

5G HETEROGENEOUS NETWORKS FOR CONNECTED VEHICLES: A COOPERATIVE MULTI-LAYER APPROACH

Von der Fakultät für Elektrotechnik und Informationstechnik
der Rheinisch-Westfälischen Technischen Hochschule Aachen
zur Erlangung des akademischen Grades eines Doktors
der Ingenieurwissenschaften genehmigte Dissertation

vorgelegt von

Master of Science
Jose Angel Leon Calvo

aus Madrid, Spanien

Berichter: Universitätsprofessor Dr. rer. nat. Rudolf Mathar
Universitätsprofessor Dr.-Ing. Gerd Ascheid

Tag der mündlichen Prüfung: 14. November 2018

Diese Dissertation ist auf den Internetseiten
der Hochschulbibliothek online verfügbar.

Acknowledgments

First of all, I would like to thank my supervisor Univ-Prof. Dr. rer. nat. Rudolf Mathar for providing me the opportunity of pursuing my Ph.D. at the Chair of Theoretical Information (TI) at RWTH Aachen. I would also like to thank him for his continuous support and giving me the freedom to conduct my research. Moreover, I would like to express my gratitude to Univ-Prof. Dr.-Ing. Gerd Ascheid for taking the effort to assess this thesis as the second supervisor and contribute new ideas and valuable comments.

The colleagues at the TI group have contributed immensely to my personal and professional time during my Ph.D. The group has been a source of friendship as well as good advice and collaboration. Especially to Florian Schröder and Ehsan Zandi for having a really nice time sharing the office during these years.

A special thank-you goes to Saeed Shojaee, Alireza Zamani and Emilio Balda for helping me during the last stages of my dissertation proof-reading and adding new concepts to this dissertation. Moreover, I would like to express my gratitude to Gholamreza Alirezaei and Arash Behboodi whose continuous support helped me through my Ph.D. bringing new ideas and solutions.

También me gustaría agradecer a mi padres por su constante apoyo y ayuda. Siempre me enseñaron a esforzarme al máximo y luchar por conseguir mis metas. Para ellos va dedicada una gran parte de esta tesis doctoral. Por último, la persona más importante en mi vida, mi pareja Riman, que en todo momento me ha apoyado, ayudado y que sin su cariño no hubiese podido completar esta tesis. Gracias. ¹

¹I would also like to thank my parents for their constant support and help. They always taught me to do my best and fight to achieve my goals. A large part of this doctoral thesis is dedicated to them. Finally, the most important person in my life, my partner Riman, who at all times has supported me, helped me and without his affection I could not have completed this thesis. Thank you.

Table of Contents

1	Introduction	1
1.1	Outline	2
2	Fundamentals of Vehicular Networks for Intelligent Transportation Systems	5
2.1	Introduction to Intelligent Transportation Systems	5
2.2	Intelligent Transportation Systems - Main Use Cases	7
2.2.1	Autonomous vehicles	7
2.2.2	Road safety systems	8
2.2.3	Traffic efficiency routing	9
2.3	Connected Vehicles	9
2.3.1	In-vehicle ITS equipment	10
2.3.2	Cooperative ITS scheme	11
2.4	Vehicular Communication Technologies	12
2.4.1	IEEE 802.11p/ITS-5G	13
2.4.2	3GPP LTE-V2X	15
2.5	Vehicular Communications as a 5G Technology	18
2.5.1	Technical requirements for vehicular communications in 5G	18
2.5.2	Short packets in vehicular communications	19
2.5.3	Low latency in vehicular communications	20
2.6	Summary	20
3	Heterogeneous Network Architecture for Intelligent Transportation Systems	21
3.1	Cloud Assisted Multi-Tier Network Architecture	21
3.1.1	Spectrum expansion	23
3.1.2	Spectrum efficiency enhancement	24
3.1.3	Network densification	24
3.1.4	Ubiquitous and dual connectivity	25
3.1.5	Small cell connectivity	25
3.2	Static Environment Optimization	26
3.2.1	Umbrella coverage deployment	26
3.2.2	Integer program formulation	27
3.2.3	Metaheuristic algorithm	28
3.3	Dynamic Environment Optimization	30
3.3.1	Density-based road-side unit placement	30
3.3.2	Vehicles clustering using spectral clustering and K-means algorithm	32
3.3.3	Head-cluster selection	38
3.3.4	Cluster dynamics prediction	40
3.3.5	Mobile relay nodes	43

Table of Contents

3.3.6	Group handover prediction	45
3.4	Summary	47
4	Radio Channel Modeling for Vehicular Communications	49
4.1	General Features of Vehicular Radio Channel Modeling	49
4.2	V2N Radio Channel Model	50
4.2.1	Deterministic ray-tracing algorithm	50
4.2.2	Stochastic radio channel model	51
4.2.3	Semi-stochastic radio channel model	52
4.3	3-D Beamforming for backhaul links	53
4.4	V2I Radio Channel Model	55
4.4.1	Fingerprint-based prediction scheme using predictor antennas	56
4.4.2	Numerical results	59
4.5	V2V Radio Channel Model	59
4.5.1	Three-waves channel model	60
4.5.2	Outage probability for URC	61
4.5.3	Parameter estimation for URC in V2V scenarios	62
4.5.4	Numerical results	64
4.6	Summary	65
5	Cooperative Scheme for Connected Vehicles	67
5.1	Cooperative Autonomous Systems	67
5.1.1	General concepts	67
5.1.2	Implicit and explicit coordination scheme	68
5.2	Cooperative Platoon Formation	71
5.2.1	Platoon formation and advantages	71
5.2.2	Game theoretical approach for platoon creation	72
5.2.3	Coalitional formation game-theory approach	73
5.2.4	Cooperative adaptive cruise control	76
5.2.5	Numerical results	81
5.3	Cooperative Communication Scheme	85
5.3.1	Semi-persistent scheduling optimization	86
5.3.2	Scheduling scheme for out-of-coverage networks	88
5.3.3	Infrastructure-based prediction scheme using sub-pools	89
5.3.4	Numerical results	90
5.4	Cooperative Connected Vehicles Security	92
5.4.1	System model	94
5.4.2	Proposed security scheme	95
5.4.3	Ring-based signature for platoon joining	95
5.4.4	Smart contracts	97
5.4.5	Blockchain-based microtransactions	97
5.4.6	Scalability and time-critical applications	99
5.5	Summary	99
6	A Practical Vehicular Network Deployment - Two Case Studies	101
6.1	Case Study I – City of Cologne	101
6.1.1	Performance network parameters	102
6.1.2	Umbrella coverage deployment	103
6.1.3	Small cells formation	104

6.1.4	Discussion of results for case study I	105
6.2	Case Study II – Occupational Safety at Seaport	106
6.2.1	Innovations in maritime sector	106
6.2.2	Case study	107
6.2.3	Barriers and success conditions	108
6.2.4	An innovation success model	110
6.2.5	Proposed system model	111
6.2.6	Simulation results	113
6.2.7	Discussion of results for case study II	116
6.3	Summary	117
7	Conclusions	119
7.1	Summary and Contributions	119
7.2	Future Research	120
	Acronyms	123
	List of Figures	127
	List of Tables	129
	Bibliography	131
	Curriculum Vitae	143

1 | Introduction

The number of vehicles on the road is increasing every year, and with it, the appearance of more complex road cases, leading to potentially dangerous situations. Several studies and research projects have been conducted by both industry and academia, reaching the conclusion that the main solution to overcome these challenges is automated vehicles. The idea of autonomous vehicles driving without human interaction requires significant improvements on the underlying communications systems and on-board equipment, which allow the vehicles to communicate with each other. In order to obtain an optimized cooperative vehicular network, it is important to implement coordination strategies as relying solely on the communication between the vehicles is not sufficient. The cooperative nature of these vehicles, which is based on their communication systems, result in defining them as *cooperative connected vehicles*. Cooperative connected vehicles are envisioned as the future of transportation due to their increased safety and road traffic optimization. Nonetheless, the stringent requirements for the communication technologies, regarding reliability and latency for safety-related applications, provide a major challenge for practical implementation.

The main barrier to implement cooperative strategies among different vehicles is to obtain a global perception of the environment using communication schemes while meeting the aforementioned requirements. Several technologies have been developed involving communication between vehicles and the infrastructures deployed alongside the road to help meet these requirements. By using inter-vehicular communication, the state information is exchanged using short-range links to acquire the local knowledge of the surrounding vehicles. However, the inter-vehicular communication scheme acquires only local information, and hence, it is required to extend the electronic horizon of the vehicles by means of communication links with the infrastructures. By combining both communication approaches, a general cooperative scheme among vehicles and infrastructures can be achieved. Typically, a cooperative scheme based solely on these communication schemes is not sufficient to acquire the complete awareness of a vehicle's surroundings. Therefore, a widely used concept to perceive the near environment is to equip the vehicle with a large set of sensors.

This dissertation contributes to the development of a framework for cooperative connected vehicles implementing different perception layers including the network deployment, management, and optimization. First, in order to set the basic notions of vehicular networks, these concepts are introduced and the state-of-the-art technologies are discussed. For the deployment of the associated infrastructures to vehicular networks, two different approaches are combined seeking to achieve an optimal solution. The first one considers the static environment, i.e., the particular scenario along with the road network, where the main goal is to obtain ubiquitous connectivity for the users.

The second approach exploits the rapidly changing environment to optimize the network applying a density-based scheme. To that end, a novel multi-layer network approach is proposed in the present work. Additionally, the communication channels between the network elements are analyzed and divided into several layers in order to model them properly. Since the aim of each of these layers is different, diverse radio channel models are proposed. A special focus is given to the vehicle-to-vehicle communication where ultra-reliable communications are required. Furthermore, once the communication requirements are fulfilled, it is the turn to develop a cooperative strategy between the vehicles. In this case, we provide a theoretical framework, supported by simulations, where the safety and traffic efficiency are improved by means of adaptive cooperation. The last part of this dissertation focuses on the cooperative scheme for connected vehicles, once a reliable network connectivity is provided. A platooning scheme is defined based on coalitional game-theory concepts including an incentive to motivate the formation of these platoons. Moreover, by including a cooperative adaptive cruise control achieved by inter-vehicular communications, the platoon formations are successfully managed fulfilling the safety and stability constraints.

1.1 Outline

First, the fundamental concepts of intelligent transportation networks are presented in Chapter 2. We define the idea of connected vehicles along with the predominant communication technologies. Moreover, the challenges and technical requirements of vehicular networks are defined within the framework of 5G technologies.

The proposed system model for heterogeneous vehicular networks is detailed in Chapter 3, showing the methodology behind this concept. Different strategies are described to meet the stringent requirements for vehicular networks. Throughout this chapter, two different network optimization approaches are built according to the static and dynamic behavior of the network.

In order to obtain a feasible communication link between the different members of the network, the radio channel model is divided into several layers and analyzed in detail throughout Chapter 4. Moreover, a realistic simulation is implemented, and thereafter the results are compared with real measurement data in order to show the accuracy of our channel model.

In Chapter 5, a cooperative scheme for autonomous vehicles is defined and analyzed in terms of implicit and explicit coordination. A coalitional game-theory approach is used to motivate the creation of platoons, which optimizes the traffic and improves the safety of the vehicles. Moreover, a novel platooning scheme is proposed using inter-vehicular communication to provide stability to the formation while maintaining the smallest inter-vehicular gap. Additionally, the exchange of messages between vehicles is protected using a blockchain scheme exploiting the platoon formation. In the last part of this chapter, we make use of our proposed heterogeneous network to optimize the network resources predicting the behavior of the vehicles.

To sum up all the concepts and contributions of this dissertation, two case studies are developed in Chapter 6. The relevant parameters are analyzed showing the improvements of the proposed framework, both in an urban and on-port scenario inferring the concepts

used for safety in vehicular networks. The conclusions of this dissertation and directions for future research are discussed in Chapter 7.

Parts of this dissertation have been published in [1–10] and additional papers submitted to different conferences and journals are still under revision as of the submission date. Furthermore, analogous concepts to the ones used for vehicular networks are applied for increasing the occupational safety in on-port environments and the obtained results are published in [11, 12].

2 | Fundamentals of Vehicular Networks for Intelligent Transportation Systems

Throughout this chapter, the fundamental concepts in the field of vehicular networks for Intelligent Transportation Systems (ITS) are described and compared to the traditional cellular systems. Several use cases are defined along with their technical requirements in order to obtain a feasible framework. Additionally, the idea of connected vehicles together with the new communication technologies adopted to overcome these design challenges are described in depth. Finally, the stringent requirements and constraints faced by the ITS technology are analyzed from a communication perspective.

2.1 Introduction to Intelligent Transportation Systems

Nowadays the number of vehicles is continuously growing, particularly in urban areas, affecting the people needs and daily life. This increase in the number of vehicles results in several disturbing effects such as traffic congestion, accidents, and larger vehicle pollution emissions. Several different strategies have been implemented in recent years in order to reduce accidents and traffic congestion. However, these efforts did not significantly improve the road safety, as they focused solely on the road infrastructure. The little improvement and the necessity to have an effective way of enhancing the transportations systems, motivated research institutions and industry to center their attention on the area of ITS [13]. ITS are envisioned as the future of transportation, due to their increased safety and higher efficiency compared to the traditional transportation systems. In summary, ITS are defined by the 5G Automotive Association (5GAA) [14] as *application of information and technologies for safe and efficient transportation of people and goods*. In other words, use connectivity as the key enabler for road safety and higher traffic efficiency.

Connectivity involves not only pure communication schemes but also electronics, control, robotics, sensors, and signal processing as shown in Figure 2.1. Hence, ITS can be understood as a global phenomenon which attracts the interest of many partners from different backgrounds. However, in this work, we are mainly focusing on the communication perspective, a brief insight into the rest of the ITS components will nevertheless be given in Section 2.3.1.

The development of ITS requires the integration of the automotive industry and the telecommunication companies, which are already collaborating in the 5GAA, to ensure a feasible network from both technical and economical point of view. In this ecosystem, the telecommunication companies will provide the crucial network connectivity for ITS

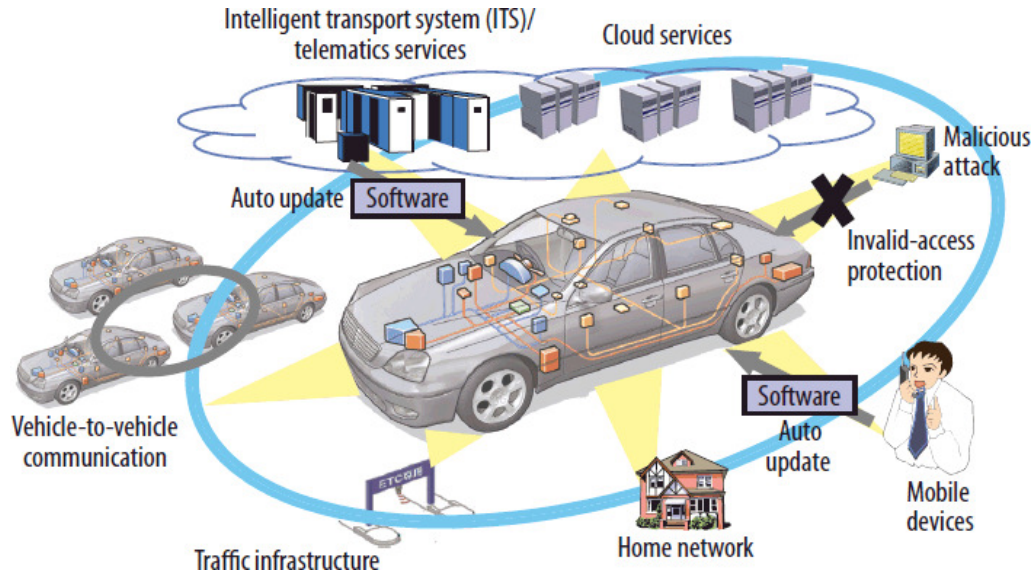


Figure 2.1: In-vehicle ITS technologies [15].

services, and the automotive industry will ensure the proper commodities and technologies required to efficiently implement the ITS services. The efforts from the ITS community to obtain a fully automated, accident-free system are divided into 5 different phases as shown in Figure 2.2.

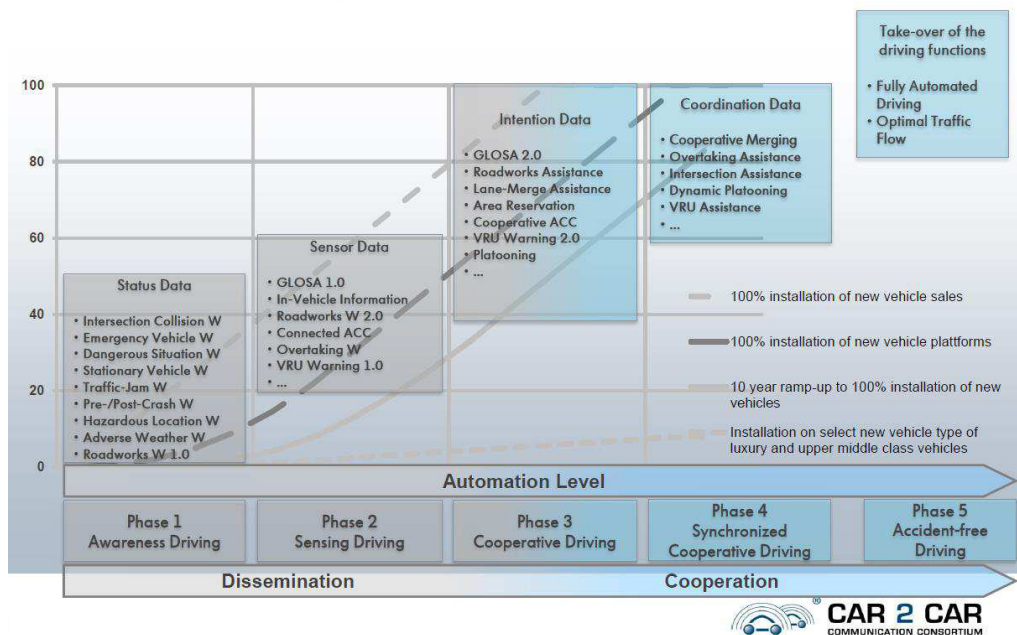


Figure 2.2: Vehicle-to-X application roadmap [16].

The first two areas focus on the data obtained by the On-board Unit (OBU) of the individual vehicles and are currently implemented in most of the commercial vehicles. These two phases cover the data acquiring and dissemination stage. The last three

phases cover the cooperation and coordination functions until complete automation. These stages focus on the coordinated maneuvers of the vehicles using the shared information which is obtained by a combination of sensors and communication schemes. In order to achieve these last levels of automation, it is required to incorporate vehicular communication schemes to obtain a fully cooperative system. At this point, we use the definitions provided by Petit and Shladover [17] for the ITS elements to clarify the following concepts:

- **Automation:** no human interaction in the control and management of the vehicle.
- **Autonomous Vehicle:** driving based on the readings obtained from the OBU of the vehicles, without active communication or collaboration with any other entity. This is the actual definition of a self-driving vehicle.
- **Cooperative Automation:** autonomous vehicle which integrates the information obtained from the different network elements (other vehicles and infrastructures) within the local environment knowledge gathered by the OBU.

Therefore, the final goal and motivations of this work are to obtain fully autonomous vehicles which cooperate, by means of vehicular communications, with the remaining vehicles and infrastructures in order to obtain an optimal and stable system.

2.2 Intelligent Transportation Systems - Main Use Cases

There are different scenarios in which the ITS will significantly impact our daily life. Using these cases as a road-map, the different aspects and technical requirements for ITS can be described. In this work, we highlight three of them as the most relevant ones, namely autonomous vehicles, road safety systems and efficient routing for road traffic.

2.2.1 Autonomous vehicles

Autonomous driving is considered to be the next big thing in the upcoming years, and both industry and academia have already turned their eyes upon it [18]. It is the key enabler element for the future of ITS, and hence, all efforts are focused to make this concept feasible. Currently, the main developments in the area of autonomous driving are concentrated on a single vehicle traveling without cooperating with the remaining vehicles or the environment. In this case, advanced technologies, such as Light Detection and Ranging (LIDAR) and high-resolution maps are used to avoid collisions when following a predefined route [19]. However, these developments cover only the first two phases (see Figure 2.2), which are far away from the final goal. Nevertheless, these approaches have shown the potential of autonomous driving, achieving a great success in terms of the number of accidents per kilometer driven surpassing human driving. Nonetheless, it is worth mentioning that a single autonomous vehicle will not improve the overall traffic flow, since it does not take into consideration the remaining vehicles on the road for more than merely collision avoidance [20].

It is critical to implement autonomous driving since many studies have shown the low efficiency of human-based driving systems due to human distraction, delayed reaction and inappropriate maneuver decision [21, 22]. Ultimately, a fully autonomous driving

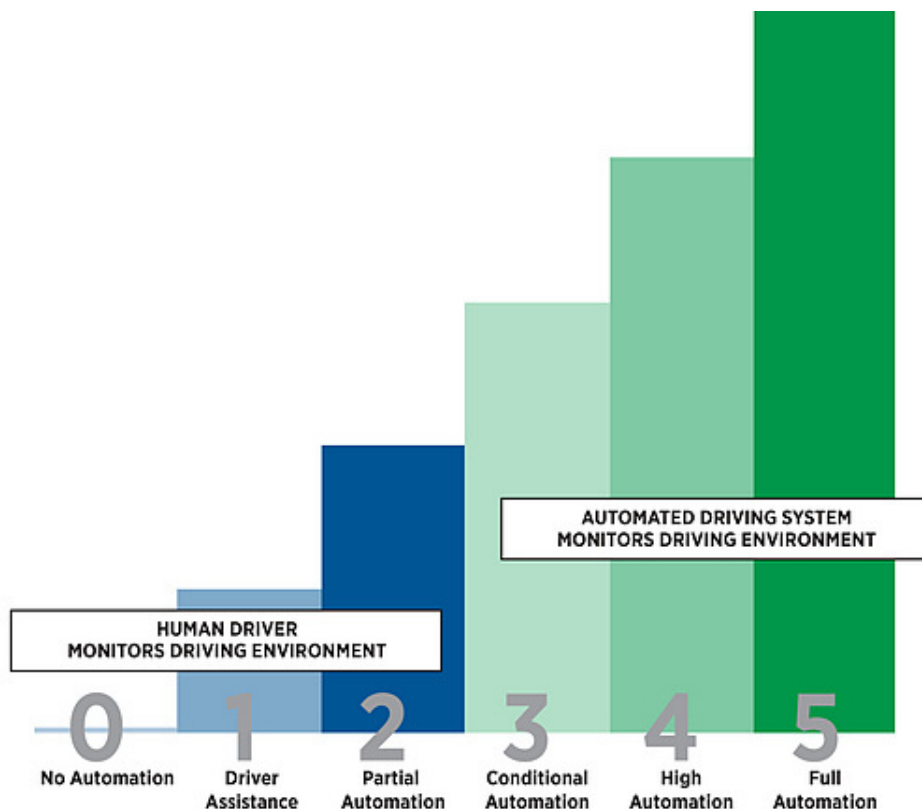


Figure 2.3: Automation levels according to SAE International Standard.

system may replace human drivers, automatically making and executing maneuver decisions. According to the SAE International Standard J3016 [23] and following the previously given definitions, a fully automated driving system is one which operates without human interaction while the remaining vehicles are also autonomous as shown in Figure 2.3 in its fifth level. Therefore, a fully automated vehicle must have knowledge about the surrounding environment, and it should also be able to obtain and share information concerning the general traffic status. The current state-of-the-art technology involving autonomous vehicles is moving between level 2 and level 3, i.e., partial and conditional automation. In order to achieve the last level of automation, it is required to use communication schemes which are analyzed in Section 2.4.

2.2.2 Road safety systems

The World Health Organization assesses the number of road traffic deaths as higher than 1.25 millions worldwide per year [24], and considering Europe alone this number reaches up to 50000 per year according to Eurostat statistics [25]. Therefore, one of the main goals of ITS is to provide an enhanced road safety system for all vehicles and pedestrian. In order to obtain a higher road safety, the first required step is to increase the driver’s awareness of its surroundings. In the near future, when autonomous vehicles become a reality, the driver’s assistance will not be needed and this awareness will be transferred to the vehicle itself. As we stated in the previous point, it is not sufficient to obtain the individual vehicle knowledge but to create a collective perception. This idea includes the

information obtained from the OBU of each vehicle, which will be discussed in Section 2.3.1, and the periodically broadcast status information from the vehicles. These broadcast messages can be classified into two different domains:

- **Cooperative Awareness Message (CAM):** these messages contain the status information of the vehicle (e.g., position, acceleration, heading, etc.) and are periodically sent, typically every 0.1 seconds.
- **Decentralized Environmental Notification Message (DENM):** the DENM are event-driven messages, i.e., they are only sent when an unexpected incident or event appears in the network. The nature of these events can be in a wide range (e.g., traffic jam, accident, icy road, etc.).

Both types of messages are disseminated in the network, either to the individual vehicles or to a central infrastructure where it can be aggregated to the rest of messages and information, helping to create the collective perception. As a result of the achieved collective perception, the vehicles and pedestrians in the network can extend their electronic horizon [26], which is defined as the physical limit of the OBU and communication technologies. Several applications, such as improved collision avoidance, see-through and bird's eye at intersections are based on this extended electronic horizon.

2.2.3 Traffic efficiency routing

On the basis of information dissemination and collective cooperation, the direct consequence is the capability of routing the traffic efficiently. This use case belongs to the last level of ITS (see Figure 2.2) and assumes some preconditions such as collaborative perception and communication, along with a centralized architecture. As an example, using the information contained in the CAMs and DENMs, it is possible to adjust the speed of the vehicles entering an intersection; consequently, optimizing the traffic flow. Moreover, due to the collaborative perception and extended electronic horizon, the centralized architecture can optimize the traffic flow using the vehicle's status.

In order to enable an efficient traffic routing, one of the proposed technologies is a cloud-assisted network, where the information gathered by all users is collected. Using the cloud functionality, every participant has full knowledge of the network. Therefore, as a solution for connected vehicles, a heterogeneous cloud-based network is extensively analyzed in Section 3.1.

2.3 Connected Vehicles

In order to implement the previous use cases, we require a new concept of vehicle, different from the current autonomous vehicle idea, such as the one developed by Google [27]. This new concept of a vehicle is defined as Connected Vehicle in the United States or as Cooperative Intelligent Transportation Systems (C-ITS) in Europe [28]. Due to their communication equipment, the vehicles have the capability of sharing and disseminating their status with other vehicles in the network and sense their local environment using their OBU. Connected vehicles are equipped with advanced software which enables new

technologies, creating a new label of applications, platforms, and infrastructures. The on-board equipment in vehicles has grown from basic technology, such as lighting systems, to cruise control or collision avoidance systems, where several types of sensors provide the vehicle with knowledge about the internal and external environment.

2.3.1 In-vehicle ITS equipment

The connected vehicle fleet has to be equipped with a set of different discrete elements to sense the local environment and make proper decisions. In order to detect obstacles, other vehicles or pedestrians, a combination of LIDAR with vision cameras is generally used to map the 3D environment [29]. The LIDAR technology allows us to detect non-metallic obstacles with a higher accuracy due to its shorter wavelength laser light. In addition to this technology, there is a variety of different sensors, including radar, ultrasonics and acoustic sensors installed in the vehicles, as shown in Figure 2.4.

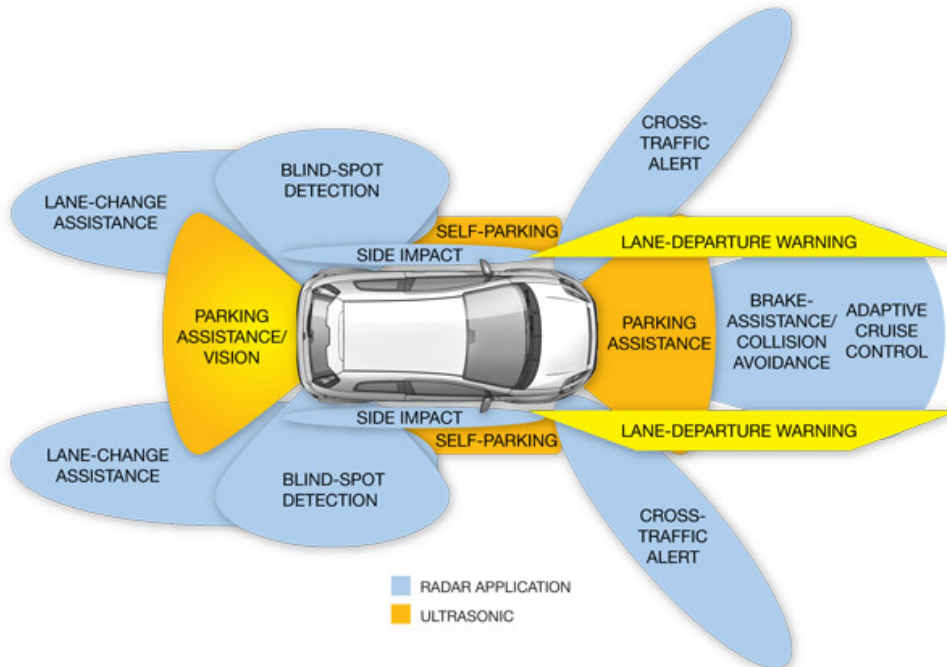


Figure 2.4: In-vehicle sensors and active safety systems.

These sensors constitute the active safety system of each vehicle responsible for bringing integrity to the system [30]. Since the information coming from all sensors has a widely different nature, it is important to implement signal processing techniques to rapidly acquire the information. The vehicle works as a sensor fusion center where the readings from the different sensors are collected in order to make an accurate decision.

This sensor fusion center is the main component of the in-vehicle ITS system and can be classified using the categorization from Armingol et al. in [31] as follows

- **low level** applications, raw information is obtained from different sources and combined afterward, obtaining new information.

- **medium level** applications, in this abstraction level several pre-processing steps are performed for each individual sensor, before combining the readings.
- In **high level** approaches, the detection and classification techniques are applied to the sensors individually, and in the last step, the output from each sensor is combined to obtain the final accurate reading.

This classification is the traditional way of combining the information gathered by the OBU. However, new approaches are being developed, where the readings from different types of sensors, such as cameras and radar, are combined to improve the estimation. Moreover, the readings from the sensors can be used to obtain an additional security layer for authentication and communications. A secure communication scheme exploiting these sensor's readings is introduced in Section 5.4.

2.3.2 Cooperative ITS scheme

The next step to create connected vehicles is to provide a reliable communication scheme to share the information obtained from the OBU of each vehicle. These communication technologies are analyzed in Section 2.4. This field is occasionally a neglected aspect of connected vehicles even though it enables the cooperative component among vehicles. Nevertheless, by making use of the communication schemes as the enabling factor, different approaches for managing the vehicular network have been proposed, predominating the platooning systems [32–34]. These platooning systems provide increased safety, efficiency in terms of vehicles on the road and reduced fuel consumption.

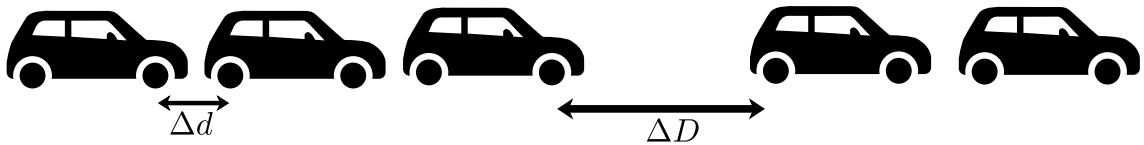


Figure 2.5: Standard platoon formation.

A platoon system, as shown in Figure 2.5, is a group of vehicles connected electronically one to each other. It can be comparable to a train, where the vehicles are wagons and all of them are traveling in the same direction and with the same speed. The first vehicle in the platoon is denominated as the platoon leader, and it is in charge of keeping the pace for the platoon. The distance between vehicles, Δd , stays constant, and it is the main parameter required to achieve platoon stability. Additionally, the distance between two consecutive platoons is defined as ΔD being it in the order of ten times bigger than Δd . It has been shown in one of the published contributions of this work [8] that in order to obtain an optimal platoon system, a reliable inter-vehicular communication scheme is required. Therefore, the next step in our work is to analyze the vehicular communication technologies in order to implement a feasible cooperative scheme.

2.4 Vehicular Communication Technologies

The predominant concept in the 5GAA vision for vehicular communication management is a heterogeneous network formed by different sized cells and infrastructures. The suggested communication technology for these heterogeneous networks is the Long Term Evolution-Vehicle to Everything (LTE-V2X) proposed by the Third Generation Partnership Project (3GPP) in its Release 14 [35] which involves both centralized and decentralized networks. Nevertheless, the Vehicle to Everything Communication (V2X) communication network concepts implemented in this work are independent of the used technology. In our scheme, a heterogeneous network is formed by different protocols and layers, with a first (upper) layer where the Evolved Node B (eNodeB) provides umbrella coverage, i.e., total connectivity for all the users. The second layer is constituted by smaller infrastructures called Road Side Unit (RSU) which are connected to the eNodeB by backhaul links. The last layer is formed by the vehicles and pedestrians which share their information with the rest of users as well as the upper network layers.

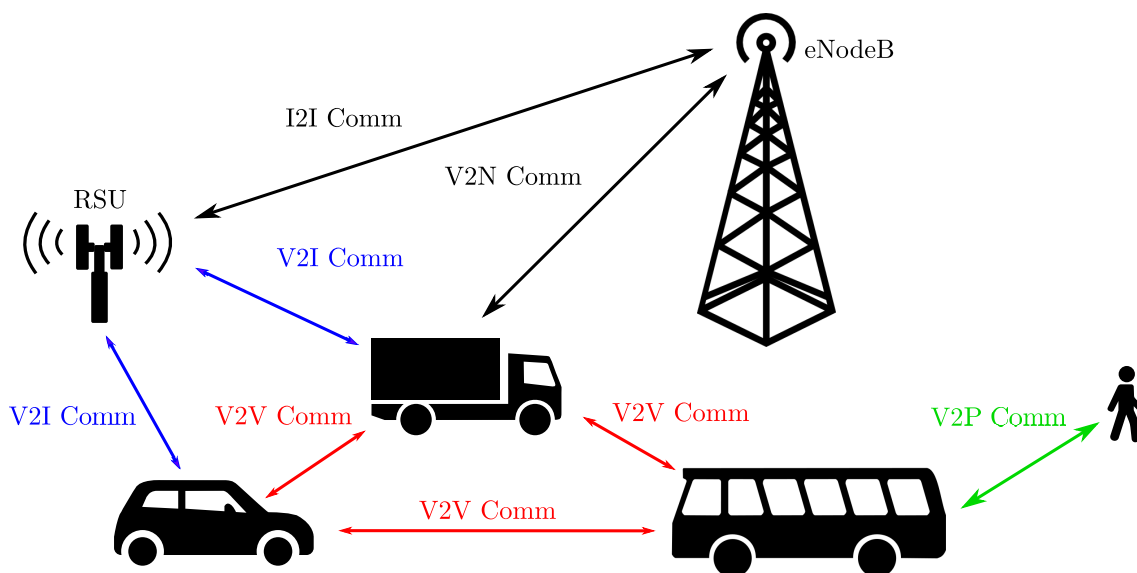


Figure 2.6: V2X communication network overview.

A standard V2X communication network is depicted in Figure 2.6, which includes the following communication protocols:

- **Vehicle to Network Communication (V2N):** this protocol layer connects the macro-cell infrastructure (eNodeB) directly with the vehicles. It is usually used to transmit the control data, i.e., CAMs and DENMs, from the vehicle directly to the network reducing the end-to-end latency. Moreover, the infrastructure informs the vehicle about its allocated resources.
- **Vehicle to Infrastructure Communication (V2I):** the vehicle and the infrastructure, usually an RSU, exchange information whenever the vehicle is in the proximity of the infrastructure. In this case, the infrastructure might play a double role, acting as a communication node or as a relay forwarding information.

- **Vehicle to Vehicle Communication (V2V):** this layer has two different modes. Usually, the information is broadcast to all the vehicles in range, but it can also be sent to specific users. The V2V application transmits specific information about the vehicle status (e.g., location, vehicle dynamics), and hence, the payload must be flexible to adapt its content to different types of information.
- **Vehicle to Pedestrian Communication (V2P):** this layer is usually used in the uplink direction, i.e., the pedestrian sends information to the vehicle or infrastructure, whenever the proximity and authorization requirements are fulfilled. This layer is used to detect areas with a high density of pedestrians, using the beacon signal sent from the pedestrian's mobile phone.

All these types of communication protocols are used to provide a collaborative perception and offer smarter services to the end-users. Therefore, using the aforementioned layers, the transportation entities, such as vehicles, pedestrians, RSUs, and macro-cells gather information to extend their local knowledge. Due to the characteristics of the communication scheme, especially considering the V2V layer, the main concepts for vehicular communications are similar to the ones used in Device to Device (D2D) [36] for smart meters or sensor networks, where the nodes continuously share their status and information about the environment. However, in the case of vehicular networks, the mobility of the users is different. In order to overcome the challenging particularities of vehicular networks, i.e., high density of nodes, fast mobility, highly variable scenario, and high network load, two new communication schemes are proposed to fulfill the Quality of Service (QoS) requirements, namely IEEE 802.11p/ITS-5G and LTE-V2X. In the following sections, we focus on the PHY and MAC layer of both protocols in order to evaluate the most suitable schemes for vehicular communications.

2.4.1 IEEE 802.11p/ITS-5G

IEEE 802.11p is a communication protocol from the 802.11 family with a modified PHY and MAC layer and has the objective of enabling vehicular communications. IEEE 802.11p has been proposed as a candidate for ITS for the last 10 years [37]. This protocol is proposed mainly as a distributed system where the nodes can communicate with each other without requiring a central infrastructure. Hence, the IEEE 802.11p technology constitutes a decentralized system which is based on the broadcast messages from the nodes. The MAC layer of IEEE 802.11p can be divided into two different schemes: Punctual Coordination Function (PCF) for infrastructure-based networks without contention mechanisms, and Distributed Coordination Function (DCF) which is used in distributed networks, such as vehicular networks.

IEEE 802.11p distributed MAC layer is based on the Carrier Sense Multiple Access with Collision Avoidance (CSMA/CA) mechanism and it operates at a frequency of 5.9 GHz. Due to its simplicity and distributed media access control mechanism, this standard is suitable for vehicular network applications. However, by means of the highly dynamic environment of vehicular networks, it does not fulfill the ITS requirements in terms of reliability [38]. In particular for IEEE 802.11p, the maximum latency of communications cannot be guaranteed as the number of nodes increases. Nonetheless, the ad-hoc nature

of the communication scheme allows the nodes to communicate immediately without any additional infrastructure. The diagram for CSMA/CA is depicted in Figure 2.7.

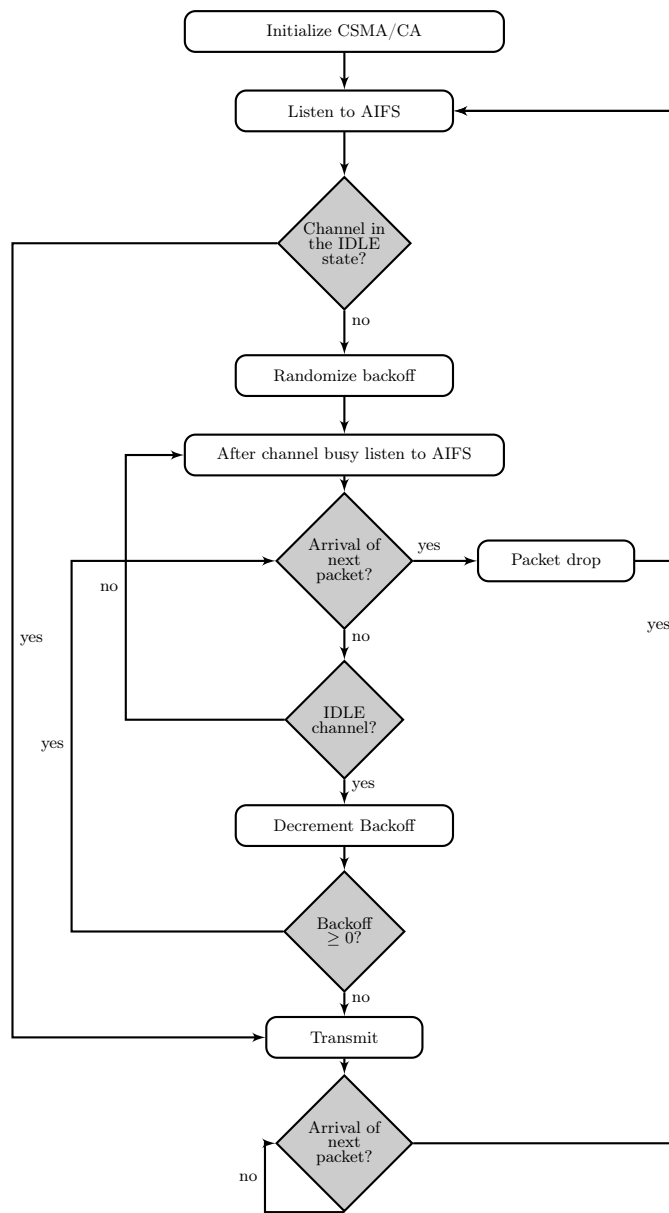


Figure 2.7: Flowchart for the CSMA/CA according to the standard.

The CSMA/CA scheme works as follows: the transmitter node senses the channel during an Arbitration Inter-frame Space (AIFS) interval. If the channel is free after this time period, the node transmits the packet. Once the node can send the packet, it checks whether the upper layers have a new packet ready to be sent. In case the transmitter node finds a busy channel during the sensing operation, it will get a back-off value which will be decreased every time the node has to wait to transmit until the value gets to zero and the packet can be transmitted. Moreover, this scheme suffers from the hidden terminal issue, where not all the communication nodes are in a reciprocal range. In addition to the reliability issue, IEEE 802.11p suffers from scalability in dense scenarios, where it is not

able to provide the required time-probabilistic characteristics. Hence, in an environment where latency and reliability are so critical, the MAC layer of 802.11p is not a good candidate to fulfill the requirements.

2.4.2 3GPP LTE-V2X

As discussed in the previous section, the IEEE 802.11p technology is not suitable for dense scenarios due to the non-guaranteed QoS. In contrast, the LTE-V2X technology addresses this problem developing an enhanced PHY and MAC layer. LTE-V2X has been proposed as a centralized-based architecture, i.e., the network revolves around an eNodeB, but it can also work as a distributed architecture without the requirement of an infrastructure. Although the requisite of a centralized infrastructure can be considered to be a drawback, it provides practical advantages (e.g., the communication range can be extended and the eNodeB can perform the role of a smart architecture). Moreover, due to the fact that the infrastructure in LTE and LTE-V2X can be reused, the deployment cost is therefore considered relatively low.

LTE-V2X has been recently proposed as a new scheme for vehicular communications, extending the services of Long Term Evolution (LTE). The different protocol layers are shown in Figure 2.8. The upper layers of the protocol stack are reused and adapted to the requirements defined by the automotive associations (e.g., SAE, ETSI, 5GAA). These upper layers are used to tune the congestion parameters. The lower layer, specially PHY, and MAC are redefined using several use cases, in order to fulfill the high reliability and low latency requirements. The main changes in these layers with respect to the cellular LTE are implemented in order to obtain an enhanced performance in the MAC/PHY layer and provide congestion control. In addition, a deterministic access control and resource scheduling are also proposed.

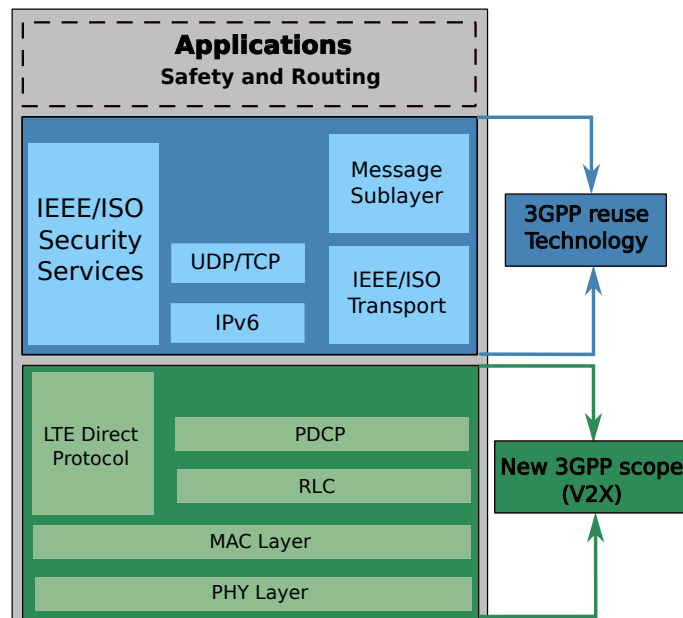


Figure 2.8: LTE-V2X Release 14 architecture.

The radio protocol architecture of LTE can be divided into user and control plane. The user plane is further divided into three different components:

- **Packet Data Convergence Protocol (PDCP)** this component provides service to the Radio Resource Control (RRC) and user plane layers. The main functions of this layer are header compression, ciphering, integrity protection, and transfer of user and control data.
- **Radio Link Control (RLC)** its main function is to adapt the packet size from an upper layer into a format that can be transmitted over the radio interface. In the case of a packet reception failure, this component is also responsible for retransmissions.
- **Media Access Control (MAC)** this layer decides the amount of data that can be transmitted in each radio bearer. Moreover, this layer is in charge of meeting the requirements negotiated in the QoS agreement for each radio bearer.

LTE-V2X PHY layer

The LTE-V2X physical layer for Sidelink (SL) is based on Single Carrier Frequency Division Multiple Access (SC-FDMA) for the uplink connection. The resource block architecture of LTE-V2X in time domain is shown in Figure 2.9.

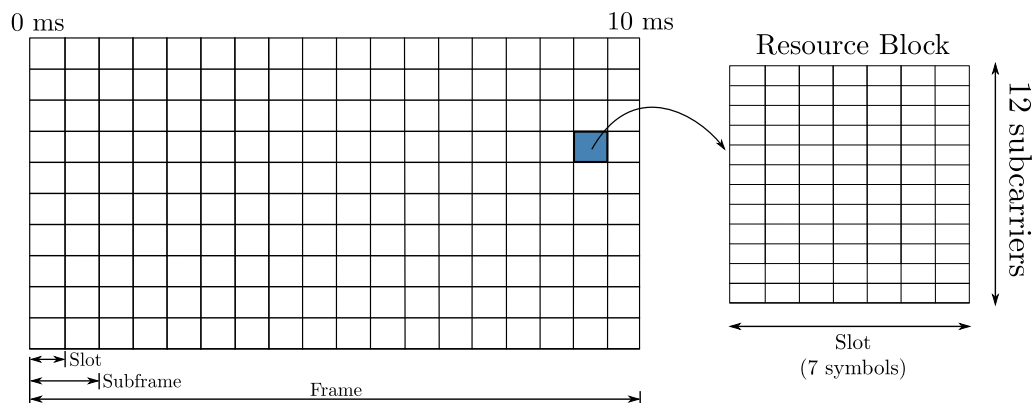


Figure 2.9: LTE resource block architecture.

LTE-V2X Sidelink transmission is organized in frames of 10 ms of duration. Each of these frames is divided into slots of 1 ms of duration in time domain. At the same time, each of these 1 ms slots is divided into 7 symbols, creating the minimal data structure (Resource Block), as shown in Figure 2.9. LTE-V2X Sidelink (SL) was released in March 2017 as part of the LTE 3GPP Release 14 to enable direct communication between User Equipment (UE)s and can be operated with or without the assistance of the eNodeB. When the vehicles UE are in the coverage range of the eNodeB, it can perform resource scheduling of the sidelink communication using the global knowledge, which is known as centralized scheduling or mode 3 scheduling of LTE-V2X SL communication.

LTE-V2X MAC layer

Principally, the eNodeB can mitigate the interference problem by assigning UEs with diverse time and frequency resources. Alternatively, when the vehicle's UEs are out of eNodeB coverage, distributed scheduling is applied. In such a distributed scheduling scheme, UEs access physical resources following a sensing-based Semi-Persistent Scheduling (SPS) scheme. According to this scheme, one UE keeps sensing the resource usage in one resource scheduling period all along. By decoding the received message or measuring the energy in every resource block, which is organized in different subframes and subbands in LTE-V2X SL, UE can be aware of the resource reservation condition and knows which resources are free to use in the next scheduling period. Afterward, from the determined idle resources, the UE randomly selects the needed number of resources for transmission. According to SPS, once a UE selects the resources successfully, it tends to keep occupying them during the next few scheduling periods avoiding costly reconfigurations. The infrastructure-based LTE-V2X has three different modes of operation shown in Figure 2.10.

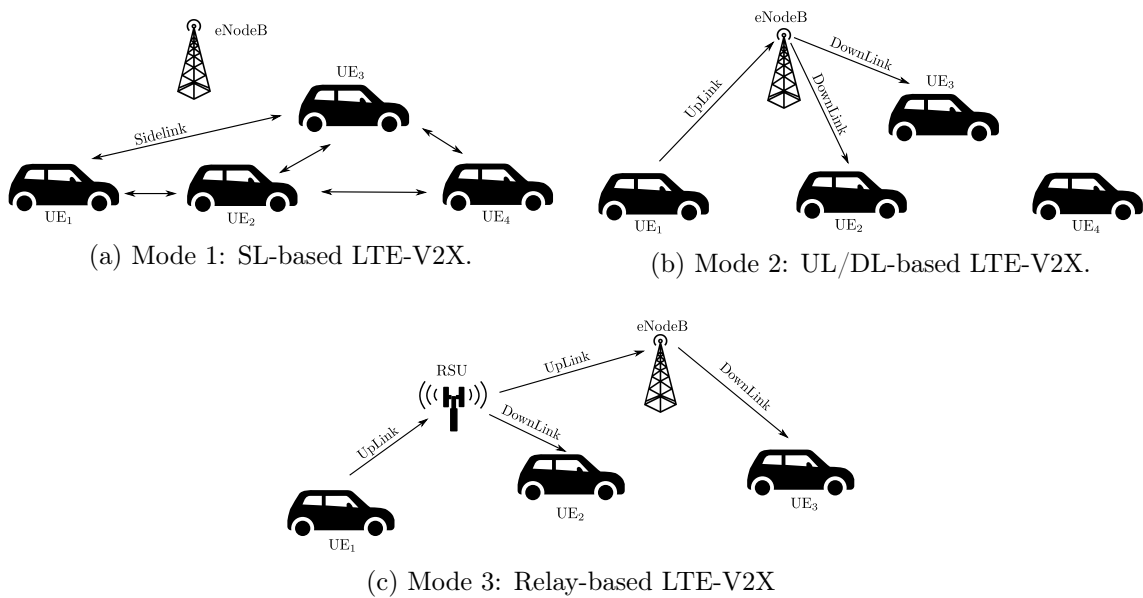


Figure 2.10: Modes of operation for V2X communications.

The first mode in Figure 2.10(a) depicts the direct exchange of information between vehicles using the PC5 interface, without the assistance of the infrastructure. In this mode, the information, usually CAM or DENM, is shared between the vehicles in a one-hop broadcast manner without the assistance of the infrastructure. Figure 2.10(b) shows the infrastructure-based operation mode where the information is shared within a two-hops transmission method. In this mode, the information is gathered at the infrastructure, and afterward, forwarded to rest of vehicles. The last operation mode is shown in Figure 2.10(c) where the communication can be done in more than two hops using RSUs for the dissemination of the information. This mode can be seen as the generalized mode where the UL/DL and the SL coexist.

2.5 Vehicular Communications as a 5G Technology

The different concepts for the future ITS presented throughout this chapter require an enhanced network in order to provide the required connectivity, latency, and reliability. Accordingly, vehicular communications has to be designed using a new paradigm, in contra-position with traditional cellular systems. For this particular reason, vehicular communications are encompassed in the 5G framework.

The 5G networks have a completely different vision in comparison with the 4G networks, where the latter focuses on user data and its rate improvement, whereas in the former, the majority of communication exchanges will not involve human-users, but Machine-to-Machine (M2M) communications, and in most of the cases these machines will be autonomous. Therefore, the communication trend will change to the following two new wireless modes [39]:

- **Massive M2M communication:** huge number of devices, usually sensors, exchanging information in a specific area.
- **Ultra-Reliable and Low-Latency Communications (URLLC):** reliability communication level close to 100% with delay values inferior to 1 ms. This kind of communications is not implemented in the current 4G communication systems.

Vehicular communications fall into the URLLC category where the short messages need to be exchanged with low latency, typically < 1 ms, and the reliability has to be 99.999%. Since we are focusing our study on autonomous driving and safety applications, URLLC are the main goal, however, it is noteworthy that for other applications such as infotainment or traffic routing, the requirements in terms of latency and reliability are not so stringent.

2.5.1 Technical requirements for vehicular communications in 5G

Vehicular communications as a specific use case for 5G has the following technical requirements given by 5GAA in [14]:

- **End-to-end latency (ms):** in the case of using the PC5 transport layer (direct V2V communication) it can be defined as the delay from the air interface. In the case of using the infrastructure mode, the end-to-end latency is defined as the uplink required time and any additional routing.
- **Reliability (10^{-x}):** maximum packet loss rate at the application layer. A packet is considered lost if the reception is not possible at a specific time interval, which is acknowledged as the maximum acceptable end-to-end latency.
- **Node mobility (km/h):** maximum speed for the vehicles in a given under a specific reliability value.
- **Network density (vehicles/km²):** maximum number of vehicles in a given area under a specific reliability value.
- **Security:** security features specified by the application layer.
- **Communication range (m):** maximum distance between two communication entities which assures the required reliability.

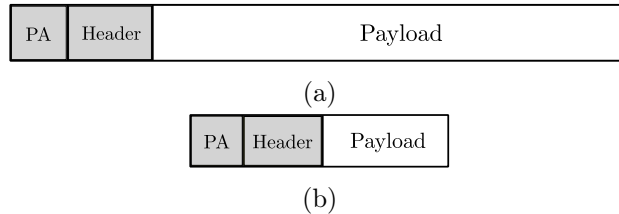


Figure 2.11: Packet structure consisting of metadata (preamble + header) and payload
 (a) Traditional long packet for current cellular systems. (b) Short packet for vehicular communications.

The V2X services can be classified into three different categories [40]: i) safety-related services, ii) non-safety services and iii) automated driving services. The safety related-services are based on sporadic messages (DENMs) to provide update information to the vehicles. The non-safety services are connected to the traffic flow optimization and are usually based on V2I links where the latency and reliability requirements are not so stringent. For safety reasons, automated driving services V2V require extremely high reliability. These services are based on periodic messages (typically every 0.1 s) where the requirements in latency (e.g., < 10 ms end-to-end latency) and reliability (99.999% of successful communications) are extremely stringent to secure the safety of the users.

2.5.2 Short packets in vehicular communications

Before considering the mechanisms of ultra reliable and low latency communications, the specific approach for V2X technology needs to be explained. Traditionally, the messages sent over the network have an amount of data (payload) k_i than can be considered to be much larger than the metadata (control information), k_0 , such as $k_i \gg k_0$. However, in the particular case of vehicular communications, most of the exchanged messages, CAM and DENM, have a length comparable to the control data, as shown in Figure 2.11. In the traditional way, the channel capacity can be defined as

$$C = \lim_{\epsilon \rightarrow 0} C_\epsilon = \lim_{\epsilon \rightarrow 0} \lim_{n \rightarrow \infty} R^*(n, \epsilon), \quad (2.1)$$

where ϵ is the packet error probability and n is the packet length. However, in our case the packets cannot be arbitrarily long, and hence, a more refined expression is required. For our case of short packets, Polyanskiy et. al [41] redefined the usual metrics showing that the maximal code rate $R^*(n, \epsilon)$ can be expressed as

$$R^*(n, \epsilon) = C - \sqrt{\frac{V}{n}} Q^{-1}(\epsilon) + \mathcal{O}\left(\frac{\log n}{n}\right), \quad (2.2)$$

where C is the positive channel capacity. Moreover, the packet length is defined as in the traditional way as $n = k_0 + k_i$ after going through the channel encoder. Here, V is the channel dispersion and $Q^{-1}(\cdot)$ is the inverse of the Gaussian Q function. Therefore, using the expression in equation (2.2) it is possible to derive the packet error probability ϵ for short packets.

2.5.3 Low latency in vehicular communications

The end-to-end latency in communication networks faces two main constraints: the distance between both communication ends and the number of devices connected to the same cell simultaneously. Both of these limitations will be addressed and overcome in Section 3.1 as a result of our proposed multi-tier network architecture. The second limitation faced by communication networks is the radio interface design, which is not designed specifically for low latency transmissions. In this case, the two main strategies used to enhance this aspect are introduced in the following:

- **Fast Uplink Access (FUA)** this mechanism eliminates the overhead created by the signaling each time a vehicle wants to transmit. This mechanism uses SPS to allocate the resources beforehand. It has been proposed in LTE Release 13.
- **Transmission Time Interval (TTI) Shortening:** the minimum resource unit in LTE systems is the TTI. Hence, if this value is shortened the latency will be drastically reduced. Some of the values considered for the shortened TTI are 0.5 ms (7 OFDM symbols) and 0.14 ms (2 OFDM) which have been proven to reduce the latency [42].

2.6 Summary

This chapter has established the state-of-the-art concepts for Intelligent Transportation Systems (ITS) from the communication technology's perspective. Additionally, the two main candidates for the future ITS communication (IEEE 802.11p and LTE-V2X) along with their strengths and weakness are outlined. Moreover, the concept of connected vehicles and their on-board equipment have been described including the different levels of automation. To conclude the chapter, the novel V2X technology has been presented in the 5G framework, stating the main requirements and challenges this technology faces in terms of communication reliability and latency.

3 | Heterogeneous Network Architecture for Intelligent Transportation Systems

In this chapter, a novel heterogeneous network architecture for vehicular networks is designed. The proposed heterogeneous network is formed by different layers creating several cell sizes. The main objective is to reduce the latency and increase the reliability, while at the same time, provide enhanced service to all the users by means of network densification. Additionally, the network architecture is optimized using two different approaches, namely a static and a dynamic environment optimization.

3.1 Cloud Assisted Multi-Tier Network Architecture

A heterogeneous network is defined as a network topology formed by multiple different sized cells under the coverage of macro-cells. Heterogeneous networks are a cornerstone element for the future 5G technologies where a larger number of users and devices are connected simultaneously. This new paradigm requires different methodologies and strategies in order to fulfill the 5G requirements. Andrews [43] summarized the main aspects which impact the research on next-generation networks. Among these topics, the topology, cell association, and mobility are the fundamental aspects addressed in our work. In the case of connected vehicles, the network has to fulfill even more stringent requirements than those needed for 5G technology due to the constraints for safety applications. Hence, the main aspects to fulfill are:

- **A massive amount of data** due to the rise of hungry-data applications and proliferation of devices. These devices will generate various types of data traffic; going from the several gigabytes of a high-quality video to the few bytes used by M2M protocols or warning systems in V2X.
- **Increase in the number of users** as a result of the new technology businesses, such as M2M, Internet of Things (IoT), and V2X communications. The biggest transformation comparing 4G to 5G is the addition of a huge number of automated devices periodically sending their data. It is considered that in the year 2020 the number of connected devices will be up to 25 billion. Among these autonomous devices, connected vehicles play a major role.
- **Ubiquitous connectivity** the always-on concept is a requirement for many new applications, such as vehicular safety, which creates a brand-new challenge in the conception of the communication networks. Moreover, in our case, reliability is a critical parameter due to non-fault-tolerant communications.

- **QoS requirements** due to the different applications and services supplied by the network, the latter has to provide different QoS depending on the user. In the case of a high-resolution video, a high data rate is required, while in the exchange of safety messages between vehicles, the main requirement is latency and reliability. Therefore, the network should be able to fulfill both by adapting its parameters.

In the particular case of vehicular networks, the number of users and the amount of data to transmit (we only focus on the three aspects mentioned in Section 2.2) do not experience a great transformation compared to traditional cellular systems. However, the requirements of ubiquitous connectivity, ultra-reliable and low-latency communications are the cornerstone features that our network must fulfill. Thus, we propose in this work a scheme focusing on the requirements of vehicular networks, considering an architecture that provides service to all users. From the first description of ITS involving connected vehicles, the network revolved around the idea of installing RSUs. The RSUs are usually located closer to the vehicles than the cellular infrastructure (macro-cells), and therefore, the communication delay and reliability are enhanced. However, any infrastructure is costly to deploy, making it infeasible to install one for each Small Cell (SC) required in the network. Therefore, we use in this current work the concept of Moving Relay Node (MRN) [44] for limiting costs and improve connectivity.

Consider a multi-tier heterogeneous network where a set \mathcal{K} of communication infrastructures, Donor Evolved Node B (DeNodeB), are deployed and a set \mathcal{L} of SCs are formed. We define the macro-cell infrastructures as DeNodeB since they are connected to both the final users and intermediate relays. The SCs can be defined in two different ways: i) in areas with an estimated high density of vehicles, where a set of \mathcal{M} RSU is installed, ii) a set of \mathcal{N} MRNs is defined, forming Mobile Small Cell (MSC) in order to provide service for the remaining areas, exploiting the platoon organization of the vehicles as shown in Figure 3.1. Moreover, each individual vehicle is defined using the set \mathcal{I} . Therefore, each vehicle, $i \in \mathcal{I}$, is associated simultaneously to a single SC that can be defined either as i_m^k or i_n^k which denotes the SC created by the RSU $m \in \mathcal{M}$ or MRN $n \in \mathcal{N}$, both of them associated to the DeNodeB $k \in \mathcal{K}$.

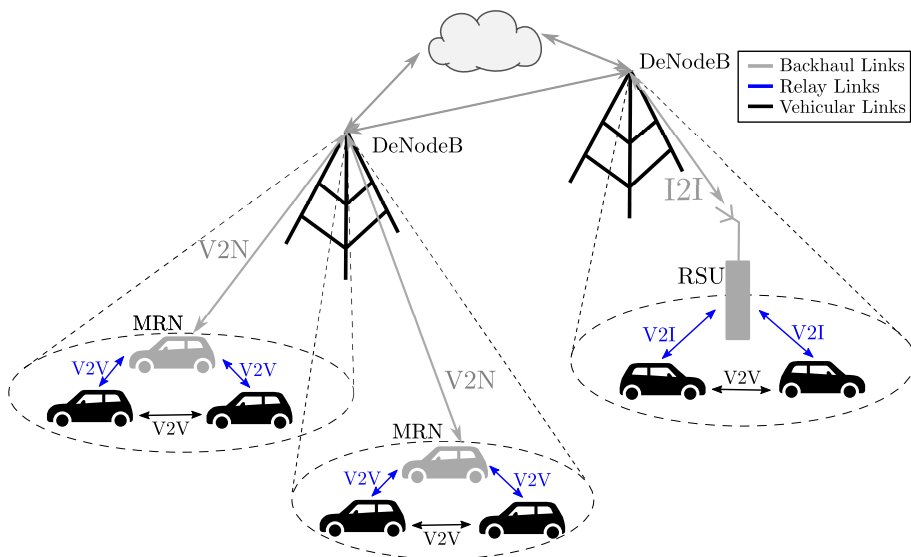


Figure 3.1: Cloud-assisted heterogeneous network overview.

Table 3.1: Cloud-assisted heterogeneous network notation.

Symbol	Description
\mathcal{K}	the set of DeNodeBs
\mathcal{L}	the set of SCs
\mathcal{M}	the set of RSUs
\mathcal{N}	the set of MSCs
\mathcal{I}	the set of vehicles

The DeNodeB provides *umbrella* coverage for the entire network forming macro-cells since ubiquitous connectivity is one of the main requirements in vehicular communications. Additionally, the DeNodeBs are connected to a cloud system which manages the network. As a result of using a cloud-based network the monitoring, management and network organization can be easily performed as follows

- **Management and control** with a large number of deployed SCs since the network is difficult to handle due to the different technologies and protocols. Therefore, in a highly variable environment caused by the vehicle's mobility, a cloud-based network is able to monitor and adapt the network resources accordingly.
- **Facilitating real-time optimization**, not only allocates the network resources efficiently to support different technologies, it also optimizes the traffic routing due to the gathered information. Using the information obtained by the macro-cells, the cloud's server has the updated information of each vehicle at every moment, enabling an optimal traffic routing.
- **Interference management** as the network density increases, the inter and intra-cell interference is more likely to affect the communication. In our case, due to the vehicle's simultaneous connection to the macro-cell and SC, enabling certain mechanisms to mitigate the interference is critical to obtain reliable communications. The cloud-based management can help to provide joint transmissions or optimal beam-forming for the backhaul links.

The vehicles are equipped with a dual communication scheme, i.e., equipment for LTE (2.4 GHz) which handles the control plane between the infrastructure and vehicle, along with high frequency equipment (5.9 GHz) for V2V and V2I communication inside the SC to allow higher data rates. In addition to this model, in our proposed network scheme, the vehicles additionally send their CAMs to the macro-cell infrastructure by the control links, using the dual-connectivity concept. In this work, we focus only on the vehicular network. However, it is worth mentioning that in the future 5G heterogeneous networks, vehicular communications have to coexist with different radio technologies which is another advantage of cloud-assisted networks [45]. In order to develop a 5G network with the previous characteristics, most of the efforts should be done in three different aspects: spectrum expansion, spectrum efficiency enhancement, and network densification.

3.1.1 Spectrum expansion

In order to achieve the high requirements of ITS, the radio spectrum needs to be expanded. In our proposed network, the vehicles are equipped with dual equipment, and the intermediate infrastructures and relays transmit on a dedicated carrier (5.9 GHz) are

different from the ones of the DeNodeB (2.4 GHz). On the one hand, the high carrier frequency communications are used in the short-range communications, i.e., between vehicles and for providing intra-SC communications, due to their higher pathloss. On the other hand, for long-range communications, as expected for the links between DeNodeBs and vehicles, the lower frequency is more suitable. Additionally, short-range communications have a higher bandwidth which enables higher data rates, while the V2N communication is only used for short packets, not requiring such high data rates.

3.1.2 Spectrum efficiency enhancement

The overall network capacity can be increased not only by expanding the radio spectrum using different technologies, it can also be improved using techniques to enhance its usage. In the current proposed network, we suggest two different mechanisms:

- **Full Dimension Multiple Input Multiple Output (FD-MIMO)**
Multiple-input multiple-output (MIMO) technology along with coordinate network schemes are technologies that attract a lot of attention as promising solutions. MIMO has been a popular technology in the past due to the potentially achievable gain [46] using a high number of antennas at both ends of the communication link. Usually, beam-forming has been applied to the azimuth or horizontal plane which concentrates the power into the desired direction. However, in some applications, a further step into the beam-forming concept can be applied [47, 48] by combining it with the LTE technology. For this purpose, the concept of 3D beam-forming [49] has been introduced. This scheme does not only adapt the horizontal dimension of the antenna pattern but also uses the vertical orientation of the antenna pattern to achieve a great gain and at the same time mitigate interference. The 3D beam-forming does not require a huge number of antennas at the transmitter, as opposed to massive MIMO [50], making this technology easier to develop and obtaining a significant improvement compared to traditional 2D beam-forming. This scheme will be analyzed in depth in Section 4.3 in order to create the backhaul links.
- **D2D connectivity** using the characteristics of the V2V communication, it is possible to connect vehicles in close proximity using the LTE-SL (PC5), without previously sending the data to a central infrastructure. This feature helps to alleviate the load of the network, hence increasing the spectral efficiency.

3.1.3 Network densification

Network densification is considered to be the predominant aspect required in order to achieve the main requirements of vehicular communications: low latency and high reliability. It is achieved by deploying RSUs and SCs, which bring the network closer to the users, consequently reducing the latency and increasing the network capacity. The infrastructures which form the SCs usually have lower transmission power and a decreased coverage range compared to the macro-cells, because they are intended to provide service to a lower number of users. The deployment of SCs is challenging due to network management in addition to the increased costs of deploying numerous

infrastructures. In order to optimize the network densification and resource allocation, two different optimization strategies are proposed in this work.

The first one is based on the large-scale deployment of the macro-cells to provide ubiquitous connectivity, considering the surrounding scenario and its characteristics. The second strategy is based on the highly dynamic component of the vehicles. For this purpose, we focus on the dynamic behavior and accurately predict the network load to allocate the proper resources. Both optimization strategies are analyzed in Section 3.2 and Section 3.3, respectively.

3.1.4 Ubiquitous and dual connectivity

Dual connectivity improves the robustness of user connectivity since each user is connected simultaneously to two cell tiers (DeNodeB and SC). Additionally, it brings redundancy to the network, which is an important mechanism to provide ultra-high reliability in safety-related applications. Using the concept of dual-connectivity from LTE networks [51, 52], the control- and user-plane are divided, offloading and enhancing the management of the LTE network. In our scheme, the DeNodeB manages the control plane of all users utilizing vehicle-to-network (V2N) links, while the RSUs and MRNs control the user-specific data using vehicle-to-infrastructure (V2I) links.

3.1.5 Small cell connectivity

In our network scheme, we define two different SC architectures: some small cells are created by fixed infrastructures (RSUs), and other ones are formed by using vehicles in the network, performing as relays. The first ones are deployed using a density-based algorithm in order to deploy the costly infrastructure at the expected high density spots (as shown in Section 3.3.1). The RSUs are connected by means of a wireless backhaul link to the DeNodeB in order to enable inter-cell coordination.

The main function of the moving small cells is to provide high connectivity rates to those areas where fixed infrastructures (RSUs) are not deployed, in our case those areas with low traffic density. The MSC is formed once a platoon moves through an area which is not covered by any fixed RSU. Every vehicle in the network is under the coverage of a DeNodeB (ubiquitous connectivity), and hence, a backhaul exists between one vehicle in the platoon (the one taking the role of a MRN) and the macro-cell. The concept of moving cells is usually applied in vehicular networks using public vehicles, e.g., buses and trains, where the passengers are the connected users [53]. The main advantage of the concept of MRNs is that the users are really close to the relay node, and hence, the communication link is highly enhanced. However, in our model, we are not providing service to users inside a vehicle, instead to other vehicles in the network. Therefore, we need to modify this concept to adjust it to our requirements, exploiting the platoon concept. This idea will be extended in Section 3.3.5.

3.2 Static Environment Optimization

3.2.1 Umbrella coverage deployment

In order to obtain total connectivity from the macro-cells, every vehicle in the network has to be under the coverage of one of these macro-cells at every instant while fulfilling a required QoS. In this section, we propose the use of an environment-based planning algorithm to obtain ubiquitous coverage for every vehicle in the network. Traditionally, the planning algorithms for urban scenarios, with respect to vehicular communications, have been developed without taking into consideration the surrounding scenario [54, 55]. However, due to the high density of buildings and obstacles in these scenarios, the link quality is degraded and, in some occasions, the communication is lost. Using the radio channel model that is introduced in Section 4.2.3, a network planning algorithm is developed exploiting the benefits of the site-specific propagation parameters. For that, we extract the road infrastructure information as a set \mathcal{X} , and it is divided into a pixel form, denoted by $x_i \in \mathcal{X}$. Moreover, the different potential positions of the macro-cells are selected taking into consideration the scenario avoiding potential illegal positions, i.e., not in the middle of the road, inside a building, etc. In the following, we introduce our notation for the planning algorithm in Table 3.2.

Table 3.2: Symbol notation.

Symbol	Description
$\mathcal{X} = \{x_i\}$	the set of the road points
$\mathcal{R} = \{r_i\}$	the set of possible DeNodeB location
$\mathcal{Z} = \{z_{(i,j)}\}$	the set of possible matchings between \mathcal{X} and \mathcal{R}
$\mathbf{y} = \{0, 1\}^{n_r \times 1}$	optimization variable for the selection of r_i
$\mathbf{z} = \{0, 1\}^{n_z \times 1}$	optimization variable for the selection of $z_{(i,j)}$
$\mathbf{C} = \{0, 1\}^{n_r \times n_x}$	coverage matrix
$C(r_i) = \sum_{j=1}^{n_x} \frac{c_{ij}}{n_x}$	coverage for each potential DeNodeB location
C_{min}	minimal total coverage for optimal solution

We denote the set of possible DeNodeB locations with $\mathcal{R} = \{r_i\}$ and the set of road points with $\mathcal{X} = \{x_i\}$, where $|\mathcal{R}| = n_r$ and $|\mathcal{X}| = n_x$, where $|\cdot|$ denotes the cardinality of a set. For a pixel point x_i to be covered by a possible DeNodeB location, we consider the threshold values for received power P_{th} , maximum propagation delay τ_{th} , and the maximum distance to the road point d_{th} . Considering these constraints, we define the coverage matrix $\mathbf{C} = \{0, 1\}^{n_r \times n_x}$ with entries c_{ij} as

$$c_{ij} = \begin{cases} 1 & \text{if } x_j \text{ is covered by } r_i, \\ 0 & \text{otherwise.} \end{cases} \quad (3.1)$$

During the execution of the planning algorithm, the DeNodeBs have been configured using the setup parameters in commercial equipment following the LTE standard [56], where the transmitted power is adjusted to 28 dBm. Therefore, using the above mentioned configuration, the constraints for the optimization scheme are set as given in Table 3.3.

Table 3.3: Static optimization constraint values.

Parameter	Value
P_{th}	-110 dBm
τ_{th}	100 μ s
d_{th}	500 m

These constraint values are chosen based on the requirements for obtaining a reliable communication, as well as focusing on the priority of low delay communications between the vehicles and the DeNodeBs. This low delay communication scheme is critical for safety-oriented applications, and thus, it requires to be restrained to a maximal upper bound.

In order to achieve the required coverage, we propose to solve the optimization problem by means of two different approaches: integer program (IP) formulation and metaheuristic (MH) algorithm. The first approach gives a close optimal solution for the problem, but its performance deteriorates when a large set of data is involved. Therefore, the latter approach is defined in order to cover all possible situations.

3.2.2 Integer program formulation

The optimization variable \mathbf{y} for the selection of DeNodeB locations is defined as $\mathbf{y} = \{0, 1\}^{n_r \times 1}$, where $y_i = 1$ if r_i is selected for the deployment. Furthermore, we define the set of possible matchings between the possible DeNodeBs locations and the road points \mathcal{Z} as

$$\mathcal{Z} = \{z_{(i,j)} = (x_i, r_j) \mid x_i \in \mathcal{X}, r_j \in \mathcal{R}\}, \quad (3.2)$$

where $|\mathcal{Z}| = n_z$. The optimization variable \mathbf{z} for the selection of a possible matching from \mathcal{Z} is defined as $\mathbf{z} = \{0, 1\}^{n_z \times 1}$, where $z_{(i,j)} = 1$ means the assignment of the road point x_i to the DeNodeB location y_i . An overview of all the notation and variables is depicted in Table 3.2.

The objective of the network planning problem is to minimize the number of deployed DeNodeB while maximizing the number of covered points, i.e., the total coverage. This multi-objective optimization problem can be formulated as

$$\underset{\substack{y_j, z_{i,j} \\ (i,j) \in \mathcal{Z}}}{\text{minimize}} \quad \lambda_1 \sum_{j=1}^{n_r} y_j - \lambda_2 \sum_{(i,j) \in \mathcal{Z}} z_{i,j} \quad (3.3)$$

$$\text{subject to} \quad \sum_{\substack{j \\ (i,j) \in \mathcal{Z}}} z_{i,j} \leq 1, \quad i = 1, \dots, n_x, \quad (3.4)$$

$$z_{i,j} \leq y_j, \quad \forall (i,j) \in \mathcal{Z}, \quad (3.5)$$

$$y_j \in \{0, 1\}, \quad j = 1, \dots, n_r, \quad (3.6)$$

$$z_{i,j} \in \{0, 1\}, \quad \forall (i,j) \in \mathcal{Z}. \quad (3.7)$$

where the first term in equation (3.3) stands for the number of deployed DeNodeBs, and the second term stands for the number of covered road points. The constraint in equation

(3.4) ensures the assignment of a road point to maximum one DeNodeB, whereas equation (3.5) ensures the selection of a DeNodeB location y_j if a road point is assigned to it. The coefficients λ_1 and λ_2 can be selected to achieve a trade-off between the coverage and the number of DeNodeBs. In the present work we set $\lambda_1 = \lambda_2 = 1$. The optimal solution of this integer linear problem in the present work is calculated upon using the commercial optimization solver Gurobi [57] and it is shown in Figure 3.2.

3.2.3 Metaheuristic algorithm

In order to obtain an optimal number of DeNodeBs and their location, a metaheuristic algorithm has been developed. Due to the number of constraints involved in the optimization problem in equations (3.4)-(3.7) and the complexity of the overall problem, a metaheuristic approach gives a good trade-off between the execution time and the optimality of the solution. The main principles involved in the metaheuristic algorithm are presented in the following algorithm

Algorithm 1 Algorithm for optimal DeNodeB deployment

Output: \mathbf{y} —vector of selected DeNodeB locations

```

while  $i \leq n_r$  do
  if  $\sum_{j=1}^{n_x} c_{ij} \geq C_{th} \cdot n_x$  then
     $r_i :=$  possible DeNodeB location
  else
     $y_i := 0$  in the solution
  end if
end while

```

Metaheuristic algorithm:

generate the initial vector \mathbf{y}_0 as

```

while  $i \leq n_{max}$  do
  generate  $\mathbf{y}_{i+1}$  from  $\mathbf{y}_i$ 
  if  $C(\mathbf{y}_{i+1}) \geq C_{min} \cdot n_x$  then
    return  $\mathbf{y}_{i+1}$ 
  else
     $i \leftarrow i + 1$ 
  end if
  if  $i > n_{max}$  then
    return  $\mathbf{y}_i$ 
  end if
end while

```

Algorithm 1 shows the flow of the proposed metaheuristic approach, where \mathbf{y}_0 denotes the initial vector with all the potential DeNodeB locations, n_{max} is the maximum number of iterations regarding the scenario, and $C_{th} = 1\%$ is the minimal individual coverage for a selected DeNodeB.

The metaheuristic planning algorithm used in this work is based on tabu-search [58], such that the potential DeNodeB locations, which do not cover a sufficient number of points given by C_{th} in percentage, are discarded to avoid unnecessary computations. Due to

the complex constraints in the optimization problem, a sub-optimal solution is obtained whenever the algorithm does not find a feasible optimal solution in the maximum number of iteration n_{max} . The sub-optimal solution gives the best-effort result obtained during the sequential iterations of the algorithm which did not reach the optimal criteria, i.e., the total coverage does not fulfill the given requirement C_{min} .

The metaheuristic algorithm consists of obtaining the individual local maximums of coverage for each DeNodeB, using a greedy strategy. Subsequently, the total coverage obtained with the selected DeNodeB formation is evaluated, in other words, whether the total coverage fulfills the constraints, i.e., $C(\mathbf{y}_{i+1}) \geq C_{min} \cdot n_x$. If this constraint is fulfilled, the DeNodeB formation is valid. Hence, the algorithm pursuits a twofold optimization goal:

- (i) maximizing the total coverage for the selected DeNodeB set, and
- (ii) minimizing of the number of DeNodeBs to obtain an optimal DeNodeB deployment, regarding the network cost.

Therefore, the general idea for the metaheuristic algorithm is denoted as follows

$$\max_{\mathbf{y} \in \{0,1\}^{n_r \times 1}} C(\mathbf{y}). \quad (3.8)$$

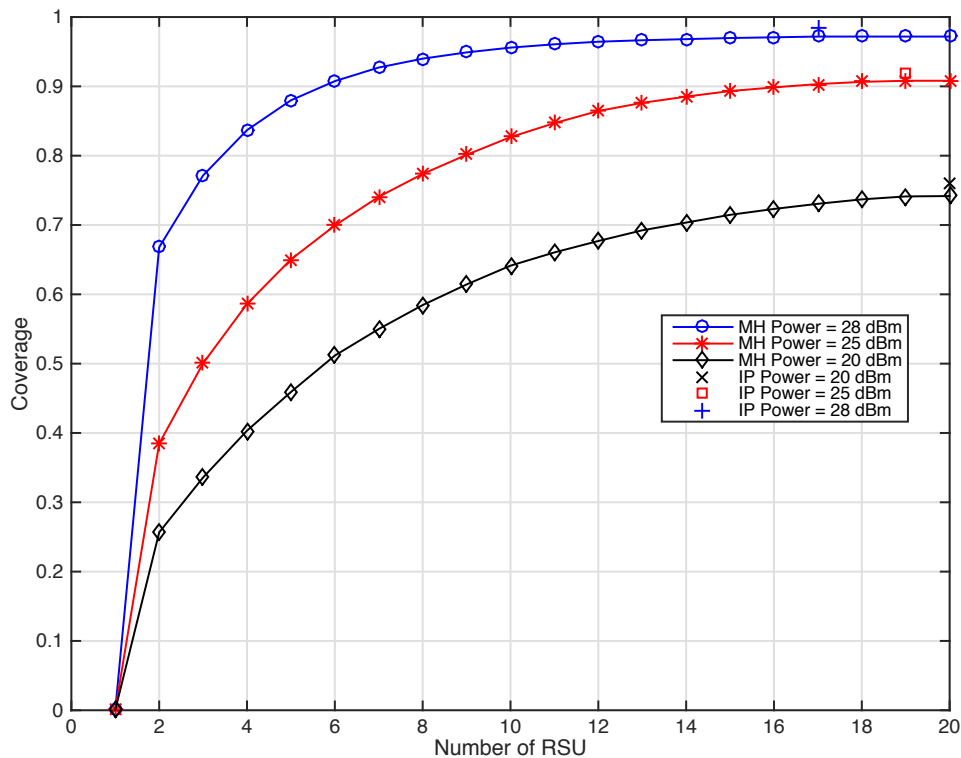


Figure 3.2: Comparison of the results from metaheuristic algorithm and linear integer optimization with three different transmitted powers.

A comparison between both optimization approaches is shown in Figure 3.2. It shows the increment of total coverage as a function of the number of allocated DeNodeBs. The curves obtained using the metaheuristic algorithm have an upper bound given by the environment, i.e., the maximum coverage due to the particular geography of the scenario. However, using the integer program formulation approach, we obtain the optimal point regarding coverage and number of DeNodeBs. It is interesting to remark that the contribution to the network by each DeNodeB, i.e., the unique road points reached by the DeNodeB, decreases when the number of DeNodeBs increases. This is consistent with our approach since we do not take into consideration the overlapping points for our algorithm, and the higher the number of chosen DeNodeBs is, the higher the probability of overlapping.

3.3 Dynamic Environment Optimization

3.3.1 Density-based road-side unit placement

Once the macro-cells are properly placed using Algorithm 1 from the previous section, the next step is to place the RSU in order to create the small cells. The RSUs are fixed infrastructures placed close to or along the road to provide the required connectivity to the vehicular adhoc networks [59]. Since the RSUs are fixed structures, the transmitted power is much higher than mobile stations, enabling a larger coverage area. Hence, the RSU deployment can be used to create networks based on vehicle-to-infrastructure (V2I) communication, which has been proven to be feasible for non-interactive applications. One of the main applications involving V2I networks is the safety-oriented applications for the vehicles in the network. Thus, an optimal deployment of RSUs increases the safety level on the roads.

Several different approaches for the deployment of the RSUs have been proposed, such as the one found in [54], where the deployment is based on placing RSUs in inverse proportion to the expected density of the vehicles, in order to minimize the notification messages. Using a graph representation developed in [60], a scheme for placing RSUs using Markov chains is created to model the traces of the vehicles. These two different approaches study the dynamic nature of the vehicular networks; however, they do not take into consideration the surrounding environment. Furthermore, the deployment strategy created in [61] aims to maximize the coverage by placing the RSUs in road intersections. A different optimization goal is obtained in [55], where a power-saving model is implemented to reduce the power consumption of active RSUs under a connectivity constraint. The power distribution for each RSU is based on the road-traffic distribution, but it also does not take into consideration the environment scenario as in the previously reviewed studies [54, 60].

In our proposed model, each RSU is connected only to one DeNodeB. In order to achieve a realistic model, the potential positions of the RSUs are located on top of buildings and traffic lights. This assumption reduces the number of possible RSU locations decreasing the complexity of the iterative algorithm. Different researchers using realistic RSU models show coverage area up to 1000 m [62]. However, in this study, the maximum coverage of each RSU is set up to $R_{RSU} = 100$ m, in order to obtain a higher reliability. By applying this coverage area reduction, it is guaranteed to fulfill the network requirements in terms of communication delay. An optimal RSU deployment scheme greatly improves

the overall performance and coverage [63] of the vehicular network, since disconnected vehicular communications show delays up to 100 seconds, as shown in [64]. The proposed density-based algorithm for the RSU deployment, using the knowledge from the scenario, is given in Algorithm 2.

Algorithm 2 Density-based RSU deployment

Input: Traffic density: $f(t) \in \mathbb{R}$, Map, $\mathbf{R}_{\mathcal{M}}(x, y)$;
Output: selected RSUs location: $\mathbf{R}_M(x, y)$;
 1: *Initialisation* : $\mathcal{A} = \{A_1 \cup A_2 \cup \dots \cup A_\gamma\}$;
 2: **for** $i = 1$ to γ **do**
 3: **if** ($f_{A_i}(t) \geq f_{th}$) **then**
 4: select a subset $M \subseteq \mathcal{M}$ of RSUs s.t. $|M| \propto f_{A_i}(t) \in \mathbb{Z}$;
 5: $\mathbf{d} = \|(\mathbf{m}_i(x, y), \mathbf{m}_j(x, y))\|$; $\forall m_i, m_j \in M, i \neq j$.
 6: $\mathbf{q} = \|(\mathbf{m}_i(x, y), \mathbf{c}_i(x, y))\|$;
 7: $\mathbf{r} = \min(\mathbf{q}, \mathbf{d})$;
 8: Obtain the total coverage $\mathbf{C}_{m,i} = \sum_{\alpha=1}^{|\mathbf{r}|} \pi \mathbf{r}_\alpha^2$;
 9: **end if**
 10: Obtain the vector $\mathbf{C}_i = (C_{1,i}, C_{2,i}, \dots, C_{M,i})$.
 11: **end for**
 12: **return** $\mathbf{R}_M(x, y)$ s.t. $\max \mathbf{C} = (\mathbf{C}_1, \mathbf{C}_2, \dots, \mathbf{C}_\gamma)$;

Algorithm 2 selects a subset $M \subseteq \mathcal{M}$ of RSU locations from the total number of RSUs locations \mathcal{M} defined as $\mathbf{R}_{\mathcal{M}}(x, y)$. The number of RSUs in the subset M is proportional to the density of traffic in the given area $f_{A_i}(t) \in \mathbb{Z}$. A related point to consider is that the observed area \mathcal{A} is divided in a discrete set of non-overlapping circular areas $\mathcal{A} = \{A_1 \cup A_2 \cup \dots \cup A_\gamma\} = \bigcup_{i=1}^{\gamma} A_i$ with the same radius following the theory of circle packing [65], which has been already tested in one of our related works for unmanned autonomous vehicle (UAV) deployment [66].

The next step is to check whether the traffic density $f_{A_i}(t)$ is higher than a given threshold for that particular area, f_{th} , in order to place a fixed RSU in that area. The constraint is calculated using the maximum physical capacity of the road as

$$f_{th} = \frac{A}{v_{length}} \cdot \xi, \quad (3.9)$$

where $A \in \mathcal{A}$ stands for the usable area of road infrastructure and \bar{v}_{length} is the mean size of a vehicle. Moreover, the parameter ξ is used to adequate the network. In our case, the parameter ξ is set to 80% of road occupancy. In case of fulfilling the constraint f_{th} , the algorithm selects the location of the RSUs from the subset M .

Moreover, this algorithm calculates the shortest value between the distance from the RSU to the center of the coverage area \mathbf{q} and the distance \mathbf{d} between the RSUs contained in the subset $M \subseteq \mathcal{M}$. Moreover, $\mathbf{c}_i(x, y) \in \mathbb{R}^2$ is defined as the center of the coverage area A_i and $r_\alpha \in \mathbb{R}$ as the radius of the selected small cell. The final step consists of storing the coverage value of the selected RSUs in a pixel point form and select the set $\hat{\mathbf{R}}_M(x, y)$ with the highest value of points covered. An example for the deployment for $M = 3$ RSUs in a given coverage area \mathcal{A} is displayed in Figure 3.3.

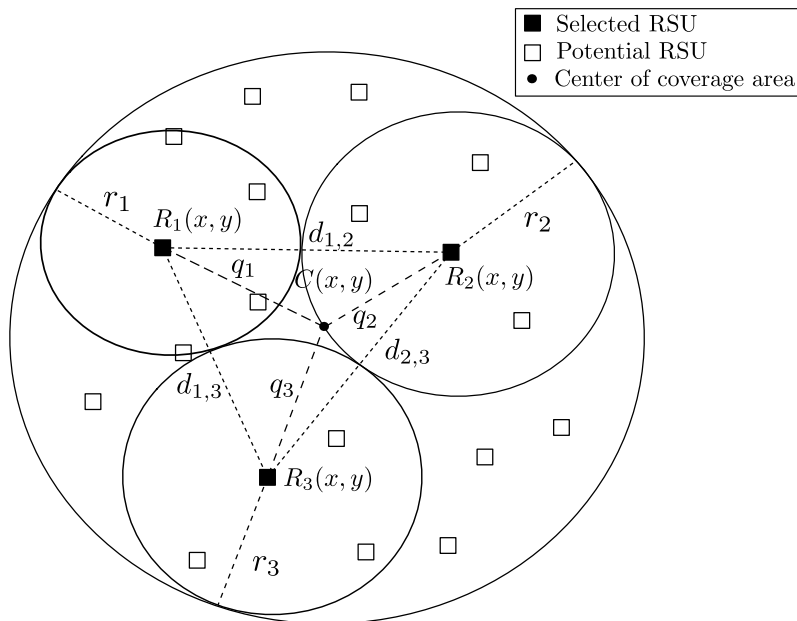


Figure 3.3: Geometry for RSU deployment.

As illustrated in Figure 3.3, the coverage area for each RSU is different, but it is still upper bounded by the maximum allowed radius $0 \leq r_\alpha \leq R_{\text{RSU}}$. It is worth mentioning that there are areas without RSU coverage in the area \mathcal{A} using the proposed algorithm. These remaining spots are covered by mobile relays (as shown in Section 3.3.5) whether it is necessary; besides they do not require a fixed infrastructure since the density is below the given threshold. Moreover, every road point in the network is covered by the macro-cells, fulfilling the ubiquitous connectivity principle.

3.3.2 Vehicles clustering using spectral clustering and K-means algorithm

In the previous sections the fixed infrastructures, namely DeNodeB and RSU, have been optimally deployed using two different approaches, i.e., obtain the total coverage of the network and an optimal placement based on the expected density of vehicles. However, the main obstacle faced while creating a low-delay and reliable network is the fragmentation and fast variation of the vehicle formation. Moreover, due to the surrounding environment, i.e., buildings and elements from the urban architecture, it is difficult to obtain a fully connected network, deriving in disconnected vehicles which are isolated from the rest of the system. Nevertheless, a common way to overcome these problems is to group the users of the network into clusters. The main goal of the clustering techniques is to reduce the number of individual entities in the system helping to improve the network management due to the smaller number of individuals.

The issue of clustering is a well-researched area and has been approached in different ways in the vehicular literature; nevertheless, most of the approaches have the common goal of obtaining the most stable cluster. The stability of a cluster is of main importance since the less number of reconfigurations, the higher stability, and less congestion is provided to the network. In the work of Kuklinski and Wolny [67], the clustering scheme is developed from a density point of view, considering the network in a graph-form and using the density

of vehicles in the connections of the graph as a metric. Most of the algorithms attempt to reduce the number of reconfigurations of the head-cluster which leads to increasing the stability of the cluster. In the related research of Mohammed and Michele [68] a technique to select the node which is most likely to last longer as the head-cluster based on the structure of the road is used. This approach uses the precise knowledge of the road lanes, while the nodes broadcast their location and obtain the optimal head-cluster. Additionally, in [69], a beacon-based clustering algorithm was developed. This algorithm uses the general scheme implemented by IEEE 802.11p, broadcasting every message to all the elements in the cluster. Thereafter, the cluster is re-organized using the information contained in the beacons. Nonetheless, broadcasting periodic messages to all the users in the cluster leads to a highly congested network which impacts the reliability and latency of the communications.

Our heterogeneous multi-tier network scheme presents an architecture which has not been extensively studied so far, since the majority of studies [70–73] use the IEEE 802.11p architecture without additional infrastructure, i.e., a Vehicular Ad-hoc Network (VANET). These studies use a node as a head-cluster where all the information is gathered by the short links and use the LTE technology to provide the long-range communications. Moreover, in [71] the selection of the head-cluster is solely based on geographical properties, i.e., the proximity to the rest of vehicles, which in most of the cases is not the optimal choice for the head-cluster in terms of stability. A delay efficient network is introduced in [72], where the long-range links are based on LTE and the short-range ones between the vehicles are implemented using IEEE 802.11p. The method for clustering the different network nodes in the present study is similar to the one introduced in [71], where the vehicles with the strongest path, i.e., the maximum signal strength between vehicle and infrastructure, are selected as head-cluster to disseminate the intra-cluster messages, acting as a mobile relay node. Additionally, a multi-hop scheme is described in [73] obtaining high connectivity between the network elements but at the same time using a large part of the network bandwidth for the message dissemination. The main difference between those studies and our heterogeneous multi-tier network is that we do not store all the information sent by the nodes in a single node, instead of in the RSUs and DeNodeBs, which provides a higher smartness and cooperation to the network. The smart infrastructures are able to predict the dynamic profile of the clustered elements and provide the optimal head-cluster selection.

In our approach, we make use of the extended knowledge about the scenario, and the centralized architecture to obtain an enhanced clustering algorithm. Moreover, the information from the head-cluster is sent only to the RSUs or DeNodeBs, decreasing the network load. In order to select an optimal head-cluster, we use a similarity parameter as a metric, selecting the one vehicle that provides a better overall performance. The set of vehicles $V^m \in \mathcal{V}$ that are assigned to the same RSU and $m \in M$ are clustered using a sub-spacial spectral clustering [74, 75].

Spectral clustering

The main advantages of using spectral clustering are its simplicity to be implemented, and that the algorithm can be solved by applying standard linear algebra. Moreover, it outperforms the typical clustering techniques because it does not make strong assumptions on the form of the clusters, i.e., it works well for non-defined data shapes. Additionally,

spectral clustering can handle efficiently large data sets, as it is expected from vehicular networks, as long as the similarity matrix is sparse. Therefore, it is important to properly choose the similarity graph in order to avoid getting a local minimum or restarting the algorithm with different initial values for the linear problem.

Let denote a set of data points $\mathcal{X} = \{x_1, \dots, x_r\}$ and a similarity metric as $S_{ij} \geq 0$ for each pair of points x_i and $x_j \in \mathcal{X}$. Since the only available information for clustering is the data points and the similarity metric, the data is represented using a similarity graph as $\mathcal{G} = (\mathbf{W}, \mathbf{E})$, where every vertex $w_i \in \mathbf{W}$ represents a data point x_i and \mathbf{E} is the affinity matrix. Hence, the points (x_i, x_j) are connected by means of the similarity graph if $S_{i,j} \geq S_{th}$, where S_{th} is a given threshold. The spectral clustering algorithm is stated in Algorithm 3.

Algorithm 3 Spectral Clustering Algorithm

Input: Similarity matrix $\mathbf{S} \in \mathbb{R}^{r \times r}$, selected number of clusters \hat{k} .

Output: Selected clusters $\mathbf{y} = (y_1, y_2, \dots, y_{\hat{k}})$.

1: *Initialisation* : Construct the proper similarity graph and compute the value:

$$\mathbf{W} = \sum_{i,j=1}^r w_{ij} \text{ which states all the connections between } i \text{ and } j.$$

2: Compute the Laplacian matrix \mathbf{L} .

3: Obtain the first \hat{k} eigenvector $(e_1, e_2, \dots, e_{\hat{k}})$ from the Laplacian matrix \mathbf{L} .

4: Construct an affinity matrix $\mathbf{E} \in \mathbb{R}^{r \times \hat{k}}$ arranging the obtained eigenvector $(e_1, e_2, \dots, e_{\hat{k}})^T$ column-wise.

5: Cluster the rows of \mathbf{E} using the K-means algorithm into the clusters $\mathbf{y} = (y_1, y_2, \dots, y_{\hat{k}})$.

The similarity graph is denoted as fully connected graph. In this graph every point is connected to the remaining ones by means of the similarity metric, i.e., vertex with $S_{ij} \geq 0$. This graph represents the local relationships of the data points, and therefore, it is required to construct a meaningful similarity function which reflects the data points behavior. In our case, the behavior of the data is given by the dynamic behavior of the vehicles. Since we attempt to cluster the data points in terms of a higher dimensional data, i.e., position, direction, and speed, in our approach a subspace transformation needs to be performed.

It is important to point out that since the dataset that is compared for the similarity metric are related to different subspaces, the sense of distance becomes meaningless. Therefore, the dataset will be transformed using the analogy of an intensity matrix as follows:

$$v_i(t) \in \mathbb{R} \longrightarrow \tilde{v}_i(t) \in [0, 1], \quad (3.10)$$

$$\mathbf{p}_i(t) \in \mathbb{R}^2 \longrightarrow \tilde{\mathbf{p}}_i(t) \in [0, 1], \quad (3.11)$$

$$h_i(t) \in \mathbb{R} \longrightarrow \tilde{h}_i(t) \in [0, 1]. \quad (3.12)$$

This is considered as a feature scaling that involves dividing the input values by the range of the input variable $R \in \mathbb{R}$ resulting in a new value which is upper bounded by 1. This transformation is used to speed up the process of clustering the data. In a general form, the transformation is as follows

$$\tilde{v}_i(t) = \frac{v_i(t) - \mu_{v_i(t)}}{R_{v_i(t)}}. \quad (3.13)$$

After this transformation, all the values in the dataset are comparable, and hence, the similarity graph and the metric associated to it is meaningful. However, the different parameters $\tilde{v}_i(t)$, $\tilde{p}_i(t)$ and $\tilde{h}_i(t)$ do not have the same weight in our similarity clustering. Therefore, we denote the similarity parameter for a data point $x_i \in \mathcal{X}$ as follows:

$$\tilde{s}_i = \alpha \cdot \tilde{p}_i(t) + \beta \cdot \tilde{h}_i(t) + \gamma \cdot \tilde{v}_i(t), \quad (3.14)$$

where $\alpha \geq \beta \geq \gamma \in \{0, 1\}$. In our case, the most important parameter is the position of the vehicle, meaning that points with the same behavior in speed and heading but at far away locations will not be clustered together. Moreover, the heading is predominant over the speed since vehicles with a similar position and heading are most likely to drive to the same locations.

This clustering method uses a metric based on the connection of all the nodes with a positive similarity using a full-connected graph form. For this method, we apply the Gaussian similarity function to estimate the affinity matrix \mathbf{S}

$$S_{i,j}(x_i, x_j) = \exp\left(-\frac{\|\tilde{s}_i - \tilde{s}_j\|^2}{2\sigma^2}\right) \quad \forall i \neq j \text{ and } S_{i,i} = 0, \quad (3.15)$$

where the parameter σ controls the similarity threshold between the neighbor nodes, and \hat{s}_i, \hat{s}_j are the similarity parameter of the data points x_i and x_j forming the cluster, respectively. The spectral clustering works well for different dataset structures even when it does not have a convex form. The second required input parameter for the algorithm is the number of clusters. Usually, selecting the number of clusters is the most complicated step for all clustering techniques. In our case, we decide to use the gap statistic defined in [76] which uses the output of the clustering algorithm and calculates the dispersion under a given number of clusters.

The gap statistic method is iterative and obtains the optimal number of clusters from a given range of $\mathcal{Q} = \{1, 2, \dots, Q\}$. Hence, using this statistic is possible to obtain the number of clusters which groups more efficiently the data, obtaining a higher amount of information. An example of the use of the gap statistic is given as follows

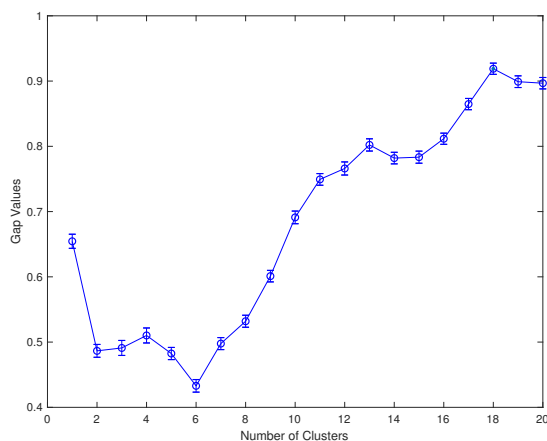


Figure 3.4: Gap statistic for dataset 1.

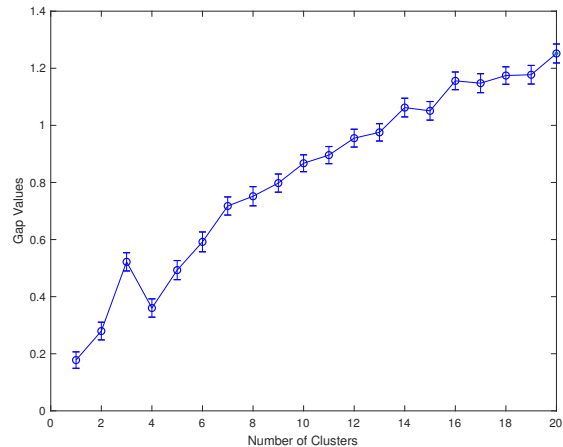


Figure 3.5: Gap statistic for dataset 2.

As shown in Figure 3.4 and Figure 3.5, the obtained amount of information generally grows accordingly to the number of clusters. However, increasing the number of clusters as much

as possible is not always the best approach due to the higher computational complexity for managing the network. Moreover, in the case of Figure 3.4, the highest amount of information is obtained when the number of clusters is not the maximum. Therefore, we need to find a trade-off between the amount of information and number of cluster.

The second step of the spectral clustering algorithm states to compute the Laplacian matrix \mathbf{L} . Hence, we define the matrix \mathbf{L} as:

$$\mathbf{L} = \mathbf{D} - \mathbf{W}, \quad (3.16)$$

where $\mathbf{D} \in \mathbb{R}^{r \times r}$ is defined as a diagonal matrix with diagonal entries d_1, \dots, d_r . These d_i values are calculated as

$$d_i = \sum_{j=1}^r w_{ij} \text{ for a vertex } w_i. \quad (3.17)$$

Therefore, $d_i \neq 0$ for all the vertices adjacent to w_i . Using the top eigenvectors from the affinity matrix \mathbf{E} , the spectral clustering algorithm obtains great results in reducing the amount of computational time due to its simple structure. As an example of the algorithm output, we use the data obtained from clustering applying the k-means algorithm [77].

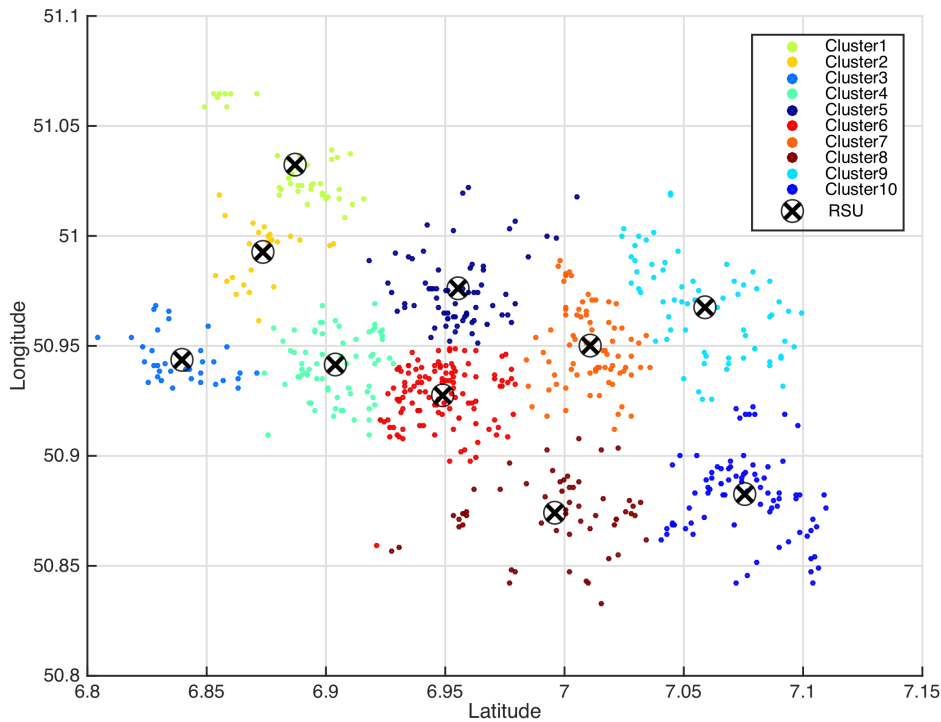


Figure 3.6: K-means clustering algorithm.

As shown in Figure 3.6, the values are grouped around the RSUs, which have been defined as the centroids of the k-means algorithm. In this case, we use the spectral clustering algorithm for one of the clusters.

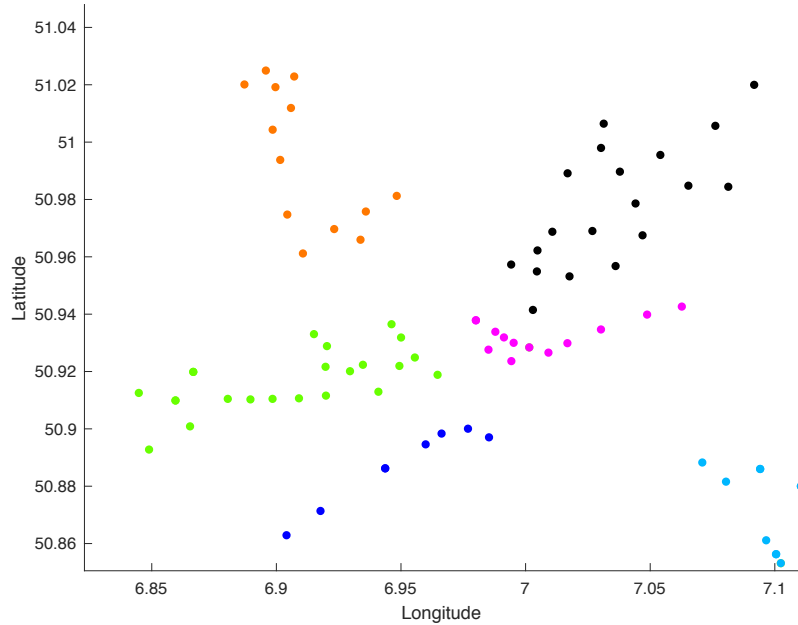


Figure 3.7: Spectral clustering of one cluster obtained using K-means.

Figure 3.7 depicts the cluster obtained using K-means, which is further divided into smaller cluster depending not only on the position but also including the other two dimensions, i.e., heading and speed. The simulation shows the great performance of spectral clustering when the data does not have a standard form and it is able to group the points successfully.

In order to verify the suitability of our approach, it has to be compared with other typical clustering schemes. First, we analyze the different common methods to cluster ad-hoc networks in the domain of MANETs and VANETs.

1. **Lowest-ID** consists of selecting as head-cluster the node with the lowest ID in range as developed in [78]. The IDs are distributed to each node once it enters the network and they do not change. This clustering scheme works well in networks with a low dynamic profile due to the low number of reconfigurations.
2. **Highest Degree** is based on the connectivity among the nodes [79]. The algorithm creates a graph scheme to select the head-cluster using the broadcast messages among the nodes and selects the node with the highest degree of connectivity.
3. **Utility Function** [80] uses a similar clustering approach as the method introduced in the present work. It takes the head-cluster which is closer in distance and speed to the rest of nodes in range and selects it as head-cluster. However, it does not use the information from other clusters, through infrastructure connectivity, to optimize the selection.

The comparison of our approach with the ones proposed in the literature is done by means of two main parameters, i.e., number of beacons and head-cluster stability.

Number of beacons

This parameter is of special importance due to the high number of nodes that can simultaneously be in a cluster [81]. The protocols IEEE 802.11p and LTE-V2X broadcast the messages to all the nodes in the same cluster, however, in our approach this is not needed since the infrastructure controls the status of all the nodes.

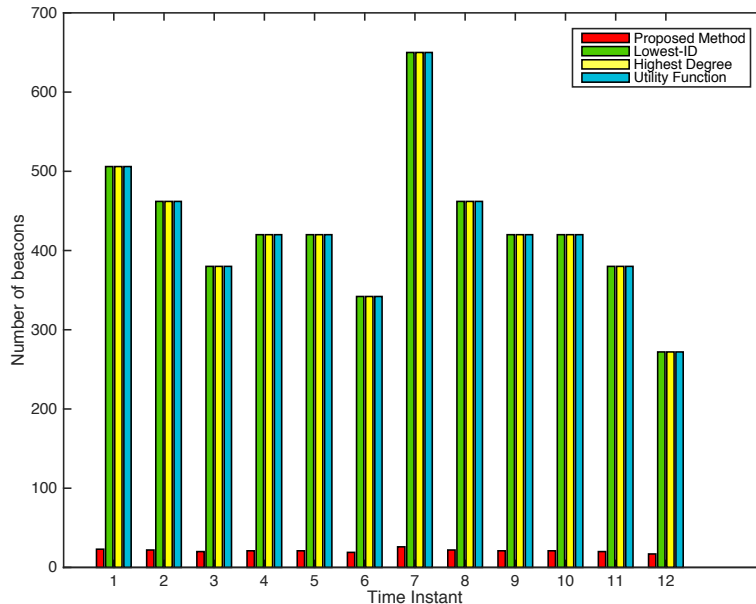


Figure 3.8: Number of beacons in a cluster.

As shown in Figure 3.8, the number of beacons in the three common clustering techniques, Lowest-ID, Highest Degree and Utility Function is identical, being this value $l(l-1)$ where $l \in \mathbb{Z}$ is the number of nodes in the cluster. In our proposed model, the number of beacons is greatly reduced in comparison with the rest of schemes, providing a less congested network. Nonetheless, the main drawback of this approach is the requirement of installing an infrastructure which can be costly in terms of an economic and logistic point of view.

3.3.3 Head-cluster selection

Once the nodes are clustered using the scheme described in Section 3.3.2, the next step is to choose the head-cluster with the expected highest lifetime, i.e., longest time as a member of the cluster. In this section, a scheme to select the head-cluster based on coalitional game theory is developed. The main goal of a coalitional game is to obtain the maximum payoff from the collaboration of all the nodes in a coalition. A coalition inside a cluster can be defined as $R \subseteq N$, where $N = \{n_1, \dots, n_l\}$ is the set of all nodes in the cluster. In coalitional games, the maximum output is always given by the payoff function obtained by the collaboration of all nodes, creating a grand coalition. In the present approach, the coalition R is formed by all the nodes forming a cluster, connected to the same infrastructure, obtained using the spectral clustering method. Since all the nodes

forming the cluster have similar properties as mentioned in Section 3.3.2, it is reasonable to assume that the nodes will have a common goal that can be maximized, obtaining an optimal solution for all the nodes. The proposed coalitional game assumes that the infrastructure is myopic, i.e., the head cluster is selected considering the actual status of the cluster, not future or past events. Moreover, every node n_i in the cluster does not know about the opponent's payoff function, they only have an estimation of about its opponent way of playing. We assume that all the players have an honest behavior, i.e., they will not try to rig the game making it unfair. It could be the case that an adversary tries to play not using fair rules, nevertheless, there are methods to avoid this misbehavior which will be analyzed in Section 5.4.

In each round of the algorithm, the infrastructure extracts the information sent in the CAMs, $m_i(t)$, by the nodes and selects the node which minimizes the payoff function. The payoff function is based on the similarity concept used to create the cluster and aims to obtain the head-cluster which best describes the entire cluster. Therefore, the payoff function $f_{i,j}(t) \in \mathbb{R}$ for a time instant t over all nodes (n_i, n_j) in a cluster is as follows:

$$f_{i,j}(t) = d(p_{i,j}(t)) + d(v_{i,j}(t)) + d(h_{i,j}(t)), \quad (3.18)$$

where $d(\cdot)$ is defined as the Euclidean distance between the pair of points. The idea is to obtain the node n_i which more likely defines the cluster. The goal is to obtain the minimal value for the payoff function in each time instant as

$$\min_{i,j} f_{i,j}(t) \quad \forall t \in \{t_0, t_1, \dots, t_f\}, \quad (3.19)$$

where t denotes the simulation time. In order to avoid costly recalculations, the period t is an interval that goes from t_0 until t_f with a sample rate of typically $\Delta t = 5$ seconds, thus $\Delta t = t_1 - t_0$. Using the values of one time period and not the instantaneous values, we ensure that the dynamic behavior is the correct one, and not an spurious value. Once the head-cluster which minimizes the payoff function is selected, it can be defined as:

$$n_{hc} := (\hat{\mathbf{p}}(t), \hat{v}(t), \hat{h}(t)) \quad (3.20)$$

where the row vector formed by $(\hat{\mathbf{p}}(t), \hat{v}(t), \hat{h}(t))$ defines the dynamic parameters of the selected head-cluster vehicle, which also best-defines the entire cluster. The entire idea of clustering the vehicles using the similarity metric, and to choose as head-cluster the vehicle with the optimal payoff function is a similar concept as platooning. Platooning has been defined as the optimal vehicle formation due to minimal inter-vehicular distance and the increased safety. A more detailed analysis of the platooning concept and its benefits using the idea of connected vehicles is given in Section 5.2.

The proposed multi-tier network uses the cooperation between the RSUs and DeNodeBs to share information, and predict the dynamics of the vehicles in the future time instants. As we stated at the beginning of this section, obtaining the dynamic prediction of every individual vehicle in real-time is infeasible, and therefore, a clustering scheme is proposed. Thus, it is interesting to verify how accurate is the position prediction, not of every individual vehicle, but of the head-cluster vehicle, which is the best indicator of the general cluster behavior, using the values obtained in equation (3.20). In order to obtain an insight

into the prediction accuracy, the predicted value has been compared with the real traffic data for one minute divided into periods of 5 seconds.

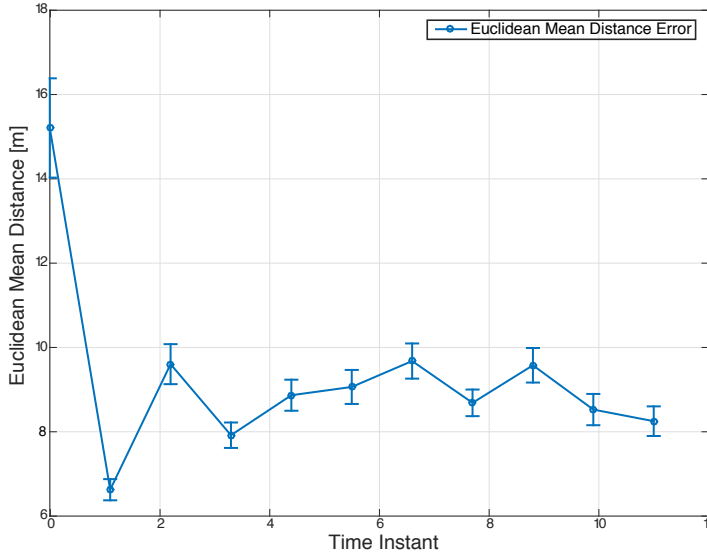


Figure 3.9: Head-cluster dynamics prediction.

As shown in Figure 3.9, the mean error distance between the predicted head-cluster and the value obtained from real traffic data is around 9 meters. The initial step in the simulation is the one with the biggest error which is consistent with our consensus-based approach, where the vehicles share their information status. Nevertheless, the error after this point is stabilized at around 8 to 10 meters. In view of the results obtained from predicting the head-clusters, it can be concluded that the idea of sharing information between the infrastructures works accurately.

3.3.4 Cluster dynamics prediction

In the case of considering only the head-clusters of the network, it is possible to define the traffic as macroscopic, i.e., instead of individual cars which make the simulation infeasible, selecting the head-clusters to obtain the general profile of the traffic. The goal of using a macroscopic traffic simulation is twofold. On the one hand, it is too complex to simulate and predict the dynamics of each individual car. On the other hand, the bandwidth usage is reduced by grouping the nodes and choosing a head-cluster. In road networks, assuming only one direction, vehicles can be modeled as a fluid which helps to anticipate traffic phenomena and predict the interaction between the network elements [82, 83]. We can define the position of each vehicle as $\mathbf{p}_i(t)$, and its velocity as $\mathbf{v}_i(t) = \frac{d\mathbf{p}_i(t)}{dt}$ along with the acceleration as $\mathbf{a}_i(t) = \frac{d\mathbf{v}_i(t)}{dt} = \frac{d^2\mathbf{p}_i(t)}{dt^2}$. However, these are not the only parameters we are interested in. Let us assume that every vehicle is moving in a one-lane road, such as a highway. The principal parameters in traffic flow models are velocity, traffic density, and flow. The traffic flow parameter $q(\mathbf{p}, t) \in \mathbb{R}$ is addressed by the following equation

$$q(\mathbf{p}, \Delta t) = \rho(\mathbf{p}, \Delta t) \cdot v(\mathbf{p}, \Delta t), \quad (3.21)$$

which is related to the conservation in the number of cars, and the relationship between the car velocity and traffic density. In equation (3.21) the density $\rho(\mathbf{p}, \Delta t) \in \mathbb{R}$ is the number of cars during an interval Δt passing through the position \mathbf{p} . Moreover, $v(\mathbf{p}, \Delta t) \in \mathbb{R}$ is the mean velocity of the vehicles driving by that point. The principal goal of this method is to obtain an accurate prediction of the geographical properties of the vehicles. Generally, the speed of each car $\mathbf{v}_i(t)$ is obtained and recorded. However, in our approach it is denominated as $\tilde{\mathbf{v}}(\mathbf{p}, t)$ which is associated to the entire cluster, being \mathbf{p} the position in space covered by the head-cluster extracted from equation (3.20). Additionally, the same concept is used for the rest of properties, i.e., the direction and position.

Using the cooperative scheme due to the interconnected infrastructures, the head-cluster selection can be modified using the dynamics prediction. Applying the knowledge of the head-cluster from different RSUs, it is possible to predict the next position of the cluster, and hence, choose a head-cluster which may not be the optimal for the time instant t , but will create a more stable cluster in future time instants. In order to show the estimation accuracy of the prediction scheme, the simulation results for different update periods Δt are displayed in Figure 3.10.

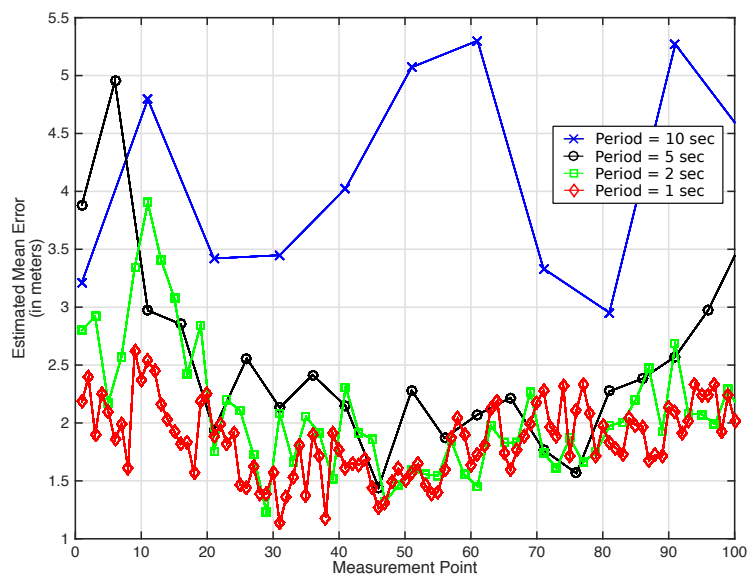


Figure 3.10: Estimated prediction accuracy for each update period Δt .

The results present the estimated mean error for all the vehicles under the coverage of a single infrastructure. The overall accuracy fluctuates in the range of 1 up to 5 meters in the worst case of an update time period of $\Delta t = 10$ seconds. It can be observed in Figure 3.10 that the schemes with a shorter update period, $\Delta t = \{1, 2, 5\}$, have a similar behavior with an estimated error of 2 meters. However, in the case of $\Delta t = 10$ seconds, the behavior is visibly worse due to the higher deviation in the predicted values. This higher error is a consequence of a longer update time used to adapt the prediction, which can not update itself as fast as the movement of the vehicles. The results are shown in Table 3.4, which displays that the predictive scheme works arguably well under the assumption of acquiring all the required information.

Table 3.4: Estimated mean values for each update period.

Parameter	Value [m]
$\hat{\tau}_{10}$	4.1232
$\hat{\tau}_5$	2.5157
$\hat{\tau}_2$	2.0872
$\hat{\tau}_1$	1.8530

Moreover, it can be observed that having an update time period of $\Delta t = 5$ seconds does not degrade the prediction results, and it positively contributes to reducing the load between vehicles and infrastructure, especially in highly dense scenarios. Our approach adds more complexity to the network, in comparison with the standard LTE-V2X scheme, due to the clustering and prediction schemes. However, having the division of the radio spectrum in several sub-pools, i.e., for the different clusters, our approach is more suitable for fast changing scenarios as discussed in the succeeding Section. 5.3.1 using an optimal SPS scheme.

Head-cluster stability

The main parameter used to test the precision and adaptability of our clustering scheme, and particularly, the head-cluster selection, is the stability of the latter. On the one hand, the best case scenario for this parameter is to have an adaptive head-cluster selection, i.e., the selection changes depending on the cluster parameters. On the other hand, having a continuous adjustment of the head-cluster leads to frequent reconfigurations in the cluster, and therefore, an excess of signaling. The results obtained from the head-cluster stability are analyzed using 12 time intervals of 5 seconds of duration as follows

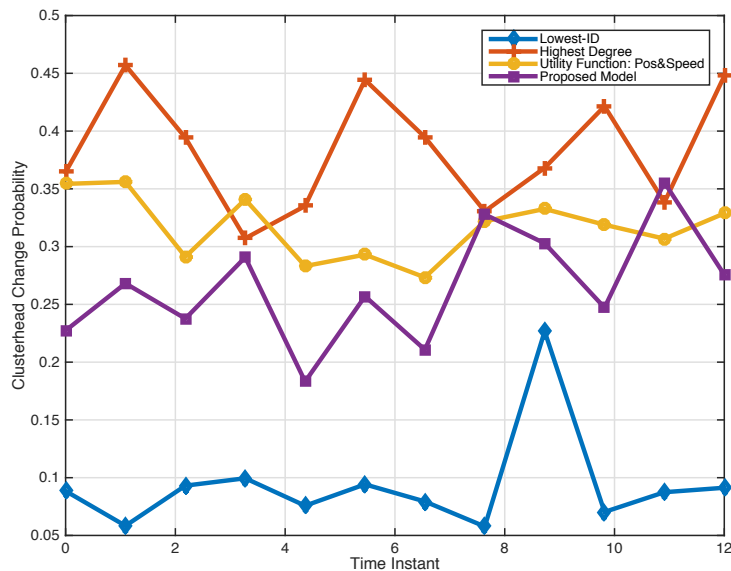


Figure 3.11: Cluster lifetime comparison.

As shown in Figure 3.11, the best approach regarding the number of reconfigurations is Lowest-ID. However, having an extremely low head-cluster variation is a drawback in VANETs, since it will not provide an optimal selection for the rapid changes in the network. Highest-Degree performs worse in this aspect, having a really volatile head-cluster. This frequent change produces a high number of exchanged messages in the network, and as it was mentioned in the previous section, the number of beacons to select a head-cluster is remarkably high, which potentially congests the network. The last clustering scheme studied is the Utility Function using the average speed and position of the cluster. It works fairly well obtaining a balance between the longevity of the cluster and the adaptation to the cluster changes. Analyzing our proposed model in this section, we can observe a better performance than the Utility Function, due to the expected prediction of the head-cluster based on the dynamics. Moreover, the proposed model adapts itself accurately to the dynamic nature of VANETs, while providing an adequate head-cluster lifetime.

3.3.5 Mobile relay nodes

Up to this point, we have proposed deployment schemes for fixed infrastructures at high density areas, in order to obtain ubiquitous connectivity. However, one question remains unanswered, what to do with the remaining areas? In this work, we propose not to install further costly infrastructures, but to use the capability of the vehicles to work as relay nodes, defined as mobile relay nodes (MRN). The idea of using vehicles in the network as relays is not new, and it has been tested successfully using parked cars as RSUs [84]. Nonetheless, in our specific case, it is possible to use the vehicles as MRNs due to the small separation between the vehicles belonging to the same platoon. The main advantages of using MRNs are the following:

- The radio channel does not change abruptly from vehicle to vehicle since the MRN and the rest of vehicles move along together.
- The signaling overhead is decreased due to the group handover scheme (GHO) explained in next Section 3.3.6.
- Generally, the distance between relay and users is smaller than the distance between users and macro-cell [85].

Moreover, in our proposed network, the energy efficiency can be enhanced depending on the network demand, where the RSUs might remain idle. The implementation of MRNs in the network has a twofold aim: i) there is no need to deploy costly infrastructure in low density areas, and ii) the flexibility of the network is enhanced by having a self-organizing architecture. For the MRN selection, we assume that the vehicles are forming clusters or platoons. A flowchart for the MRN selection scheme is given in Figure 3.12.

The system initialization uses the map and the system information, denoted by dashed lines in Figure 3.12, including the position of the deployed infrastructures. Then, the role of the DeNodeB is to identify the areas without coverage of any RSU and check if there is any platoon in these areas exploiting the cloud-based architecture. Once the platoon has been located and is out of coverage of any RSU, the infrastructure will create an MRN. The first step is to choose the member of the platoon which will play the role of the MRN. The best possible option is to choose a bus or a truck due to their higher altitude, and hence, increased probability of being in a LoS situation with the rest of platoon members.

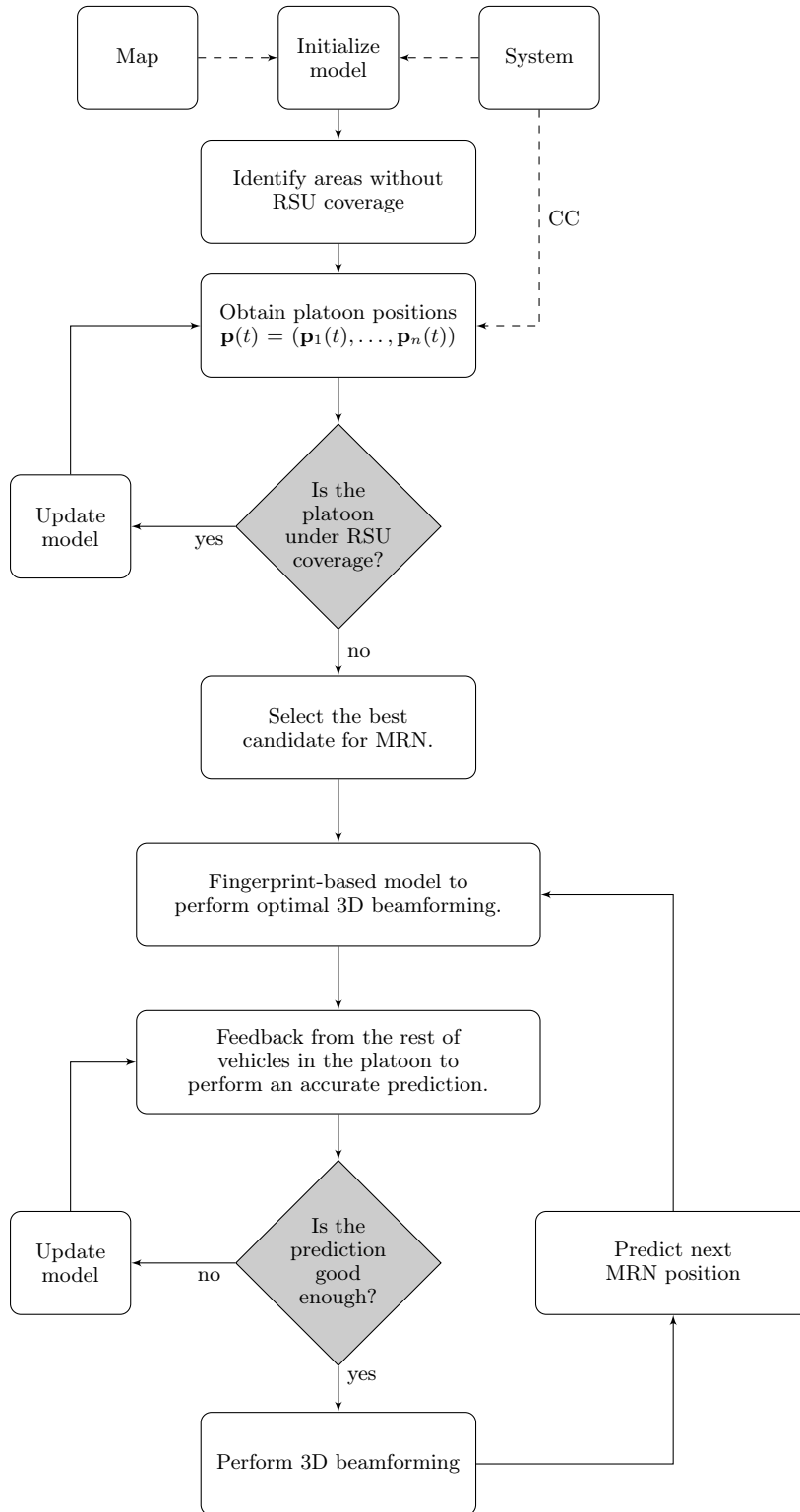


Figure 3.12: Flowchart for the MRN selection.

Following the model used in [8], all the vehicles communicate their status to the rest of vehicles in the platoon, using a V2V scheme. Additionally, all the vehicles are connected to the DeNodeB and transmit their CAMs to the centralized architecture. The platoon

leader is connected to every vehicle being part of the platoon. Since all of the vehicles in the small cell travel at the same speed and direction, the relative mobility is negligible as it is inside the bus for all the passengers [86]. Moreover, as the position of each vehicle is known at every time by the DeNodeB, it is possible to obtain an accurate 3D beam-forming for the creation of the backhaul link. This procedure is explained in Section 4.3.

3.3.6 Group handover prediction

The second aspect of the self-organized network, along with the MRN selection, is the capability of performing Group Handover (GHO), implementing the feature of centralizing the control-plane by using the DeNodeB. We assume that the vehicles are organized in clusters, i.e., all vehicles have similar heading and speed. Hence, it is reasonable to assume that they will change coverage areas at almost the same time instant. This assumption can be considered valid due to two conditions:

- (i) the distance between vehicles is small, i.e., $\Delta d = 0.1 \cdot v_n(t)$, and
- (ii) the number of vehicles in the platoon is limited by the communication range.

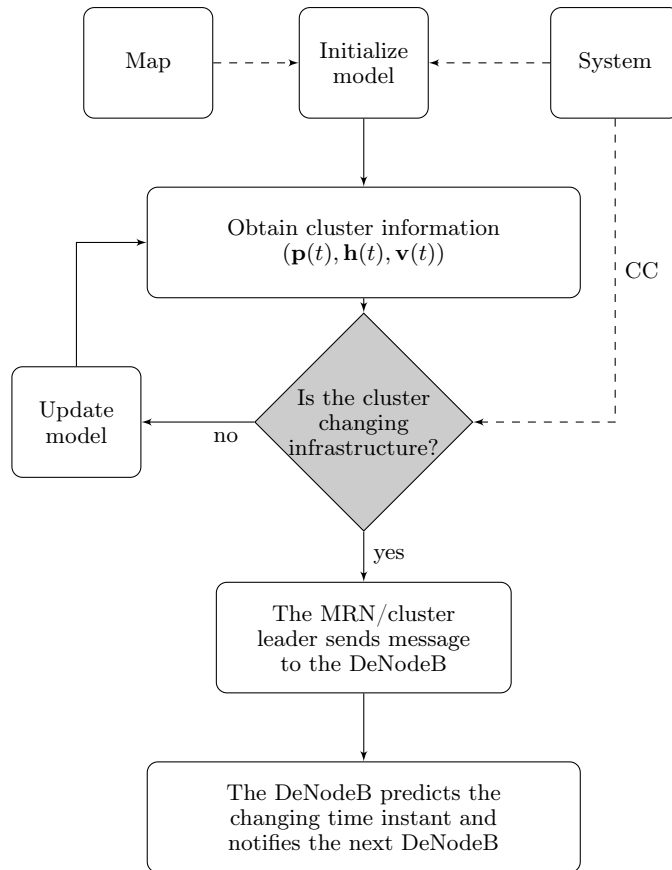


Figure 3.13: Flowchart for the group handover selection.

Hence, a cluster formation can be characterized as a train where the vehicles act as the wagons but without any physical attachment. The overall algorithm for the group handover prediction is depicted in Figure 3.13. The MRN is connected directly to the

source DeNodeB by means of a V2I communication link. A handover event is triggered once the MRN sends a specific message, i.e., the signal strength decreases as the MRN is running out of the macro-cell range. Since the DeNodeBs are interconnected, the next DeNodeB in charge of allocating the MRN (cluster) free its resources. In order to predict which DeNodeB cell will be the next one to serve the MRN and the precise time for the switching, we use the mobility parameters sent by the MRN, along with the cluster members obtaining a precise estimation of their future positions.

Once the MRN is signaled from the DeNodeB to perform the GHO, it sends messages to the new DeNodeB to synchronize with it and requests a confirmation of successful GHO from the new serving DeNodeB. The advantages of using the GHO are twofold:

- First, the signaling is greatly decreased for the handover operation since the vehicles are grouped in clusters and all the signaling is performed by the MRN.
- Second, simplifying the network management. Since the vehicles are grouped in clusters, it is needed to manage the individual clusters rather than each vehicle individually. Hence, it is possible to use the traffic flow prediction scheme introduced in Section 3.3.4.

In addition, due to the control and data channel split, the handover signaling does not interfere with the data channel, making the group handover feature a great addition to the network management. In order to create an accurate prediction scheme, the DeNodeB requires the following information:

- Updated road information, i.e., connections between the roads and traffic flow direction. Additionally, it is needed to periodically update this information to have the best prediction possible.
- Information of each vehicle and their associated cluster denoted by $\mathbf{y}_{n,i}^k(t) := (p_{n,i}^k(t), h_{n,i}^k(t), v_{n,i}^k(t))^T$.
- Communication link between the different DeNodeBs in the area. The interconnection of the DeNodeBs has a double goal: first, to obtain a higher range for prediction and second, to add redundancy to the network.

Using the information of the vehicles i and $i + 1$, where $i + 1$ corresponds to the preceding vehicle. Hence, the position and vehicle dynamics prediction are done as follows

$$p_{n,i}^k(t_1) = p_{n,i}^k(t_0) + v_{n,i}^k(t_0) \cdot \Delta t \cdot h_{n,i}^k(t_0) \quad (3.22)$$

$$v_{n,i}^k(t_1) = v_{n,i+1}^k(t_0) \quad (3.23)$$

$$h_{n,i}^k(t_1) = h_{n,i+1}^k(t_0) \quad (3.24)$$

where $\Delta t = t_1 - t_0$ is the time interval between updates. Moreover, in order to predict the position of the first vehicle in the platoon, i.e., the one with no preceding car, the updated road information is used to obtain the potential valid positions. Hence, with this information collected in the DeNodeB, it is possible to predict the cluster members and their respective DeNodeB connection.

3.4 Summary

In this chapter, a multi-tier heterogeneous network architecture based on LTE-V2X has been proposed. The network fulfills the stringent requirements for 5G communication technologies, and specifically, for vehicular networks. These requirements are achieved mainly by means of network densification, deploying small cell infrastructures. The deployment strategy is done using two different approaches: First, the macro-cells are deployed prioritizing the ubiquitous connectivity of the vehicles. Second, small cells are created using a density-based approach based on the expected density of vehicles at a given time. The last feature implemented in the proposed network architecture is to group the vehicles by means of spectral clustering using the available information. Furthermore, taking advantage of the clustering techniques, the vehicles are properly grouped, such as to enable the creation of mobile relay nodes and the application of group handover which reduces the signaling overhead.

4 | Radio Channel Modeling for Vehicular Communications

In this chapter, the most relevant features of the radio communication channel in the field of vehicular communication are investigated. Due to the particular characteristics of vehicular networks, such as dynamic environment, high mobility of vehicles, and a lower antenna height, new models and parameter characterizations need to be established in contrast to the traditional cellular systems. Throughout this chapter, different models for the diverse environments involved in vehicular communications are defined. Moreover, a 3D radio channel model to enable backhaul links between macro-cells and relays is built. To finalize the chapter, a theoretical framework is defined to study the reliability in vehicle-to-vehicle communications, where the requirements are particularly stringent.

4.1 General Features of Vehicular Radio Channel Modeling

There are plenty of existing radio channel models in the literature, which have been widely and successfully used for traditional cellular systems. However, in the case of vehicular networks, using the same characterizations and parameters do not provide accurate results as reported by Viriyasitavat et al. [87]. The discrepancies between traditional cellular systems and the ones used for vehicular communications arise mainly due to the particular characteristics of the vehicular environment. These main characteristics are:

- diverse environments for vehicular networks, such as urban, rural, tunnels, highways, overpasses, etc. Each of these environments requires a particular way of modeling the radio channel. Additionally, due to the rapid mobility of the users, the constant changes in the radio channel conditions need to be addressed.
- several scatterers affecting the communications. Due to the dynamic environment, not only the buildings and static objects need to be taken into consideration, but also different vehicles and pedestrians interfering with the channel. These scatterers affect the communication link in two main ways, i.e., blocking the direct line-of-sight between the receiver and transmitter, and introducing Doppler shift in the case of moving obstacles.
- combination of different schemes and protocols, as shown in Chapter 3 for our proposed network. Using this multi-tier network architecture as a guideline, the radio channel modeling is divided into three different layers: V2N, V2I, and V2V. Each one of these schemes has its own characteristics and constraints.

Furthermore, designing and modeling the parameters for a particular scenario does not ensure that the model will be accurate for all scenarios of the same class. Using an appropriate channel modeling is critical for precisely evaluate the communication protocols and applications before investing in a real deployment. Thus, the optimal modeling approach is to consider a particular scenario and adapt the parameters accordingly. This is the basic motivation behind our proposed semi-stochastic radio channel in Section 4.2.3 for V2N communications.

4.2 V2N Radio Channel Model

The first channel model to analyze is the one involving the connection between the infrastructure (DeNodeB) and the vehicles. This model is analogous to the traditional cellular systems due to the high altitude of the infrastructure and its static nature. Hence, in this case, we can use a combination of a deterministic and a stochastic radio channel model, obtaining a semi-stochastic channel model as defined in [88]. The main goal of this layer is to obtain a complete coverage for every vehicle under the range of the infrastructure, i.e., obtaining the highest possible coverage and reliability (ubiquitous connectivity).

4.2.1 Deterministic ray-tracing algorithm

The first component of the here proposed radio channel model is the deterministic ray-launching algorithm Parallel Implemented Ray Optical Prediction Algorithm (PIROPA) [89] developed at the Institute for Theoretical Information (TI) RWTH Aachen University. It is defined as a deterministic component since the calculated parameters for a given scenario do not change, i.e., there is no randomness involved in the parameters calculated by the algorithm. In order to execute PIROPA, there is some prerequisites and information needed:

- the geographical data of the scenario including the shape of the obstacles and building, along with their height.
- the position of the transmitter and all the possible receivers points (multiple receivers can be simulated).
- the transmitter has to be static and the parameters of only one transmitter can be calculated for each simulation.

Once the location of every element in the network is decided, the ray-launching algorithm is used to calculate the large-scale parameters for every link between the transmitter and the receiver with a minimum granularity of one meter. This algorithm can be understood as physical rays being radiated through infinitesimal small tubes, called paths, which are normal to the surface of the scatterers. Moreover, regarding the angular domain, each of the rays is launched in a spherical form, i.e., for the azimuth angle θ the rays are located in the interval $[0, 2\pi)$, and the same goes for the elevation angle φ in the interval $[0, \pi)$. By using this method every single potential path between transmitter and receiver is reached by the algorithm.

The propagation path is based on refractions and reflections considering the obstacles as vertical surfaces and neglecting other forms. Each ray can be traced back using a tree, where the surface of the impact of each obstacle is treated as a leaf node in the tree. This algorithm continues monitoring the rays until it reaches its destination, or the power of the ray is below an estimated power threshold, caused by the attenuation from the different bouncing off objects.

4.2.2 Stochastic radio channel model

The second component of the semi-stochastic channel model is the WINNER II model [90] which is defined as a Geometry-Based Stochastic Model (GBSM) that models the channel using stochastic properties. Using the WINNER II model, the radio channel parameters and the antennas at both sides of the radiolink can be treated independently. The channel parameters are stochastically generated based on statistical distributions extracted from the channel measurements [91]. The rays in WINNER II channel model are grouped into clusters which are defined as a propagation path diffused in space and delay, into the same angle domain as shown in Figure 4.1.

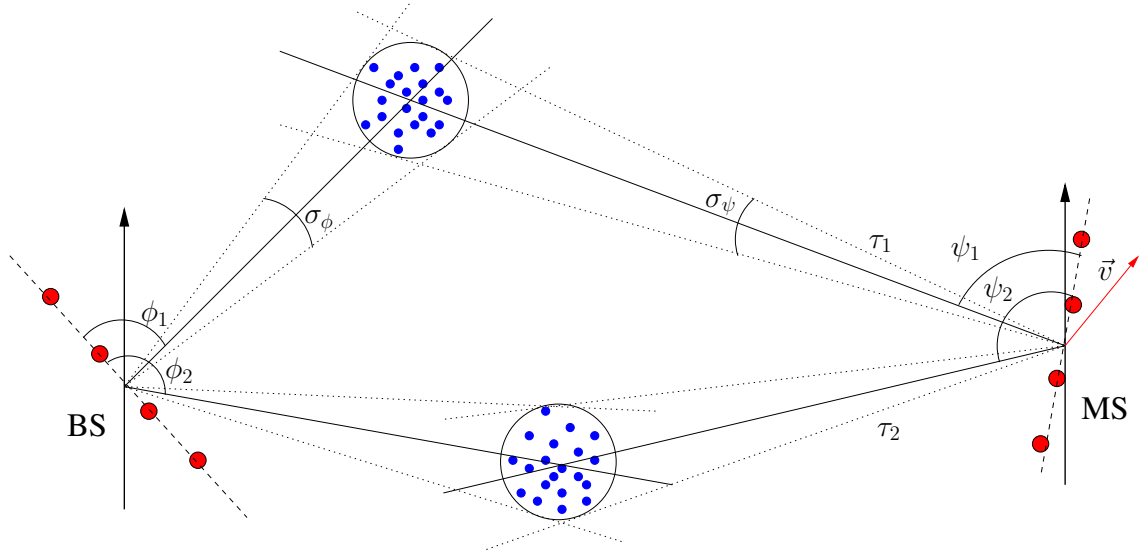


Figure 4.1: WINNER II channel model overview.

Consider a signal vector $\mathbf{x}(t) = [x_1(t), x_2(t), \dots, x_N(t)]^T$ is transmitted, then the received signal vector $\mathbf{y}(t) = [y_1(t), y_2(t), \dots, y_N(t)]^T$ can be obtained as

$$\mathbf{y}(t) = \int_{\tau} \mathbf{H}(t; \tau) \mathbf{x}(t - \tau) d\tau + \mathbf{w}(t), \quad (4.1)$$

where $\mathbf{w}(t) = [w_1(t), w_2(t), \dots, w_N(t)]^T$ is additive Gaussian white noise. In the WINNER II channel model, the MIMO transfer matrix, $\mathbf{H}(t; \tau)$, is defined as follows:

$$\mathbf{H}(t; \tau) = \sum_{n=1}^N \mathbf{H}_n(t; \tau), \quad (4.2)$$

where N is the number of clusters as defined before and τ is the time delay. If the antenna arrays at both ends of the link are included, the transfer matrix changes to introduce these values as follows

$$\mathbf{H}_n(t; \tau) = \int \int \mathbf{F}_{Rx}(\varphi) \mathbf{h}_n(t; \tau, \phi, \varphi) \mathbf{F}_{Tx}^T(\phi) d\phi d\varphi, \quad (4.3)$$

where $\mathbf{F}_{Rx}(\varphi)$ is the antenna pattern of the receiver antenna, $\mathbf{h}_n(t; \tau, \phi, \varphi)$ is the impulse response of the multipath channel and $\mathbf{F}_{Tx}^T(\phi)$ is the antenna pattern of the transmitter antenna. The generic model of WINNER II is a stochastic model with two level of randomness. The first level of randomness is formed by a large scale (LS) parameters, e. g., delay, power, and direction of arrival and departure, among others. The second level is the one formed by the small scale (SS) parameters, e. g., shadow fading and delay spread.

4.2.3 Semi-stochastic radio channel model

The combination of the deterministic and stochastic channel model constitutes the semi-stochastic channel model. This proposed radio channel model is a hybrid approach with an improved accuracy as confirmed in [1], which combines the deterministic ray-tracing algorithm, PIROPA, to obtain the large-scale parameters, and the stochastic model, WINNER II, to determine the small-scale parameters. The implementation of this radio channel is based on the assumption that the clusters, as defined in WINNER II, are equivalent to the ray paths in PIROPA. Under this assumption, the radio channel is created using the output parameters from PIROPA and importing them in order to generate the stochastic parameters for WINNER II.

Since the ray-tracing algorithm is a component of the radio channel model, the resulting radio channel model is site-specific, i.e., the obtained propagation parameters are calculated for a particular given scenario. The ray-tracing algorithm predicts the large-scale propagation parameters, such as pathloss, delay, and angular domain for a specific positioning of the transmitter and receivers in the selected environment. Afterward, using the mathematical concept of the *double directional channel* [92] to merge both approaches, the channel impulse response is calculated as

$$\mathbf{h}(\tau, \phi, \varphi) = \sum_{n=1}^N a_n e^{j\theta_n} \delta(\tau - \tau_n) \delta(\phi - \phi_n) \delta(\varphi - \varphi_n), \quad (4.4)$$

where a_n is the amplitude of the received signal for each ray, δ denotes the Dirac delta function, τ_n is the delay for each ray, θ_n is the phase of the received signal, and ϕ_n, φ_n are the angle of arrival and angle of departure, respectively. Using this radio channel model, the multi-path components of the channel are arranged in clusters, obtaining a complete profile of the channel behavior. The obtained channel impulse response from equation (4.4) is calculated based on the output from the deterministic ray-tracing algorithm, along with the random phase for each ray θ_n . Therefore, in order to add the random nature of the radio channel, i.e., the fast-fading parameters, the WINNER II channel component has to be included in the model.

In our approach, this random nature is given by the small-scale parameters, such as the phase of the rays within a cluster, the intra-fading in a cluster, cross polarization, and fast-fading phenomena associated with urban scenarios which are computed using WINNER II channel model. Table 4.1 shows a summary of the parameters used in the environment-based channel model, as well as, the method used to calculate them.

Table 4.1: Environment-based channel model parameters

Parameter	Symbol	Approach
cluster path power	P_n	PIROPA
cluster AoA, AoD	φ_n, ϕ_n	PIROPA
propagation delay	τ_n	PIROPA
number of clusters	M	PIROPA
per ray AoA, AoD	$\varphi_{n,m}, \phi_{n,m}$	WINNER II
initial phase	$\Phi_{n,m}$	WINNER II
sub clusters delay	$\tau_{n,m}$	WINNER II
cross polarization	$r_{tx,s}, r_{rx,u}$	WINNER II

The channel impulse response of the environment-based channel model $\mathbf{h}_{u,s,n}(t, \tau)$ is calculated as a combination of the large-scale parameters, i.e., the parameters which are highly influenced by the environment, from the deterministic ray-tracing algorithm and the small-scale parameters are computed using WINNER II channel model. Hence, the joint channel impulse response $\mathbf{h}_{u,s,n}(t, \tau)$ is defined as

$$\begin{aligned} \mathbf{h}_{u,s,n}(t, \tau) = & \sqrt{\frac{P_n}{M}} \sum_{m=1}^M \sqrt{G_{rx,u}(\varphi_{n,m})} \sqrt{G_{tx,s}(\phi_{n,m})} \cdot \exp(j2\pi\lambda_0^{-1}(\bar{\varphi}_{n,m} \cdot \bar{r}_{rx,u} + \Phi_{n,m})) \\ & \cdot \exp(j2\pi\lambda_0^{-1}(\bar{\phi}_{n,m} \cdot \bar{r}_{tx,s})) \cdot \exp(j2\pi\nu_{n,m}t) \delta(\tau - \tau_{n,m}), \end{aligned} \quad (4.5)$$

where the parameter P_n is given as

$$P_n = |\mathbf{h}(\tau, \phi, \varphi)|^2, \quad (4.6)$$

being $\mathbf{h}(\tau, \phi, \varphi)$ the channel impulse response obtained in equation (4.4) by using the output from the ray-tracing algorithm. Further λ_0 is the wave length of carrier frequency, $\phi_{n,m}$ is AoD unit vector, $\varphi_{n,m}$ is AoA unit vector, $\bar{r}_{tx,s}$ and $\bar{r}_{rx,u}$ are the location vectors of element s and u respectively, and $\nu_{n,m}$ is the Doppler frequency component of ray n, m . Moreover, P_n is the received power calculated using the ray-tracer algorithm as in equation (4.4). As a result, the impulse channel response $\mathbf{h}_{u,s,n}(t, \tau)$ obtained in equation (4.5) combines the advantages of both approaches. Consequently, the total received power for the environment-based channel model is calculated as

$$P_{tot} = |\mathbf{h}_{u,s,n}(t, \tau)|^2. \quad (4.7)$$

4.3 3-D Beamforming for backhaul links

The next step in our scheme is to model the communication link between the DeNodeB and the intermediate infrastructures, i.e., the relays, implementing a 3-D beamforming

scheme using the angular domain knowledge obtained from the previous layer. There are many potential applications for 3-D beamforming, also known as full-dimension MIMO (FD-MIMO) [49], nonetheless, the focus in this layer is the implementation of backhaul links, where the application of 3-D beamforming is a real improvement for the network. The main application of the FD-MIMO scheme is to provide both relay schemes, as well as fixed RSUs and MRNs, with the required capacity for the vehicles under their coverage in order to handle the high number of users.

This beamforming scheme does not only adapt the horizontal dimension of the antenna pattern but also uses the vertical orientation of the antenna pattern to achieve a great gain and at the same time mitigate the interference. This functionality has been implemented in the 3GPP Technical Specification (TS) 36.211 Release 10 Standard [93], however, there was not a specific application for it. The proposed model consists of using the angular knowledge obtained from the ray-tracing algorithm, both φ_n, ϕ_n , and apply a 3-D beamforming scheme. For this purpose, it is assumed that the base station is equipped with several transceivers each of this transceiver feeding a great number of antennas, $N_{Tx} \times M_{Tx}$, forming a large array, which allows us to perform the beamforming. The antenna array is designed as a 2-D planar array, where N_{Tx} is the vertical dimension and M_{Tx} is the horizontal one. In order to exploit all the advantages of FD-MIMO, the DeNodeB is equipped with separate transceivers, which independently control the feeding of the 2-D planar array elements [94] as shown in Figure 4.2.

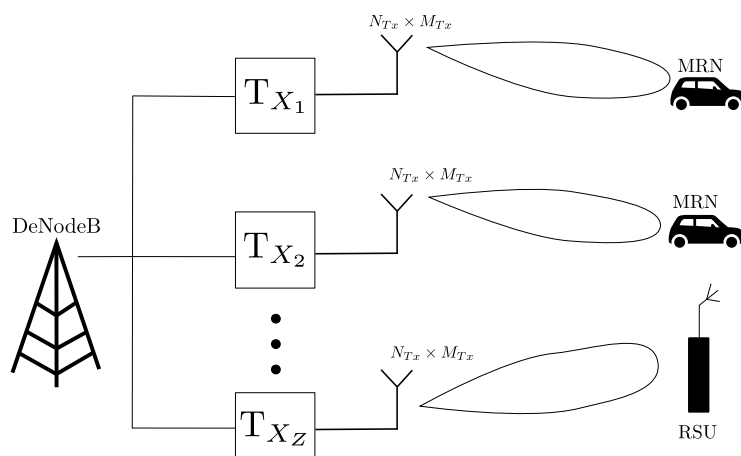


Figure 4.2: Full-Dimension MIMO for backhaul links.

The figure shows a base station equipped with a set of bi-dimensional arrays of antennas ($M \times N$) and a set of transceivers $\mathcal{T} = \{T_{X_1}, T_{X_2}, \dots, T_{X_Z}\}$ which controls the transmissions. In order to perform an optimal 3-D beamforming, it is required to obtain the azimuth and elevation directions, along with the multi-path components. The deterministic algorithm predicts the attenuation, delay, and what is more important for our model, the angle of departure and elevation from the base stations of the predominant paths. Using this knowledge, the antenna array at the transmitter can be calibrated, i.e., input power for each antenna element, to obtain the desired antenna pattern. Therefore, since the proposed channel model is a 3-D model, a radio channel model which considers also the elevation dimension is required.

The radio channel model is defined using the WINNER II channel model framework including the elevation angles as follows

$$\begin{aligned} \mathbf{H}_{u,s,n}(t, \tau) = & \sqrt{\frac{P_n}{M}} \sum_{m=1}^M \begin{bmatrix} F_{rx,u,V}(\varphi_{n,m}) \\ F_{rx,u,H}(\varphi_{n,m}) \end{bmatrix}^T \begin{bmatrix} \alpha_{n,m,VV} & \alpha_{n,m,VH} \\ \alpha_{n,m,HV} & \alpha_{n,m,HH} \end{bmatrix} \\ & \begin{bmatrix} F_{tx,s,V}(\phi_{n,m}) \\ F_{tx,s,H}(\phi_{n,m}) \end{bmatrix} \cdot \exp(j2\pi\lambda_0^{-1}(\bar{\varphi}_{n,m} \cdot \bar{r}_{rx,u})) \cdot \\ & \exp(j2\pi\lambda_0^{-1}(\bar{\varphi}_{n,m} \cdot \bar{r}_{tx,s})) \cdot \exp(j2\pi\nu_{n,m}t) \delta(\tau - \tau_{n,m}), \end{aligned} \quad (4.8)$$

where $F_{rx,u,V}$ and $F_{rx,u,H}$ are the antenna element u field patterns for vertical and horizontal polarizations respectively, $\alpha_{n,m,VV}$ and $\alpha_{n,m,VH}$ are the complex gains of vertical-to-vertical and horizontal-to-vertical polarizations of ray n,m respectively. In order to obtain the ray-tracing prediction, the estimated position of the vehicles is required along with the scenario information, i.e., surrounding buildings and road information. Following the specifications suggested by the LTE standard, the antenna patterns in both angular dimensions, i.e., elevation and azimuth, are as follows

$$A_H(\phi) = -\min \left\{ 12\left(\frac{\phi}{\phi_{3dB}}\right), A_m \right\}, \quad (4.9)$$

$$A_m = 20 \text{ dB},$$

$$A_H(\varphi) = -\left\{ 12\left(\frac{\varphi - \varphi_{tilt}}{\varphi_{3dB}}\right), SLA_v \right\}, \quad (4.10)$$

$$SLA_v = 20 \text{ dB},$$

where ϕ is the angle in the horizontal direction. φ is the vertical angle and φ_{tilt} is the angle for down tilt in the vertical direction. ϕ_{3dB} and φ_{3dB} are the 3 dB beam-width of the horizontal and vertical beam, respectively. Finally, A_m is the side lobe attenuation and SLA_v is the front-to-back loss. In order to achieve a coordinated antenna scheme, the vehicles send their CAMs to the base station which include the dynamic properties of the vehicle, i.e., the position, direction, and speed. Once this information is collected at the base stations, the adaptive antenna scheme can be performed.

4.4 V2I Radio Channel Model

The second layer of our proposed radio channel modeling corresponds to the connection between a fixed infrastructure (RSU) and the vehicles in its range following the scheme depicted in Figure 2.6. The main difference with the previous upper layer (V2N) is that the distance between both ends of the link is shorter. Additionally, the main goal of this layer is to provide high reliability and data rate in order to enable vehicular applications. Since the communication range is smaller, the RSU height is lower compared to the DeNodeB, and consequently, the number of vehicles in the range is also lower, it is possible to predict and estimate the radio channel using a fingerprint-based scheme.

4.4.1 Fingerprint-based prediction scheme using predictor antennas

In order to adapt the radio channel model for the links between the RSUs and the vehicles, the standard strategy is to use the feedback from the receiver side in order to adjust the parameters. However, in vehicular networks due to the time-critical applications and the rapid movement of the vehicles, this feedback is not enough. Therefore, in order to estimate the channel parameters, we propose to use the information obtained from the deterministic ray-tracing algorithm, in combination with the feedback from the vehicles.

Using the ray-tracer algorithm, the coverage area A_i , as defined in Algorithm 2, is divided into smaller pixel areas b of one m^2 , i.e., the minimal granularity provided by the ray-tracer algorithm, and the power and angular domain are calculated for each single pixel area $b \in A_i$. Hence, a fingerprint-based scheme for the coverage area can be obtained, which has proved to greatly increase the performance of the adaptive beamforming [95]. In addition to this, using the control plane between vehicles and DeNodeB, in order to avoid congestion, the vehicles send their feedback to the infrastructure. However, as we stated before, the feedback delay τ is usually too high in the fast moving environment and, hence, we need to find an alternative method to obtain this feedback.

Here we propose to exploit the platoon formation of the vehicles, using a similar concept as the *predictor antennas* implemented in [96]. In the cited work, the authors use two antennas, situated on top of a vehicle, separated by a distance of a few wavelengths to predict the channel, exploiting the high correlation $\mathbf{C}(\tau)$ between both channels $\mathbf{h}(t)$ and $\hat{\mathbf{h}}(t - \tau)$

$$\mathbf{C}(\tau) = \mathbb{E}[\mathbf{h}(t)\hat{\mathbf{h}}(t - \tau)]. \quad (4.11)$$

However, this approach requires large vehicles, and more importantly, it is expensive to deploy redundant equipment on each vehicle. In contrast, our proposed scheme does not require installing several antennas on top of the vehicles but uses the short distance among the participants of the same platoon to obtain the prediction based on the preceding vehicles.

The fingerprint prediction is performed in pixel form, i.e., the DeNodeB coverage area A_i is divided in pixels of one meter $b \in A_i$, and the received power P_b and angular domain $\Psi_b := (\phi_b, \varphi_b)$ are calculated for each one of these pixel points b . Therefore, the channel impulse response for a single pixel area b can be defined as $\mathbf{h}_b(t)$ whereas the past values for the same pixel area can be denoted as $\mathbf{h}_b(t - \tau)$. For any short period of time, a static Autoregressive Moving Average (ARMA) model for the fading channel coefficient can be constructed to well represent the correct fading behavior [97]. For complexity reasons, it is important to keep the model order low. In our case, the order is given by the number of participants in the platoon which due to communication limitation is generally around $n \approx 6$. Since fading channel coefficients commonly exhibit oscillatory behavior, autoregressive models are suitable. The estimated channel impulse response for the time instant t_n at a given pixel position b is given by

$$\hat{\mathbf{h}}_b(t_n) = \mathbf{h}_b(t_0) + \beta_b(t_1) \cdot \hat{\mathbf{h}}_b(t_1) + \dots + \beta_b(t_{n-1}) \cdot \hat{\mathbf{h}}_b(t_{n-1}), \quad (4.12)$$

which in a compressed form is equivalent to

$$\hat{\mathbf{h}}_b(t_n) = \mathbf{h}_b(t_0) + \sum_{i=1}^{n-1} \beta_b(t_i) \cdot \hat{\mathbf{h}}_b(t_i), \quad (4.13)$$

where $\mathbf{h}_b(t_0)$ is the initial fingerprint-based prediction obtained using the ray-tracer algorithm at the initial time. The past values for the prediction are defined as $\hat{\mathbf{h}}_b(t_i)$ with $i = \{1, 2, \dots, n-1\}$ which covers the time instant until present t_n , i.e., where the prediction is taking place. The parameters used for the autocorrelation $\{\beta_b(t_i)\}_i^{n-1}$ are tuned accordingly to the actual local environment and based on the feedback from the vehicles.

The received signal for each vehicle in the platoon which is located at a point b is defined as:

$$\mathbf{y}_b(t_n) = \sqrt{P_b} \mathbf{h}_b^H(t_n) \cdot \mathbf{x}_b(t_n) + \mathbf{w}(t_n), \quad (4.14)$$

where P_b is the transmitted power at position b , $\mathbf{h}_b(t_n)$ is the channel impulse response, $\mathbf{x}_b(t_n)$ is the transmitted signal vector and $\mathbf{w}(t_n)$ is the Gaussian noise. Using an analogous signal model as the one used in equation (4.13), we define the predicted signal using the expression obtained as

$$\hat{\mathbf{y}}_b(t_n) = \sqrt{P_b} \hat{\mathbf{h}}_b^H(t_n) \cdot \mathbf{x}_b(t_n) + \mathbf{w}(t_n), \quad (4.15)$$

where $\hat{\mathbf{h}}_b$ is the estimate channel impulse response for each vehicle at position b obtained using equation (4.12). Nevertheless, for vehicular communications where the feedback delay is extremely stringent, it is not possible to estimate the desired signal $\mathbf{y}_b(t_n)$ based solely on the previous estimations t_i with $i = \{1, 2, \dots, n-1\}$. Therefore, at this point, it is required to predict the future signals using the concept of *predictor antennas* exploiting the platooning formation. This concept is described using Figure 4.3.

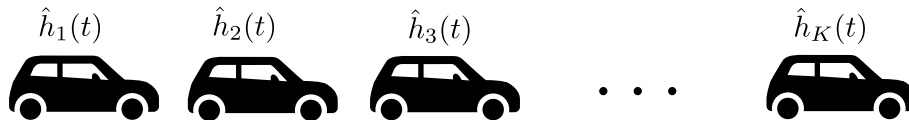


Figure 4.3: General scheme for predictor antennas using a platoon formation.

The proposed scheme exploits the distance between the vehicles in the platoon, which as tested in [8], can be defined as $\Delta d = 0.1 \cdot v(t)$. In the case of urban scenarios (assuming a $v_{max} = 50 \text{ km/h}$), the maximum distance between two consecutive vehicles is around 1.5 meters. Therefore, the channel impulse responses $\mathbf{h}(t)$ and $\mathbf{h}(t + \Delta t)$, where $\Delta t = \frac{\Delta s}{v}$, are highly correlated due to the stationarity property of the radio channel model. Using this assumption, it is possible to predict the radio channel model at successive positions using equation (4.15). In this case, we assume, as before, that each vehicle position is mapped to a pixel position b . Hence, for the channel impulse response $\mathbf{h}_1(t)$ using the preceding vehicle as a predictor, we can define the future prediction as $\hat{\mathbf{h}}_1(t + \tau) = \hat{\mathbf{h}}_2(t)$ where $\tau = \Delta t$. This concept uses the chained predictions from the platoon member to obtain a similar solution as the one obtained in equation (4.13), and it is illustrated in Figure 4.4.

However, in this case, we are not using the predictions from different vehicles at a different time instant, but at different physical positions b_i in the same time instant. The resulting future predictions are

$$\hat{\mathbf{h}}_b(t + \tau) = \alpha_{b+1}(t) \cdot \hat{\mathbf{h}}_{b+1}(t), \quad (4.16)$$

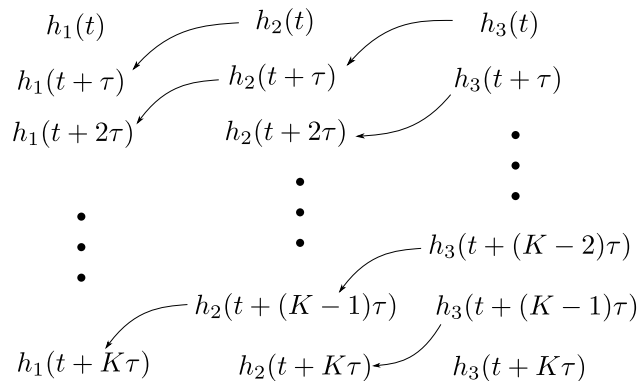


Figure 4.4: General scheme for predictor antennas using a platoon formation.

where α is a complex-value scalar gain in order to tune the future prediction. Hence, the adaptive scheme is performed at the base station using the predicted complex channel values. The estimated channel matrix is obtained using

$$\begin{aligned} \hat{\mathbf{h}}_1(t) = & \alpha_2(t + \tau) \cdot \hat{\mathbf{h}}_2(t + \tau) + \alpha_3(t + 2\tau) \cdot \hat{\mathbf{h}}_3(t + 2\tau) \\ & + \cdots + \alpha_n(t + n\tau) \cdot \hat{\mathbf{h}}_n(t + n\tau), \end{aligned} \quad (4.17)$$

which can also be written as

$$\hat{\mathbf{h}}_b(t) = \sum_{i=b+1}^n \alpha_i(t + i\tau) \hat{\mathbf{h}}_i(t + i\tau), \quad (4.18)$$

where $\hat{\mathbf{h}}_b(t_i)$ is the predicted channel corresponding to the past estimations and $\alpha_b = \mathbf{R}_b^{-1} \mathbf{p}_b$ is the vector that weights the previous predictions. The variable $\mathbf{R}_b = \mathbb{E}[\tilde{\mathbf{h}}_b \tilde{\mathbf{h}}_b^H + \sigma^2 I_L]$ is the autocorrelation matrix and $\mathbf{p}_b = \mathbb{E}[\tilde{\mathbf{h}}_b \hat{\mathbf{h}}_b^*]$ is the autocorrelation from previous and current channel matrix.

This scheme works because the short-term fading parameters (which cannot be predicted by the ray-tracer algorithm) can be assumed from previous channel estimations. Once the prediction and the feedback values are stored in the infrastructure, we realize a comparison and check if the prediction is *good enough* (analogously as in Figure 3.12) using the Normalized Mean Square Error (NMSE) metric

$$\text{NMSE} = \sum_{b=1}^B \frac{\mathbb{E}|\mathbf{h}_b(t) - \hat{\mathbf{h}}_b(t)|^2}{\sigma_{\mathbf{h}_b}^2}; \quad \sigma_{\mathbf{h}_b}^2 = \mathbb{E}|\mathbf{h}_b(t)|^2. \quad (4.19)$$

Therefore, by using the combination of a fingerprint-based scheme, adapting the past estimations and exploiting the platoon formation of the vehicles by means of *predictor antennas*, it is possible to estimate the actual channel impulse response at time t_n and to predict the future channel parameters.

4.4.2 Numerical results

The last step to complete the proposed model is to compare our results with real measurement data. Using the measurements obtained from [98] to compare the estimated results and the fingerprint-based model.

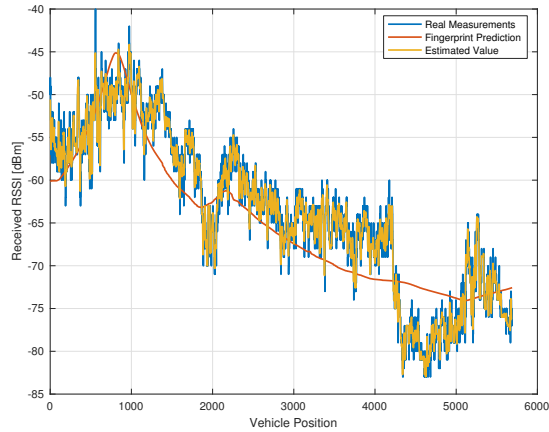


Figure 4.5: RSSI comparison for the two different models.

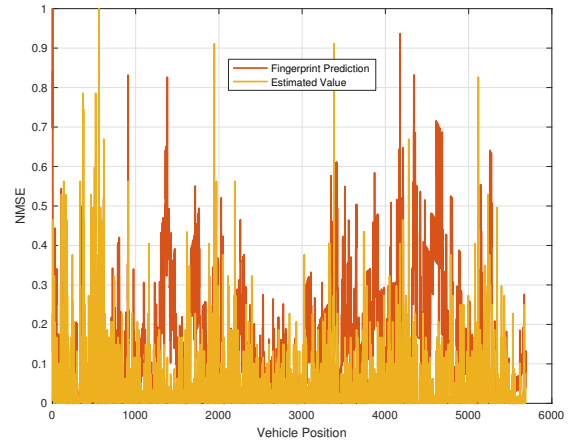


Figure 4.6: NMSE comparison.

Figure 4.5 shows the Received Signal Strength Indicator (RSSI) in dBm for the three different approaches. The fingerprint scheme uses the parameters obtained from the ray-tracer algorithm, where there is no fading involved. Moreover, using the expression obtained in equation (4.13), it is possible to achieve an accurate estimation of the received signal. In this case, the model order has been kept as $n = 6$ to obtain a practical estimation scheme.

Table 4.2: Statistical analysis for both models.

	Mean Error[dB]	Std. Dev. (SD) Error [dB]
Fingerprint Scheme	3.8325	2.3771
Predictor Antennas Scheme	0.9750	0.8739

In order to show the improved performance in a better way, Figure 4.6 depicts the NMSE as calculated in equation (4.19). Performing an statistical analysis of the obtained results, it shows that our scheme provides a high accuracy when compared with the real measurements as shown in Table. 4.2.

4.5 V2V Radio Channel Model

In recent years, different approaches to model the vehicular channel have been developed. Some models using a pure ray-tracing algorithm, such as the one developed by Maurer et al. [99]. This model uses a high detailed description of the scenario and calculates the channel statistics analyzing the strongest paths obtained using the ray-tracing algorithm. Karedal et al. [100] proposed a different perspective; where the model parameters are

extracted from several measurement campaigns done in highway and urban environments. Other models, as the one proposed by Mangel et al. [101], include information about the street architecture and intersections to the model. However, every approach has its own drawbacks, such as non-site-dependent properties, because the parameters are obtained from different measurement campaigns, or the requirement of a highly detailed scenario information, which sometimes cannot be easily obtained. Moreover, using an abstract realization of the scenario, it is not possible to model the particularities of the environment, hence, obtaining a less accurate channel model.

In the case of V2V communications, the main parameters to optimize is the reliability and latency. In general, for cooperative *connected vehicles*, the required reliability is in the order of 99.999% (the five nines) for packet reception, and a latency in the order of (1 ~ 10) ms. The focus here is in the outage probability induced by rare fading events and not by the noise-related ones. Therefore, it is required to approach the channel model in a different perspective as for V2N and V2I communications. We have to focus on the modeling of rare events and the lower tail of the cumulative distribution function (CDF) of the channel. Using an approximation is possible to obtain the tail of the CDF at the levels of URC in the form:

$$F\left(\frac{P_R}{A}\right) \approx \xi\left(\frac{P_R}{A}\right)^\gamma, \quad (4.20)$$

where A is the average power, P_R is the minimum required power in order to have a successful transmission and both ξ, γ are parameters that depend on the actual channel model, i.e., they need to be estimated beforehand and tuned in real time.

In this case, since we are looking for regimes where the URC are tested, i.e., in the order of 99.999% reliability, it is not possible to use the same semi-stochastic concept used before for V2N and V2I channel models. For this particular scenario, we require a closed theoretical form in order to obtain the limits of performance of our channel model. For this objective, we propose to model the V2V channel using a three-waves channel model.

4.5.1 Three-waves channel model

For the V2V communication channel model, we use the following three-waves channel model where it is assumed a predominant path (mostly LoS) in addition to other two specular components are given by the reflections due to the environment, i.e., multipath. Therefore, the envelope r of the received signal is defined as

$$r = |A_1 + A_2 e^{j\phi_2} + A_3 e^{j\phi_3}|, \quad (4.21)$$

where the amplitude for each ray $i = \{1, 2, 3\}$ is A_i and the average received power is the sum of the rays as $\sum_{i=1}^3 A_i^2$. Moreover, we consider that the amplitude of the received rays are $A_1 \geq A_2 \geq A_3$ since they are sorted by time of arrival. It is notable, that the Rayleigh channel model is a particular case of the three-waves channel model where the two specular components A_2 and A_3 are strong enough to cancel the contribution from the strongest path A_1 . The probability density function for the three-waves channel model [102] is given by:

$$f_{3W}(r) = \begin{cases} \frac{\sqrt{r}}{\pi^2 \sqrt{A_1 A_2 A_3}} K\left(\frac{\Delta_r^2}{A_1 A_2 A_3 r}\right), & \Delta_r^2 \leq A_1 A_2 A_3 r, \\ \frac{r}{\pi^2 \Delta_r} K\left(\frac{A_1 A_2 A_3 r}{\Delta_r^2}\right), & \Delta_r^2 > A_1 A_2 A_3 r, \end{cases} \quad (4.22)$$

where $K(\cdot)$ is an elliptic integral of the first kind and the value Δr is defined as

$$\Delta_r^2 = \frac{1}{16}[(r + A_1)^2 - (A_2 - A_3)^2][(A_2 + A_3)^2 - (r - A_1)^2]. \quad (4.23)$$

The three-waves channel model has been considered due to the two following factors:

- the negligible influence in the received signal r after the third reflection given by the peak to average ratio of the specular powers as

$$\Delta_{1,2} = \frac{2A_1A_2}{A_1^2 + A_2^2} \quad \text{and} \quad \Delta_{1,3} = \frac{2A_1A_3}{A_1^2 + A_3^2}, \quad (4.24)$$

which in the cases where A_i with $i > 3$ makes no impact in the received signal. Our assumption is also supported by the empirical measurements obtained in [103].

- the information available from the ray-tracer algorithm which gives a better prediction of the channel model. In this case, the available information comprises the power of each path associated with the angular domain of these paths (useful later for calculating the doppler shift), and their delay.

4.5.2 Outage probability for URC

In the case of V2V communications, the expected exchange of messages is in the range of short packages as defined in Section 2.5.2. For the sake of simplicity, we use an approximation of equation (2.2) to calculate the communication rate

$$R^*(n, \epsilon) = C - \sqrt{\frac{V}{n}}Q^{-1}(\epsilon) + \frac{1}{2n} \log n, \quad (4.25)$$

where n is the packet size and ϵ is the outage probability. Moreover, the capacity $C(\rho)$ and the dispersion $V(\rho)$ for a given SINR ρ can be calculated as follows

$$C(\rho) = \log(1 + \rho), \quad (4.26)$$

$$V(\rho) = \rho \frac{(2 + \rho)}{(1 + \rho)^2} (\log e)^2. \quad (4.27)$$

Hence in order to calculate the outage probability for a defined required power P_R , we use the following expression

$$\epsilon = \mathbb{P}(R < C(\rho)) = \mathbb{P}(R < \log(1 + \rho)) = \mathbb{P}(P < P_R), \quad (4.28)$$

where $\mathbb{P}(\cdot)$ defines the probability and $P_R = 2^R - 1$ is the minimal required power in order to receive a given packet with rate R . Therefore, if we particularize equation (4.28) for our three-waves channel model [102], we obtain the following

$$\epsilon = \int_0^{\sqrt{P_R}} f_{3W}(r) = \frac{P_R}{4\pi\Delta_r}, \quad (4.29)$$

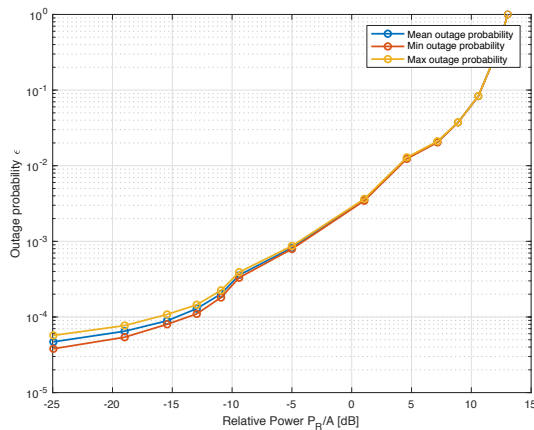


Figure 4.7: Outage probability in the three-waves channel model.

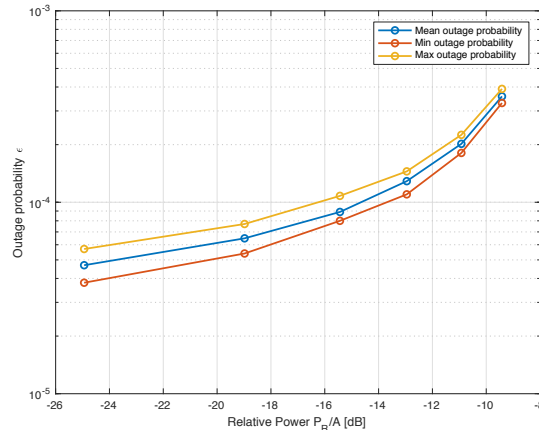


Figure 4.8: Outage probability in the three-waves channel model for URC relevant values.

using the expression from equation (4.29), we obtain a theoretical curve for the outage probability as shown in Figure 4.7 considering the amplitude of the paths as $A_1 = 1$, $A_2 = 0.7914$ and $A_3 = 0.2126$ including a Gaussian variable \mathcal{N} in order to incorporate the stochastic behavior to the channel model.

The simulation in Figure 4.7 and Figure 4.8 has been created using a high number of realizations (10^8) in order to produce results which are relevant in the values of URC $\epsilon \approx 10^{-5}$ outage probability. Moreover, the relative power $\frac{P_R}{A}$ defines the ratio between the minimum power to decode a package P_R and the received power from the different rays defined as $A = \sum_{i=1}^3 A_i^2$ including random Gaussian noise. Focusing on the relevant values for URC, we can observe that depending on the threshold power, the outage probability ϵ falls in the range of $\epsilon \approx 10^{-4}$ which fulfills the requirements for V2V, i.e., $\epsilon \leq 10^{-3}$.

4.5.3 Parameter estimation for URC in V2V scenarios

The next step in our channel model is to estimate the parameters beforehand using the information obtained from the channel model. However, since our aim is to obtain ultra-reliable communications, it is also needed to tune the channel estimation in real time. For this purpose, we use the previously introduced concept of *predictor antennas*. In this particular case, we only consider the feedback obtained from the preceding vehicles in the platoon without any further involvement of the infrastructure.

Average received power

The received average power is mainly distance dependent, i.e., knowing the distance between the receiver and the transmitter, this value is deterministic. However, as stated in equation (4.21), the phase plays also a role in the received signal value. Therefore, in order to add the stochastic nature to this variable, we simulate the phase (which cannot be predicted due to random nature) in order to estimate the worst case scenario, which

is the useful one in the reliability calculation. Moreover, another factor impacting in the received power is the shadow fading which can be estimated at the receiver side.

Doppler shift

In order to calculate the Doppler shift, it is important to consider the relative speed between the transmitter and the receiver, and the angle of the rays between them. In this case, it is convenient to use the information from the ray-tracer, which includes the angular domain for all the paths. Hence the Doppler shift can be calculated using the following expression

$$\begin{aligned} f_d &= \frac{F_c}{c} \cdot (|v_1 - v_2| \cdot \cos(\theta_1)) + (|v_2 - v_1| \cdot \cos(\theta_2)) \\ &= \frac{F_c}{c} \cdot (v_{rel} \cdot \cos(\theta_1)) + (v_{rel} \cdot \cos(\theta_2)), \end{aligned} \quad (4.30)$$

F_c being the central frequency used in the radio channel, c the speed of light, θ_1 the angle at the transmitter, θ_2 the angle at the receiver, and v_1, v_2 the speeds of the transmitter and receiver given in $\text{m} \cdot \text{s}^{-1}$, respectively. Therefore, it is possible to estimate the Doppler spread by using the predicted angle for the three rays reaching the receiver. Additionally, we assume that the speed of the vehicles is accurately obtained using the sensors equipped on them.

Fading parameters

Using the feedback obtained from the *predictor antenna*, we can consider the channel impulse response for the same spatial position p , separated in time a value of Δt as

$$\mathbf{h}_b(t) = \boldsymbol{\alpha} \cdot \hat{\mathbf{h}}_b(t - \Delta t), \quad (4.31)$$

where Δt is considered as the interval of the inter-vehicular messages (typically $\Delta t = 100$ ms). L is defined as the prediction horizon in seconds. In order to have an accurate estimation as stated in [104], the value $\Delta t \geq L$, where L depends on the velocity of the vehicle and the carrier frequency as

$$L \cdot f_d = \frac{L \cdot v}{\lambda} = \frac{L \cdot v \cdot f_c}{c_0} \quad [\text{in wavelengths}]. \quad (4.32)$$

Therefore, in our case for urban environments, we consider the speed of the vehicles is approximately 50 km/h and, hence, the value $L \approx 0.62\lambda$. Therefore, in order to estimate the fading parameters, the coefficient $\gamma = \eta \cdot \left(\frac{\sigma_b}{\hat{\sigma}_b}\right)$ needs to be estimated in order to minimize the difference between the estimated value $\hat{\mathbf{h}}_p$ and the real measurement. Both values σ_b and $\hat{\sigma}_b$ are calculated as

$$\sigma_b = \sqrt{E|\mathbf{h}_b|^2}, \hat{\sigma}_b = \sqrt{E|\hat{\mathbf{h}}_b|^2}. \quad (4.33)$$

Furthermore, $\eta \in [-1, 1]$ is the normalized value of the channel correlation.

4.5.4 Numerical results

Overtaking scenario

This scenario displays a typical situation in urban road traffic, where safety can be conditioned by the context awareness of the driver and some efforts can be done using a video assisting method. Two cars driving in the same direction, but at different speeds and in different lanes of the same road, as shown in Figure 4.9. The peculiarities of this scenario are the high mobility and different velocity of the network elements influencing the propagation parameters. In such a situation, the Doppler shift is of significance, since the spread in frequency affects the communication link reception.

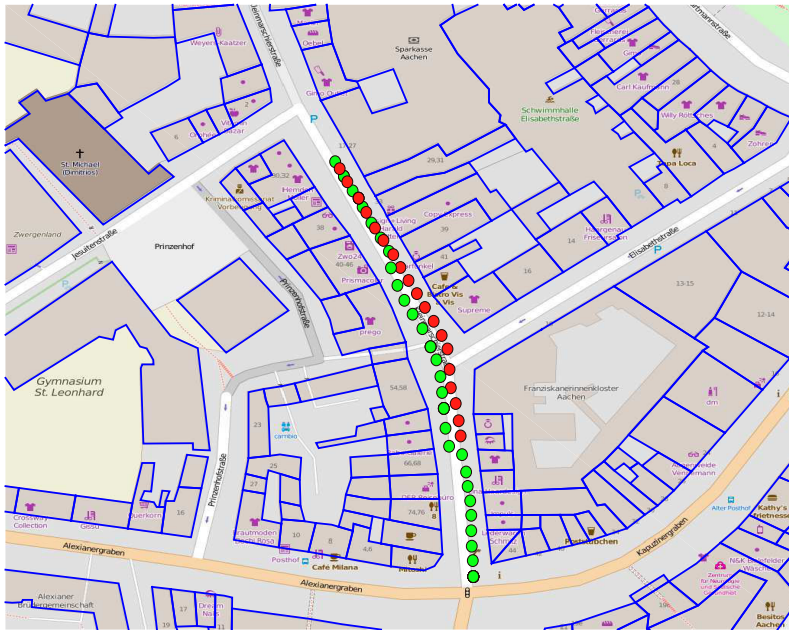


Figure 4.9: Overtaking scenario for V2V communication.

The results of the outage probability for this particular scenario are displayed in Figure 4.10. The results show that, as expected, the higher the ratio between the received power and the required power for a successful transmission, the probability of an outage ϵ is smaller. Moreover, the graph in Figure 4.10 shows the range between the best and worst case scenario. It is notable that in reliability studies is of great of importance to assume the worst case scenario for system reliability. The outage values lie in the range of 10^{-4} for the best-received power ratio, and in the worst case scenario the outage probability grows up to 10^{-2} . In the case of the Doppler shift shown in Figure 4.11, it is possible to observe that due to the constant relative speed between the vehicles, the Doppler values are in defined lower and upper bound. Moreover, it is interesting to remark that in this case, the maximum Doppler spread is in the range of $[-250, 250]$ Hz.

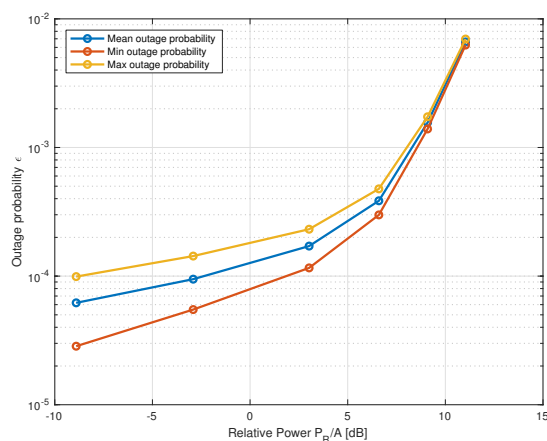


Figure 4.10: Outage probability for V2V communication link in an overtaking scenario.

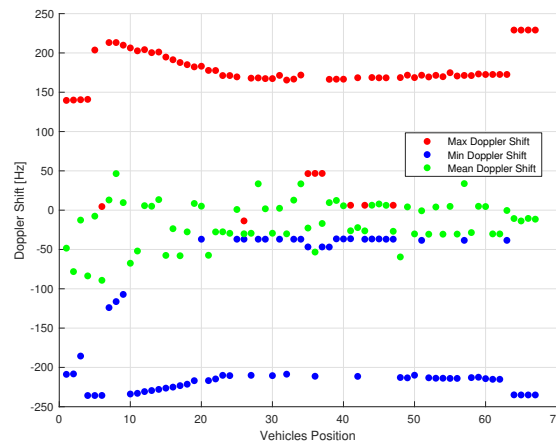


Figure 4.11: Doppler Shift value for V2V communication link in an overtaking scenario.

Crossing scenario

This scenario simulates a crossing involving two cars, as displayed in Figure 4.12. The relevance of this scenario is to show the importance of the geographical information, regarding the propagation parameters. In a crossing, the network elements suffer from different link situations, i.e., Line-of-Sight (LoS) or Non-Line-of-Sight (NLoS). Therefore, the knowledge of the surrounding scenario elements is essential. Particularly in this type of scenarios, it is expected to obtain a greater accuracy using the proposed model than applying abstract realizations of the scenario, due to the geographical input data. Moreover, this scenario is especially interesting in safety applications, since in such scenarios high numbers of collisions can occur.

The results of the outage probability for this particular scenario are displayed in Figure 4.13. In this case, the number of channel realizations is 10^8 obtaining a maximum reliability close to 10^{-6} . A behavior similar to the previous scenario (Figure 4.9) can be observed, where a higher received power ratio implies a smaller probability of having an outage. Moreover, it is also shown in this case the range of outage probabilities between the best and worse case scenario. In the relevant values for the URC, the outage probability lies in the range of 10^{-4} and 10^{-5} depending on the channel conditions. Additionally in Figure 4.14, the Doppler shift is displayed for the crossing scenario. In this case, it is possible to appreciate the moment where the vehicles pass by each other (≈ 20) in the graph, achieving the minimal Doppler value. The range of values for the Doppler shift in this scenario lies in the $[-80, 80]$ Hz range.

4.6 Summary

In this chapter, the main concepts for modeling the radio channel in vehicular networks are defined. The radio channel modeling is divided into three main layers to adapt our channel model design to the different network requirements. First, the radio channel between the fixed macro-infrastructures (DeNodeBs) and vehicles (or intermediate relays) is defined

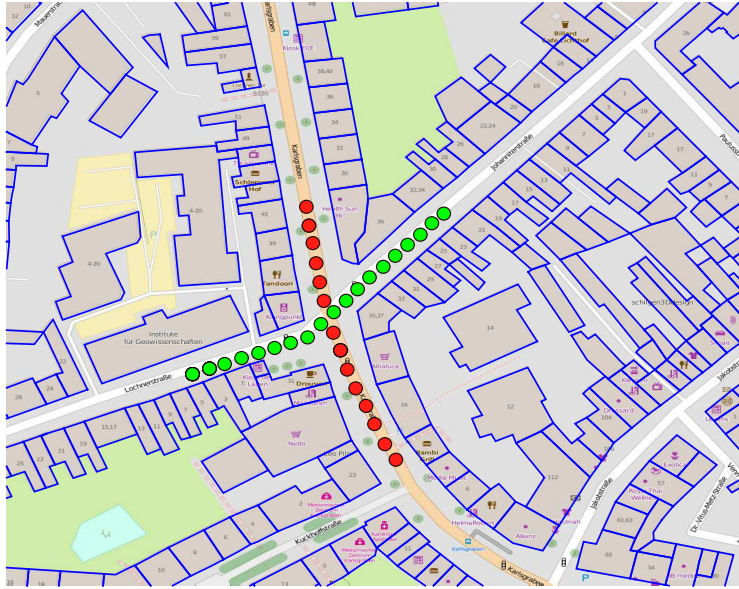


Figure 4.12: Crossing scenario for V2V communication.

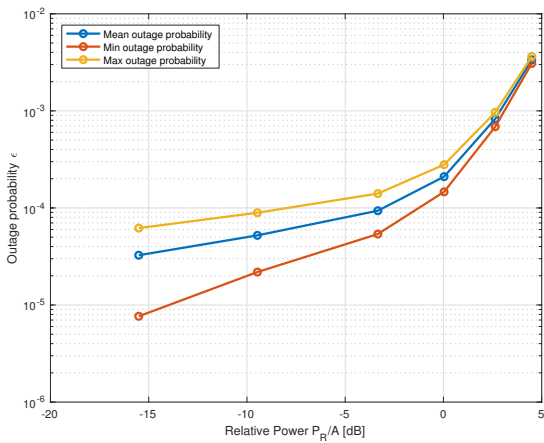


Figure 4.13: Outage probability for V2V communication in a crossing scenario.

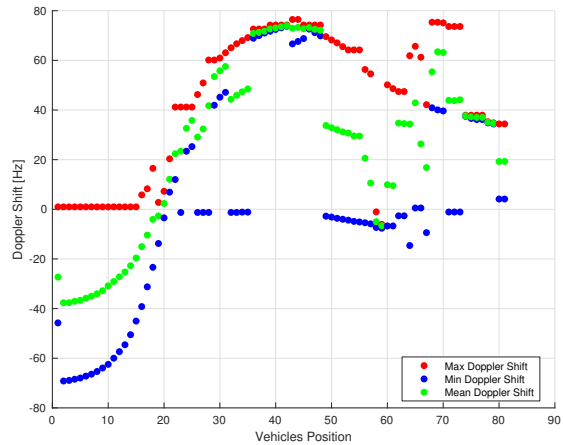


Figure 4.14: Doppler Shift value for V2V communication in a crossing scenario.

focusing on the ubiquitous connectivity required for the vehicles. For this purpose, a combination of a ray-tracing algorithm and a stochastic model is applied. The second layer is formed between the intermediate relays (both fixed and mobile), and the vehicles. In this case, we exploit the platoon formation of the vehicles to obtain accurate estimations of the channel, in addition to the semi-stochastic channel model. The last part is focused on the inter-vehicular communications. At this stage, the main parameter is the communication reliability (outage probability $\approx 10^{-4}$). In order to reach such stringent requirement, we introduced a theoretical three-waves channel model, and a predictor antennas scheme to estimate the channel parameters.

5 | Cooperative Scheme for Connected Vehicles

Throughout this chapter, the main concepts of an optimal cooperative scheme for connected vehicles are introduced. The objective of our cooperative scheme is twofold: safety and traffic optimization. For the first goal, the vehicle's coordination scheme is divided into two different layers, i.e., implicit and explicit, where only the vehicle perception is used for the first, and additional information from exchanged messages is needed for the latter. The second goal is achieved by means of a platoon formation. The main characteristics regarding stability and traffic flow optimization are explained within a platoon framework. This platoon framework was developed in collaboration with Ericsson Eurolab and some of the simulations are obtained using their own simulator. Moreover, using the previously proposed network architecture, the resource allocation for the vehicles is optimized, improving the reliability of the communications. To conclude this chapter, a secure scheme for intra-vehicular communications in platoons based on cryptographic primitives is implemented.

5.1 Cooperative Autonomous Systems

5.1.1 General concepts

The problem of coordinating a set of vehicles can be seen as calculating the best option for each vehicle while optimizing the global network. The main requirement in our system is safety, i.e., no collisions with other vehicles or pedestrians occur. Every solution of the coordination problem should satisfy the basic constraints of safety and traffic optimization. Thus, the decisions made by the vehicles will always prioritize their safety. In order to coordinate the different set of vehicles, we employ two different concepts: implicit and explicit coordination.

The first part of the coordination scheme consists of sensing the close range environment using the on-board equipment of the vehicle. After evaluating the features in a data fusion center, an individual decision (implicit coordination) is made whether an evasive maneuver is required or not. The second part uses explicit coordination between the cars to update the status of the network and inform about any unexpected event. This second part is used to extend the range of perception of each vehicle, i.e., by using the connection with the deployed infrastructures, the vehicles acquire knowledge of the entire network. In the following subsections, the aforementioned coordination schemes are explained in detail.

The objective of our coordination scheme can be understood as a *repulsion/attraction* framework usually used for swarms of dynamic agents [105]. Each vehicle should be at a minimum distance to the remaining vehicles in the network (short-range repulsion), while at the same time, it should prioritize the tasks assigned to avoid obstacles. Long-range attraction should make the vehicles converge in platoons, providing them with a reward (see game-theory approach in Section 5.2.2). Avoiding obstacles is the priority of our scheme and, therefore, we apply an implicit coordination scheme in order to obtain the fastest possible reaction. Nevertheless, maintaining a stable and optimal distance among the vehicles requires of explicit coordination, i.e., exchange of messages between the vehicles. Our coordination system should follow the three heuristic rules introduced by Reynolds [106] for multi-agent flocking in order to obtain a feasible and stable cooperative scheme:

- (i) **Flock centering:** stay at a certain distance to the remaining members of the network (*cohesion*).
- (ii) **Collision avoidance:** avoid collisions with nearby members of the network or other obstacles (*separation*).
- (iii) **Dynamics matching:** attempt to match the dynamic properties of the nearby members (*alignment*).

5.1.2 Implicit and explicit coordination scheme

Coordination is needed when the network members cannot act independently from the remaining members, and in this case, it is obvious that the safety of the vehicles is a team coordination effort. However, in dangerous situations generally, there is not enough time to exchange messages in order to perform a coordinated evasive maneuver. In this case, implicit coordination [107] is used to describe the kind of coordination which does not require any exchange of information, but instead, it is based on the shared knowledge between the network members as defined in Figure 5.1. The shared knowledge of the network is defined as the combination of the local knowledge, information obtained by the on-board sensors, and the previously exchanged information with the rest of the network. This shared knowledge helps to anticipate the actions of the remaining vehicles in the network and allows each vehicle to perform individual decisions. The general framework for the implicit coordination scheme is represented in Figure 5.1.

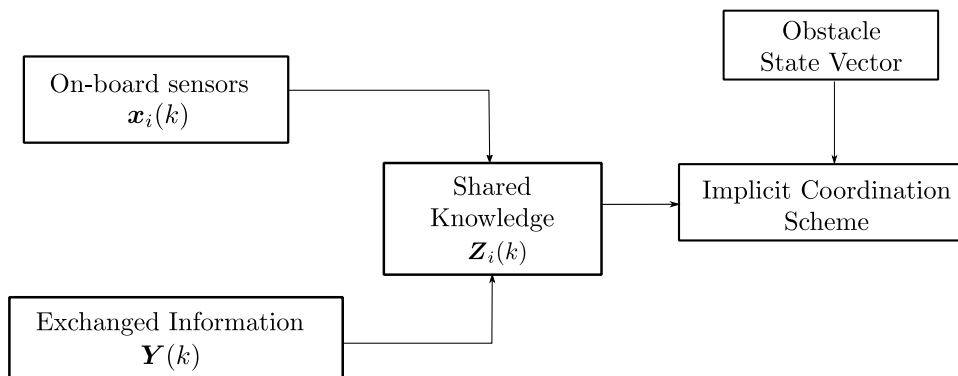


Figure 5.1: Block diagram using an implicit coordination scheme for obstacle detection.

The system is defined as a multi-agent network with discrete-time dynamics where the on-board sensors collect periodically an information row vector $\mathbf{x}_i(k) \in \mathbb{R}^q$ which denotes the readings from the sensors equipped on the i th vehicle obtained every discrete time instant k . The exchanged information $\mathbf{Y}(k) \in \mathbb{R}^{q \times N-1}$ is defined as the information shared in matrix form between vehicles and/or infrastructures using vehicular communication protocols. Therefore, the shared knowledge $\mathbf{Z}_i(k) \in \mathbb{R}^{q \times N}$ is a matrix where N is the total number of vehicles in the network, and it is mathematically defined as

$$\mathbf{Z}_i(k) = f(\mathbf{x}_i(k), \mathbf{Y}(k)). \quad (5.1)$$

In this case, the values of the sensor reading $\mathbf{x}_i(k)$ are related to the state of vehicle i , and the exchanged information matrix $\mathbf{Y}(k) = (\mathbf{y}_1(k), \mathbf{y}_2(k), \dots, \mathbf{y}_{N-1}(k))$ which includes information about the remaining vehicles belonging to the network. Moreover, it is required to achieve a consensus on information $\mathbf{Z}_i(k)$, so that each vehicle can perform an optimal decision individually. Therefore, we try to minimize the shared knowledge error $\varepsilon_{ij}(k) \in \mathbb{R}$ between the N members of the network which is defined as

$$\varepsilon_{ij}(k) = \sum_{j=1, j \neq i}^N (\mathbf{Z}_i(k) - \mathbf{Z}_j(k)). \quad (5.2)$$

Since only when all the vehicles have the same information, it is possible to perform a coordinated action, we assume that $\lim_{k \rightarrow \infty} \varepsilon_{ij}(k) = 0$, achieving strong consensus after a certain number of iterations. The general behavior of the i th vehicle can be defined as

$$\Psi_i(k+1) = f(\underbrace{A \cdot \mathbf{Z}_i(k)}_{\text{Implicit coordination}}, \underbrace{B(\mathbf{U}_i(k), \nu_i(k))}_{\text{Explicit coordination}}), \quad (5.3)$$

where $\mathbf{Z}_i(k) \in \mathbb{R}^{q \times N}$ is the state matrix for the i th vehicle, $\mathbf{U}_i(t) \in \mathbb{R}^{q \times N}$ is its control input vector and $\nu_i(k) \in \mathbb{R}$ is its utility function obtained by a coalitional game-theory approach (see Section 5.2). Additionally, we assume that both quantities (A, B) are vectors such that $(A, B) \in \mathbb{R}^q \times \mathbb{R}^q$ are stabilized to achieve a consensus. The control input of each vehicle, i.e., the update rule for each vehicle is designed in general as

$$\mathbf{U}_i(k+1) = \left(1 - \frac{1}{w_i(k)}\right) \cdot \mathbf{Z}_i(k) + \frac{1}{\sum_{j=1, j \neq i}^N w_{ij}(k)} \cdot \sum_{j=1, j \neq i}^N P_{ij}(k) \mathbf{Z}_{ij}(k), \quad (5.4)$$

which depends on the shared knowledge of each vehicle and the exchange of information with the remaining vehicles. The parameter $w_i(k) \in \mathbb{R}^+$ indicates how certain is each vehicle about its own shared knowledge, i.e., depends on the accuracy of the sensor's readings. The higher the value $w_{ij}(k)$ the more reticent is the vehicle to trust in other's readings. In order to obtain the best update in the control input of each vehicle, the difference between the readings of the rest of vehicles and the vehicle itself should be as small as possible, which is fulfilled by the strong consensus property. There exists an information flow between each pair of vehicles i and j which is weighted by the coefficients $P_{ij}(k)$, i.e., a fully-connected network. In order to obtain a realistic scenario, the communication channel between the pair of vehicles i and j can be modeled using

5 Cooperative Scheme for Connected Vehicles

the channel model defined in Section 4.5. Using this stochastic nature, in general, we define a model using a family of independent binary random variables $P_{ij}(k)$, such that

$$\mathbb{P}[P_{ij}(k) = 1] = p, \quad \mathbb{P}[P_{ij}(k) = 0] = 1 - p. \quad (5.5)$$

However, in our case, the values $P_{ij}(k) = 1$ since we assume a perfect communication channel. Using this communication link, it is possible to create a feedback channel between each pair of vehicles (i, j) in order to minimize the consensus error $\varepsilon_{ij}(k)$. It has been shown in [108] that the convergence time for fully connected networks in dynamic systems, as vehicular networks are $\mathcal{O}(\log N)$ where N is the number of vehicles in the network.

The most important requirement of our coordination scheme is safety. Hence, in order to perform implicit coordination, the map information $\Omega = \{(x_1, y_1), (x_2, y_2), \dots\}$ is required for safety constraints. It defines the set of possible map positions in pixel form excluding the invalid vehicle positions, i.e., areas where a vehicle cannot drive. Let $\mathcal{U}\{\mathbf{x}_i(k)\}$ define the geographical position of the vehicle i , thus, the set of valid positions $\Gamma_i(k)$ for this vehicle is denoted as

$$\Gamma_i(k) = \Omega \setminus \left(\bigcup_{l=1}^N \mathcal{U}\{\mathbf{x}_l(k)\} \right), \quad (5.6)$$

where $\mathcal{U}\{\mathbf{x}_l(k)\}$ is the set of positions occupied by vehicles including the own state information from vehicle i and the information contained in $\mathbf{Y}(k)$ from the remaining vehicles. The set of valid positions $\Gamma_i(k)$ is restricted due to the physical and design constraint of the vehicles, i.e., acceleration, speed and vehicle dimensions. Therefore, after estimating all the possible future positions, the coordination scheme clusters them in order to reduce the complexity. For each obtained cluster, the center of gravity, speed, and direction of the car are used to select the next safe position. As a result, every vehicle in the network has its own set of possible positions with the constraint that $\Gamma_i(k) \cap \Gamma_j(k) = \emptyset$ for every vehicle $i \neq j$.

Additionally to the implicit coordination for safety maneuvers, we propose to use explicit coordination between vehicles and infrastructures to optimize the network and achieve consensus in the shared knowledge as defined in equation (5.3). The explicit coordination concept implies the management of network elements using communication protocols in order to improve the network cognition. The main benefit of the communication between the vehicles and the different infrastructures is to extend the electronic horizon, due to the short-range of communication obtained by the on-board equipment. Additionally, this is the main motivation for deploying the infrastructures alongside the road improving the range of the network communication. Therefore, the explicit coordination scheme requires a centralized architecture to collect the exchanged information and share it with the rest of network members. In order to accomplish an optimal coordination, three different layers are implemented following as guideline the system proposed in Section 3.1:

1. **V2V communication:** between the cars which are in the same platoon and in a short-range of communications. Using the V2V scheme, the vehicles share their local knowledge. In order to obtain a feasible communication scheme, we proposed a framework based on one of our works [9], where the vehicles are clustered based on a game-theoretical approach. The vehicles share their local knowledge by means of a beacon $\mathbf{m}_i(k)$ defined by

$$\mathbf{m}_i(k) := (\mathbf{p}_i(k), \mathbf{v}_i(k), \gamma_i(k)),$$

where $\mathbf{p}_i(k) \in \mathbb{R}^r$ is the absolute car position, $\mathbf{v}_i(k) \in \mathbb{R}^r$ is the current speed and $\gamma_i(k) \in \mathbb{R}$ is the angular heading of the i th vehicle. Therefore, the beacon message $\mathbf{m}_i(k) \in \mathbb{R}^{2r+1}$ has the form of a row vector. The main application of V2V communication is to share local knowledge of the cars in the same cluster, in order to obtain the complete knowledge of their surroundings along with the information from the infrastructure. Additionally, we propose in Section 5.3.2 a system for platoon management in out-of-coverage networks supported solely by V2V communications.

2. **V2I communication:** between several cars and the infrastructure they belong to. This method of coordination is an extension of the V2V communication scheme shown before. The shared knowledge contained in the messages $\mathbf{m}_i(k)$ is, in this case, sent to the infrastructure which stores all the information from the nodes. Hence, the infrastructure plays the role of a Data Center Unit (DCU) while the vehicles serve as sensors of a bigger network (system of systems).
3. **Infrastructure to Infrastructure Communication (I2I):** between different infrastructures using a long-range communication protocol, namely LTE. The last layer of our communication scheme aims to spread the information among the different network elements obtaining a fully connected network. The main application of the I2I scheme is to optimize the traffic routing using the gathered information.

5.2 Cooperative Platoon Formation

5.2.1 Platoon formation and advantages

The concept of platooning systems has been brought up to increase the lane capacity, as one important aspect in future ITS. In a platooning system, fully automated vehicles driving in the same lane are able to form different platoons, in which vehicles are connected electronically and move together with a small inter-vehicle gap Δd , along with the intra-platoon distance ΔD as shown in Figure 5.2. In general, with the same speed, a higher lane capacity can be reached with a smaller inter-vehicle gap, however, as a trade-off, the stability of the traffic system decreases with the reduction of this inter-vehicle gap. In order to avoid traffic jams and collisions, a minimum inter-vehicle gap is required to ensure the traffic system stability such that $\Delta d > \Delta d_{min}$ so that any oscillation is not amplified upstream the traffic flow.

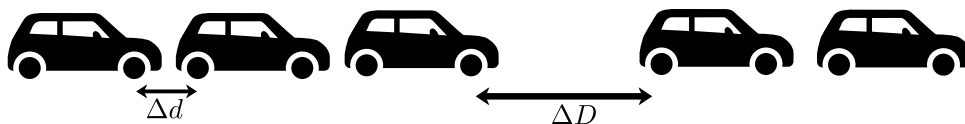


Figure 5.2: General platoon formation.

Many control schemes are proposed to achieve small demanded inter-vehicle gap under the constraint of traffic flow stability. For instance, Adaptive Cruise Control (ACC) is a local sensor-based control scheme, where via its local sensors, one vehicle is able to detect the gap towards its preceding vehicle and the speed difference between them. The maneuver decision, i.e., acceleration in longitudinal cruise control, can be determined using

the collected information, aiming at the desired speed and inter-vehicle gap. This scheme is an example of implicit coordination. Nevertheless, the aim of our system is to also include the communication system granting explicit coordination to the overall network.

For this matter, Cooperative Adaptive Cruise Control (CACC) is developed on top of the ACC. In a CACC scheme, the vehicles not only collect information via local sensors but also from wireless communication schemes, both V2I and V2V. Specifically, in car-following scenarios, one vehicle can be aware of its preceding vehicle's acceleration via V2V communication and use it as a reference value to determine its own acceleration. In addition, many studies have proved that CACC is able to maintain a smaller inter-vehicle gap than ACC under the same stability constraint. However, the performance of CACC suffers from communication delay since the received data is already outdated when the maneuver decision is made. Therefore, we need to add an adaptive behavior to our scheme in order to predict the traffic situation which is analyzed in Section 5.2.4.

Additionally, it is shown in [109] that a general leader-following scheme formed by several agents is able to achieve a system consensus based on the LaSalle invariance principle [110]. For this matter, we assume that the platoon formation consists of N vehicles including a leader, all of them connected using a graph formation denoted by \mathcal{G} . The weight of each of these connections are as follows

$$a_{ij} = \begin{cases} a_{ij}^* & \text{if vehicle in platoon} \\ 0 & \text{otherwise.} \end{cases} \quad (5.7)$$

Moreover, the vehicles can be modeled as a double integrator system, i.e., they are based on position and velocity as

$$\begin{cases} \dot{\mathbf{p}}_i(k) = \mathbf{v}_i(k), \\ \dot{\mathbf{v}}_i(k) = \mathbf{a}_i(k), \end{cases} \quad (5.8)$$

where $\mathbf{p}_i(k)$ is the vehicle position, $\mathbf{v}_i(k)$ is the velocity and $\mathbf{a}_i(k)$ is the acceleration of the i th vehicle. Moreover, $\dot{\mathbf{p}}_i(k)$ and $\dot{\mathbf{v}}_i(k)$ define the derivate with respect to the discrete time k of the vectors $\mathbf{p}_i(k)$ and $\mathbf{v}_i(k)$, respectively.

5.2.2 Game theoretical approach for platoon creation

The first step of our platooning scheme is to create cooperative platooning formations using game-theory. Similar to human behavior, game-theory approaches face the problem of the selfishness of autonomous systems. Therefore, it is required to motivate the autonomous vehicles to cooperate in order to optimize the system. A joint global goal is added to the game-theory framework, so that the autonomous vehicles will aim for the optimal decision, not only for themselves but also for the general system. Several studies have been conducted using a game-theory approach in order to implement platooning, especially for trucks. However, in most of these studies, the inclusion of communication schemes for the intra-platoon management was not considered, and hence, optimal cooperation schemes based on communication with different vehicles were not achieved [111, 112]. Following the principles of the development of autonomous systems as stated in [113], we focus on the use of utility-based functions.

In the model described in one of our previous works for out-of-coverage networks [8], the first vehicle of a platoon is considered as the platoon leader and scheduler. All the vehicles in the platoon travel using the same car-following model and the pace is marked by the preceding car. However, in a more general model, including the network model defined in Section 3.1, the infrastructure plays the role of a scheduler and not the platoon leader. Using the infrastructures in order to manage the network has several advantages, such as extending the electronic horizon due to its higher altitude, in addition to the exchange of information between different infrastructures enabling optimal traffic routing. Grouping vehicles in platoons is the optimal formation not only for the traffic flow rate but also for the fuel or energy consumption of the vehicles, especially in the case of heavy trucks [114].

In our system model, it is assumed that every autonomous vehicle has a predefined initial position and final destination known by the infrastructure. Hence with the layout of the road network, Ω is preloaded in the infrastructure, making possible to predict the position of each vehicle i at every time instant. The network can be defined as a graph by a set of links \mathcal{A} where $\alpha_{i,j} \in \mathcal{A}$ is the link between the node α_i and the node α_j (which is translated to the pair of vehicles i and j). Moreover, the density of vehicles for each link, $\lambda_{i,j}(k)$, can be predicted and updated accordingly using the information gathered by the infrastructures.

5.2.3 Coalitional formation game-theory approach

From previous sections, we conclude that forming platoons is the most efficient way to organize the vehicles in the network. Accordingly, we define our *problem statement*: a coalitional game-theory approach is defined considering the particular properties of our scenario, i.e., physical restrictions, communication among vehicles and fast changing environment while forming coalitions to optimize the traffic flow. In general, maximizing the individual utility function for each vehicle independently does not provide a global optimization, since the payoff of each player is dependent on the joint actions of the rest of players. Thus the game can be defined as Non-Transferable Utility (NTU) [115], where the value of a coalition $s \in \mathcal{S}$ is no longer a single value, but a set of utility function vectors $\nu(s) \in \mathbb{R}^{|s|}$, depending on the actions of the rest of players. Under these assumptions, a dynamic coalition formation game is mathematically defined as

Definition 1. *Dynamic Coalition Formation Game*

1. *Finite set of players \mathcal{N} forming a set $\mathcal{S} = \{1, \dots, S\}$ of disjoint coalitions such that it is satisfied $\mathcal{N} = \bigcup_{s=1}^S s$.*
2. *Creating coalitions may benefit the players involved, but there are also costs of forming a coalition, hence forming grand coalitions is usually not the optimal decision.*
3. *Finite set of potential actions \mathcal{C} for each player limited by the road network and safety constraints (see Section 5.1.2).*
4. *The game is defined as dynamic since the actions of the players may bring changes in the strength of the players and to the coalition formation.*

5 Cooperative Scheme for Connected Vehicles

The game is defined using the triplet $(\mathcal{N}, \nu, \mathcal{S})$ where the value of a coalition $s \in \mathcal{S}$ is denominated as $\nu(s)$. Since we are using a formation game, i.e., the network structure and costs to form coalitions play a major role, the value for each coalition has the *restriction property* [116], and hence, the value $\nu(s)$ has to be calculated in two steps: i) Consider the set of coalitions \mathcal{S} independent of each other and calculate the value of each one (by using the canonical definition) as

$$\nu(s) = \sum_{\forall i \in s} \phi_i(\nu), \quad (5.9)$$

where ϕ_i is the payoff given to the player i belonging to the coalition s by the Shapley value ϕ which is defined as

$$\phi_i(\nu) = \sum_{s \subseteq \mathcal{N} \setminus \{i\}} \frac{S!(N-S-1)!}{N!} [\nu(s \cup \{i\}) - \nu(s)], \quad (5.10)$$

where S and N are defined as the cardinality of the set of coalitions s and the set of players \mathcal{N} , respectively. Moreover, in the second step; ii) The resulting value of the game $\nu(s)$ is the $1 \times S$ vector of payoff functions constructed by combining all the restricted game values $(s, \nu|s)$.

Using the proposed scheme, we analyze the dynamic coalition formation game from bottom to top by means of three different utility functions; individual, coalitional and global as shown in Figure 5.3. The first level is the individual utility function ν_i for a player $i \in \mathcal{N}$ which considers the local environment, i.e., its own state vector, and the information shared by the infrastructure. The next level corresponds to the coalitional utility function which motivates the creation of coalitions. This function defines the trade-off between the maximization of the individual utility function and the global utility function of the network. Finally, the global utility function is defined where the players are not individuals, but coalitions created by several of them.

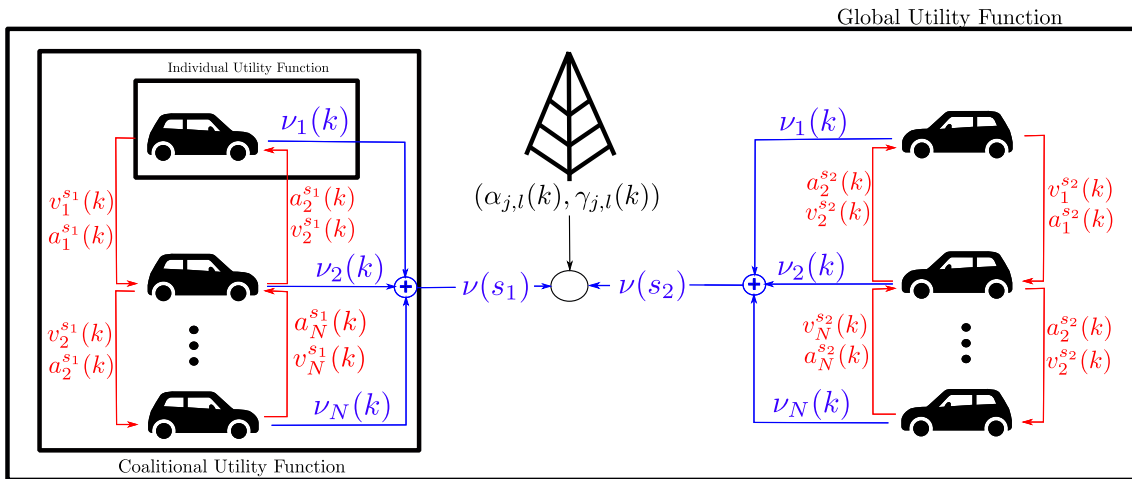


Figure 5.3: Dynamic coalition formation game overview.

Individual utility function

In order to formalize the dynamic coalitional game framework, each vehicle $i \in \mathcal{N}$ has an individual utility function as follows

$$\nu_i(k) = f(d_i(k), \tau_i(k), \xi_i(k)), \quad (5.11)$$

where $d_i(k)$ is the distance from the actual position of the player to the destination, $\tau_i(k)$ is the travel time from the vehicle position to the destination and $\xi_i(k)$ is a congestion tax created in order to stimulate the creation of coalitions. In this case, $\tau_i(k)$ is linearly related to the density of vehicles. The congestion tax variable for a given position, $\xi_i(k) = \tau_i(k) \cdot f_i(\lambda, k)$ where $\lambda \in \mathbb{Z}$ is the number of vehicles driving in the road simultaneously. The congestion tax form can be justified by the idea that in a road with more vehicles, it is more likely to create platoons (which are the optimal way of traveling). However, to avoid a high congestion in a single road path, the variable $\tau_i(k)$ is included penalizing a low speed in the given path. Using both considerations, we obtain a scheme where the platoons are created with a high probability without negatively congesting the network.

Coalitional utility function

The main goal of our approach is to create coalitions where the total payoff of this particular organization is smaller than other possible coalition \mathcal{D} , i.e., $\nu(\mathcal{S}) < \nu(\mathcal{D})$. Therefore, in order to motivate the vehicles to join a coalition, and consequently, obtain an optimal management of the traffic, the following concept must be fulfilled:

$$\nu(s) \leq \sum_{i=1, i \in s}^{|s|} \nu_i(k). \quad (5.12)$$

This concept follows the *Pareto order* which states that a player i belonging to a platoon s will stay in the same coalition if at least one player belonging to s improves its utility function without hurting any of the other players. Hence, if equation (5.12) is fulfilled no individual vehicle would have the incentive to abandon the coalition since the individual utility function outside a coalition is always smaller, or at best equal, compared to the coalitional utility function. Therefore, the optimization problem for the coalitional utility function is defined as follows

$$\underset{\substack{d_i(k), \tau_i(k), \\ \xi_i(k)}}{\text{minimize}} \quad \sum_{i=1}^S \hat{\nu}_i(k), \quad (5.13a)$$

$$\text{s. t.} \quad \hat{\nu}_i(k) = f(\hat{d}_i(k), \hat{\tau}_i(k), \hat{\xi}_i(k)). \quad (5.13b)$$

The value $\hat{\nu}_i$ is defined using the optimal values for the coalition s which satisfies equation (5.12) and fulfills the condition $\nu(s) > \nu(\mathcal{D})$, however, they do not need to be the optimal for the individual payoff function ν_i . It is important to mention that the coalitional utility function, $\nu(s)$, should be fair for each vehicle $i \in s$, i.e., no vehicle should be left starving which in game-theory is analogous to $\hat{\nu}_i(k) \rightarrow \infty$. In order to update the cost function given the parameters $d_i(k), \tau_i(k), \xi_i(k)$, the infrastructure requires the following information:

5 Cooperative Scheme for Connected Vehicles

- State vector for each vehicle i : $\mathbf{m}_i(k) = (\mathbf{p}_i(k), \mathbf{v}_i(k), h_i(k))$.
- Initial and desired final position (f_0^i, f_f^i) for each vehicle i .
- Road network information and cost coefficients $(\alpha_{j,l}(k), \gamma_{j,l}(k))$ for each path between the pair of edges (j, l) .

Moreover, each individual vehicle in this scenario is also able to take evasive and safety decisions on its own and without the assistance of the infrastructure, as a way to improve the safety against disconnections, following the principles of implicit coordination as described in Section 5.1.2.

Global utility function

Once the coalitions are formed and the coalitional function is maximized, we proceed in a way where the global utility function is enhanced by the centralized architecture. In practice, due to the communication limitations, in both range and reliability, the number of members for each platoon is limited. In order to obtain an optimal system where all the different coalitions help to maximize the general utility function, the cost coefficients $\alpha_{j,l}(k)$ and $\gamma_{j,l}(k)$ are estimated using the infrastructure. These parameters provide external information to the players in order to adjust their payoff function. The chosen coefficient will be the one maximizing the general utility function, even if it is not optimal for the individual or coalition utility function. The use of an infrastructure contributes to adding global perception to the system, along with the distributed perception of each individual vehicle.

5.2.4 Cooperative adaptive cruise control

A novel platooning control system

Based on the discussions so far, we propose a novel platooning control system that enables a prediction based control within a platoon. As shown in Figure 5.2, vehicles moving on the road can be grouped into different platoons and the platoon length is limited by the reliable communication range. Vehicles in the same platoon are time synchronized and they adapt their maneuvers simultaneously every adaptation period of T . The adaptation period T has to be larger than the maximum allowed communication delay, e.g., 100 ms for 10 Hz CAM message. At the beginning of each adaptation period, each vehicle generates a driving status message and waits for transmission. During the adaptation period, each vehicle broadcasts its own driving status message and receives the messages from other vehicles in the same platoon. Note that, since vehicles in the same platoon are within each other reliable communication range, they can receive each other messages with a high success rate. After receiving the associated messages, each vehicle determines its local maneuver decision and adapts its maneuver at the end of the adaptation period.

Time synchronized discrete control process

The proposed platooning scheme requires synchronous maneuver operation according to a common clock base, e.g., according to the Global Navigation Satellite System (GNSS) clock. During the time between two maneuver operations, which is defined as one adaptation period, we assume that the acceleration of a vehicle remains unchanged.

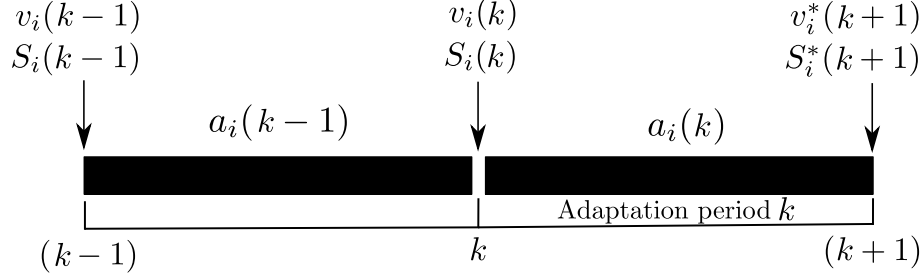


Figure 5.4: Time synchronized discrete control.

Figure 5.4 illustrates an example with two adaptation periods, where each adaptation period has a duration of $k = mT$. At time point $(k-1)$, a vehicle having velocity $v_i(k-1)$ and distance $S_i(k-1)$ towards the preceding vehicle adapts its acceleration to $a_i(k-1)$. The vehicle keeps this constant acceleration for a time period k till the next adaptation at time k when it changes its acceleration to $a_i(k)$. Since the maneuver decision of cooperative driving can only be made after the vehicle receives all necessary messages from the surrounding vehicles via V2V communication, the adaptation period k shall be large enough to accommodate the V2V communication delay, including potential retransmissions.

Traffic situation prediction

One reason for having such a synchronized discrete control scheme is that it is possible for vehicles to predict upcoming traffic situation and make their maneuver decisions based on predicted up-to-date information. For instance, at time $(k-1)$ two adjacent vehicles, e.g., vehicle i and $i+1$, broadcast their driving status messages including distance $S(k-1)$, speed $v(k-1)$ and acceleration $a(k-1)$. After a certain V2V communication delay, vehicle i receives the message from vehicle $i+1$ and tries to determine the maneuver decision, i.e., $a_i(k)$ as shown in equation (5.17), for the next adaptation period. The traffic situation experienced by vehicle N at time k is represented by its own speed $v_N(k)$, the speed of its preceding vehicle $v_{i+1}(k)$, the distance towards its preceding vehicle $S_i(k)$ and the acceleration of its preceding vehicle $a_{i+1}(k)$. $v_i(k)$, $v_{i+1}(k)$ and $S_i(k)$ can be predicted from the sensed and received information valid at time $(k-1)$ using equations (5.14)-(5.16). The prediction of $a_{i+1}(k)$ is more complicated since it further requires predicting the traffic situation experienced by vehicle $i+1$ at time k , i.e., $v_{i+1}(k)$, $v_{i+2}(k)$, $S_{i+1}(k)$ and $a_{i+2}(k)$.

$$v_i(k) = (v_i(k-1) + a_i(k-1)) \cdot T, \quad (5.14)$$

$$v_{i+1}(k) = (v_{i+1}(k-1) + a_{i+1}(k-1)) \cdot T, \quad (5.15)$$

$$S_i(k) = S_i(k-1) + (v_{i+1}(k-1) - v_i(k-1) \cdot T) + 0.5 \cdot k^2(a_{i+1}(k-1) - a_i(k-1)), \quad (5.16)$$

$$a_i(k) = f_{\text{control}}(v_i(k), S_i(k), a_{i+1}(k), v_{i+1}(k), S_{\text{min}}, k_g, T). \quad (5.17)$$

Limitations from communication system

In order to implement the control scheme in real platooning scenarios, practical issues such as communication range, delay and reliability in the communications limit the system performance. As emphasized in the previous section, prediction of the preceding vehicle's maneuver intention, i.e., acceleration in longitudinal cruise control, is crucial to determine the optimal local maneuver decision. Actually, predicting the acceleration at time instant k of any vehicle requires the known acceleration of its preceding vehicle at time k or to have the already predicted value. This scheme results in a prediction chain. The maneuver intention prediction, i.e., acceleration of the preceding vehicle, would follow a chained scheme which is done sequentially from the vehicle at the very front. Ideally, with unlimited communication range, one vehicle can be aware of the global traffic situation and predict other vehicles' maneuver intentions precisely. However, with limited communication range, the perception range is also limited.

In addition, although the inter-vehicle time gap can be reduced to zero as illustrated in Figure 5.5 and Figure 5.6. It may be reasonable to have the inter-vehicle time gap k_g , larger than the adaptation period k to avoid collisions caused by system errors.

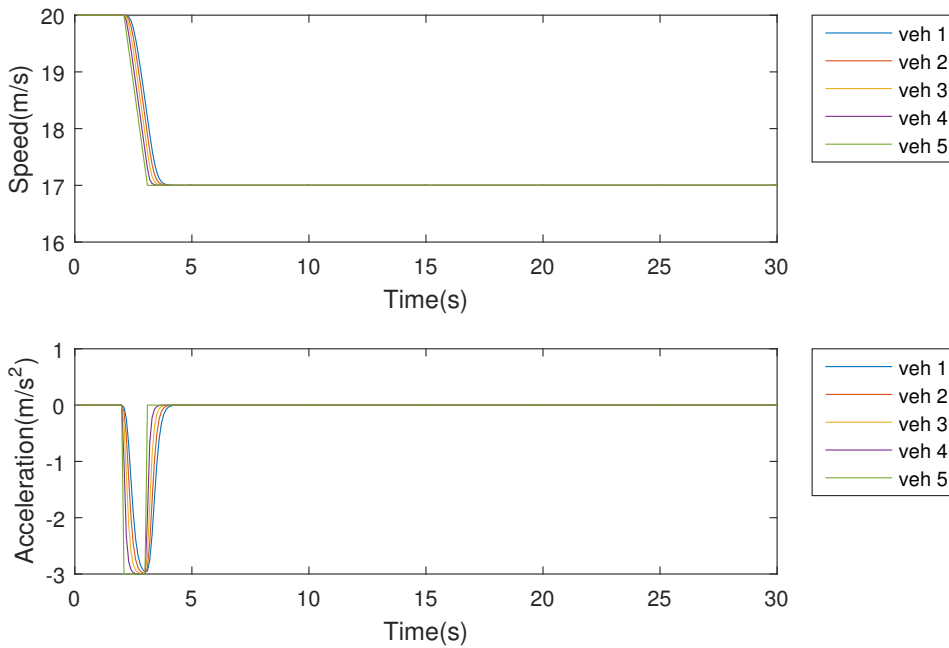


Figure 5.5: Traffic system response with 0.1s time gap.

For instance, assuming one vehicle fails to receive the message from its preceding vehicle who starts to brake, the following vehicle would keep moving with the same speed in the

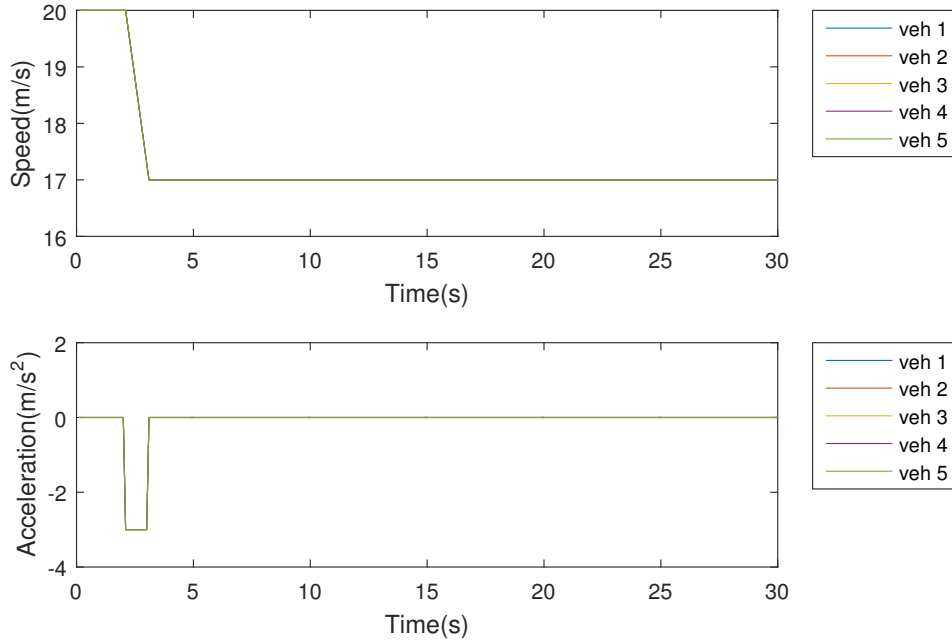


Figure 5.6: Traffic system response with 0s time gap.

next adaptation period. However, the following vehicle can be aware of the deceleration at the front by sensing, and also starts to brake after the next adaptation period. In this case, the following vehicle actually reacts to the deceleration of its preceding vehicle after a delayed time of one adaptation period k . Hence the collision can be avoided if the gap between two vehicles is larger than $v \cdot k$.

Moreover, control related V2V communication usually requires extremely high reliability for safety reasons. For instance, in future 5G ITS, a 99.999% reliability is demanded in some applications. Such reliability requirement can be used to define a reliable communication range, where any V2V communication within this range has a reliability higher than the demanded threshold and can be regarded as a reliable link.

Control law

Assuming the up-to-date traffic situation can be obtained through prediction, here we discuss the control law, i.e., the algorithm to determine the maneuver decision. Assuming a homogeneous traffic flow, where all vehicles follow the same control law, the maneuver of every vehicle aims at reaching the equilibrium as fast as possible, preferably within one adaptation period k . As also shown in Figure 5.4, if any perturbation to the traffic flow is introduced at time $(k - 1)$, then the acceleration/deceleration $a(k)$ at each vehicle is determined such that after the adaptation at time k , equilibrium, which is represented by desired speed $v^*(k + 1)$ and desired inter-vehicle gap $S^*(k + 1)$, can be achieved at time $(k + 1)$, if no further perturbation is introduced.

On the one hand, one vehicle wants to reach the maximum speed v_{max} allowed by the traffic regulations at the next time instant $(k + 1)$ as expressed in equation (5.18). On

the other hand, it also wants to keep a desired gap towards its preceding vehicle, where the desired inter-vehicle gap equation (5.19) at time $(k + 1)$ is the summation of the minimum inter-vehicle gap S_{min} , the production of speed $v(k + 1)$, and time gap k_g . The acceleration to reach the desired inter-vehicle gap at time $(k + 1)$ can be derived using predicted information at time $k = mT$ as in equation (5.20). The acceleration $\mathbf{a}(k)$ in equation (5.21), which is reached at time k , is chosen to be the smallest among velocity oriented acceleration a_v , and the inter-vehicle gap oriented acceleration a_s . The acceleration value $\mathbf{a}(k)$ is also bounded by the vehicle's maximum acceleration a_{max} and deceleration b_{max} capability as defined in equation (5.21).

$$a_v(k) = \frac{1}{T}(v_{max} - v(k)), \quad (5.18)$$

$$S^*(k + 1) = v(k + 1) \cdot k_g + S_{min}, \quad (5.19)$$

$$a_s(k) = k_a \cdot a_p(k) + k_v \cdot (v_p(k) - v(k)) + k_s \cdot (S(k) - S^*(k)), \quad (5.20)$$

$$\mathbf{a}(k) = \text{bound}(\min(a_v, a_s), -b_{max}, a_{max}). \quad (5.21)$$

Additionally, the values k_a , k_v and k_s are defined as follows

$$k_a = \frac{0.5 \cdot T^2}{0.5 \cdot T^2 + T \cdot k_g}, k_v = \frac{T}{0.5 \cdot T^2 + T \cdot k_g},$$

$$k_s = \frac{1}{0.5 \cdot T^2 + T \cdot k_g}.$$

Stability analysis

System stability is usually indicated by the transfer function in frequency domain. The system is stable if the magnitude of the system transfer function is less or equal to one $|\Gamma(z)| \leq 1$ over the whole spectrum [117]. Since the traffic system using the proposed control scheme is a discrete system, a Z transformation is applied here. Besides, in a car-following scenario, the vehicles determine their own maneuver mainly based on the acceleration/deceleration given by $a_s(k)$. Therefore, a transfer function can be derived from equation (5.17) as follows

$$\Gamma(z) = \frac{A(z)}{A_p(z)} = \frac{0.5 \cdot T \cdot z + 0.5 \cdot T}{(0.5 \cdot T + k_g) \cdot z + 0.5 \cdot T - k_g}. \quad (5.22)$$

The magnitude of transfer function $|\Gamma(z)|$ is plotted in Figure 5.7 with an assumed adaptation period $T = 0.1s$, i.e., the maximum communication delay of 10 Hz CAM messages, and different time gap values $k_g = \{0.5, 0.1, 0\}$ seconds. Owing to the properties of the transfer function, the severe fluctuation can be observed in the plot. Although the curves are not smooth, some general tendencies can be observed. First, curves are always below 0 dB within the spectrum window, which indicates that the system is always stable regardless of the chosen time gap value. Besides, when the time gap becomes larger, a more stable system is implied by the reduction of the transfer

function magnitude. Moreover, the system performance with zero time gap $k_g = 0s$ is worth mentioning. When time gap is zero, the transfer function is always equal to 1, i.e., 0 dB, within the whole spectrum. This leads to an interesting phenomenon that whenever there is no time gap between two neighboring vehicles controlled by the proposed scheme, the following vehicle would simply mimic the acceleration of its predecessor $a(k) = a_p(k)$ and all vehicles behave as one unit.

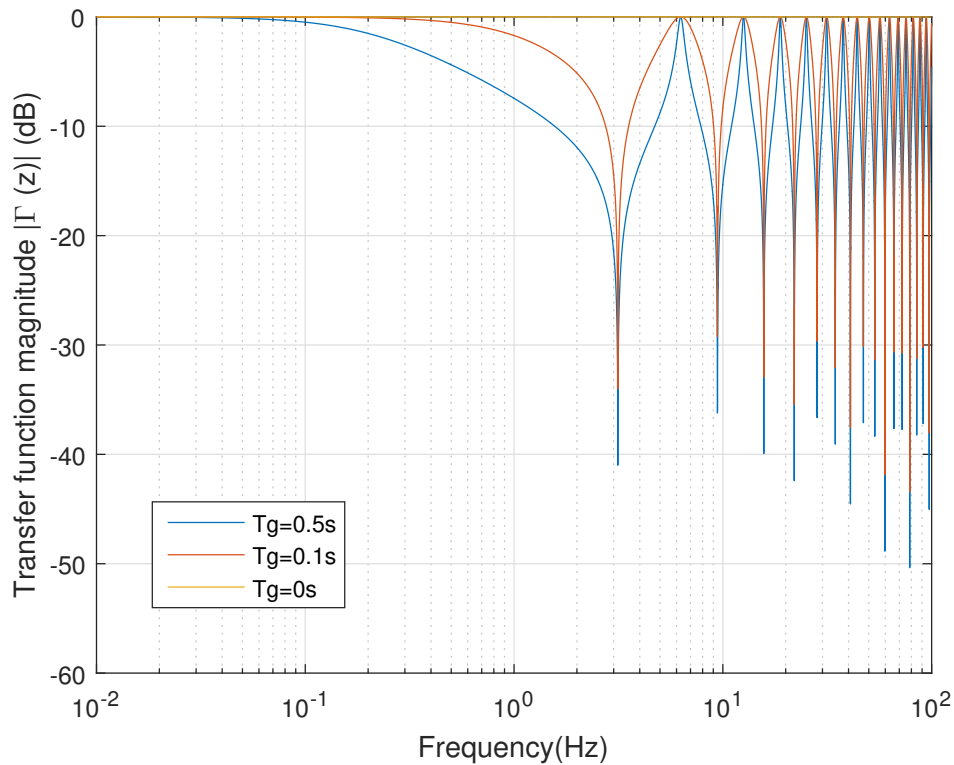


Figure 5.7: Stability analysis for the proposed platoon scheme.

5.2.5 Numerical results

In order to validate the theoretical framework introduced in the previous sections, a realistic simulation is implemented. The simulation is performed considering a road network as depicted in Figure 5.8, and its equivalent in graph form as shown in Figure 5.9. The graph-form network is formed by the nodes (roadway points), and the weights of the edges connecting these nodes. The vehicles are generated using a Poisson distribution, and the initial and final node of each vehicle is chosen randomly from the entire set of nodes. The communication scheme parameters and mobility characteristics of the system used in the simulation are shown in Table 5.1.

For the simulation parameters, the values presented in Table 5.1 were considered to be the standard values used in vehicular communications. In order to obtain a realistic simulation, we have also taken into consideration the limitations of the road network and the communication scheme as analyzed in Section 5.2.4. The proposed model is compared with two different approaches. The first one is the simplest routing algorithm, based on the

Table 5.1: Simulation parameters.

Mobility System	
Parameters	Value
Number of vehicles	40
Vehicle length	5m
Minimum inter-vehicle gap	1m
Inter-platoon time gap	1s
Intra-platoon time gap	0.1s
Adaptation period	0.1s
Max. vehicle speed	50 km/h
Communication System	
Parameters	Value
Carrier frequency	5.9 GHz
Channel bandwidth	10 MHz
Number of sub-bands	2
Sub-band bandwidth	5 MHz
CAM message size	300 bytes
Transmission power	23 dBm

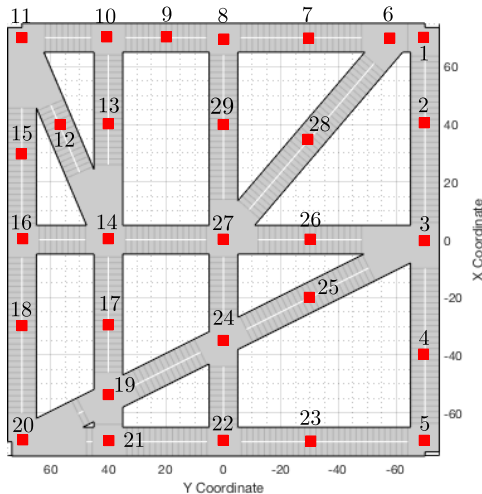


Figure 5.8: Roadmap network for the simulation example.

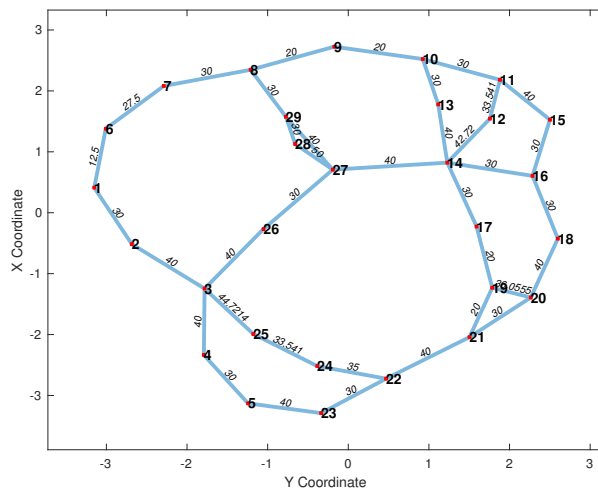


Figure 5.9: Graph form of the network including the weights for each edge.

shortest path, with no incentives to create platoons, and no inter-vehicular communication to optimize the traffic flow. The second approach is published in [112] which includes an incentive for a certain number of trucks in order to form platoons. This scheme has no centralized architecture, and additionally, does not optimize the traffic flow by means of minimizing the inter-vehicular distance.

The goal of our game-theoretical approach is to motivate the creation of platoons, hence we aim to route most of the vehicles by the same routes to motivate the creation of coalitions, nevertheless avoiding extreme congestion. Additionally, the second goal is to minimize the time to the destination of the vehicles, i.e., use the platoon formations and the global

perception to detect the fastest routes for the particular vehicles. Therefore, the first parameter to analyze is the load per path, and additionally compare it with the other two approaches as shown in Figure 5.10.

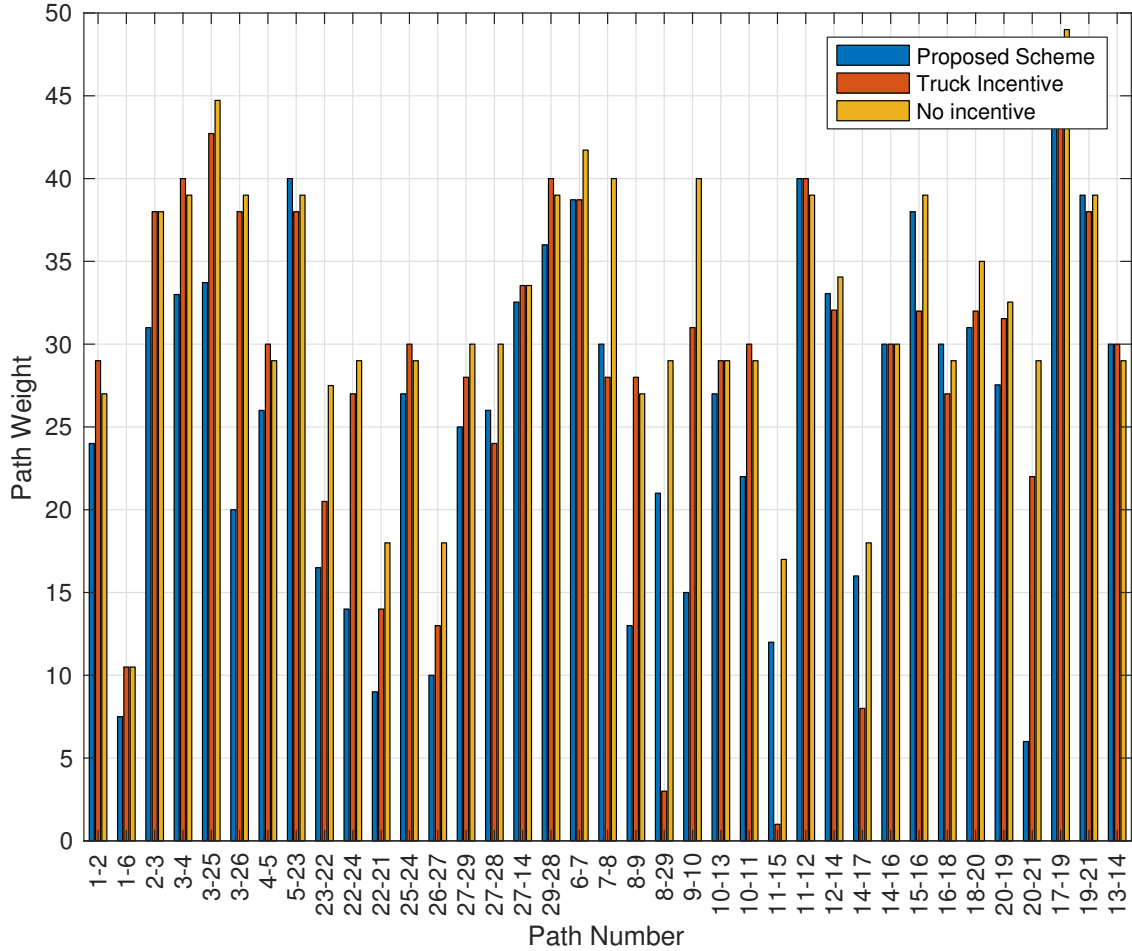


Figure 5.10: Load for each path comparing the three schemes.

Table 5.2: Statistical analysis for the load per path.

	Mean	Std. Dev. (SD)
No Incentive Scheme	31.7724	8.3413
Truck Incentive Scheme [112]	28.5292	10.8876
Proposed Incentive Scheme	25.8265	10.3222

The simulation results show a lower mean load per path (see Table 5.2) in our scheme compared to the other two, which results in a minimization of the overall network costs. Moreover, in comparison with the no incentive scheme, the standard deviation is higher indicating the motivation to drive in some paths over others in order to create platoons. Regarding the scheme proposed in [112], the mean load per path is higher than in our case, due to the lack of an inter-platoon optimization scheme, and that not every vehicle has

5 Cooperative Scheme for Connected Vehicles

the equipment to form coalitions. Moreover, the statistical analysis, in Table 5.2, shows the improvement in network costs obtained by means of the infrastructure.

The second parameter under consideration is the mean travel time to destination for the vehicles as shown in Figure 5.11. The goal of this parameter is evident, minimize the average time to destination for the vehicles. The statistical analysis shown in Table 5.3 presents that our proposed scheme outperforms both the no incentive scheme and the one proposed in [112]. It is noteworthy to mention that our scheme achieves the best results not only in average time travel to the destination, but also with the smallest standard deviation which is the indicator of a fair game, i.e., no vehicle is left starving. Furthermore, this parameter shows that introducing incentives in the network, in order to form platoons, improves the overall network performance in terms of average time to destination.

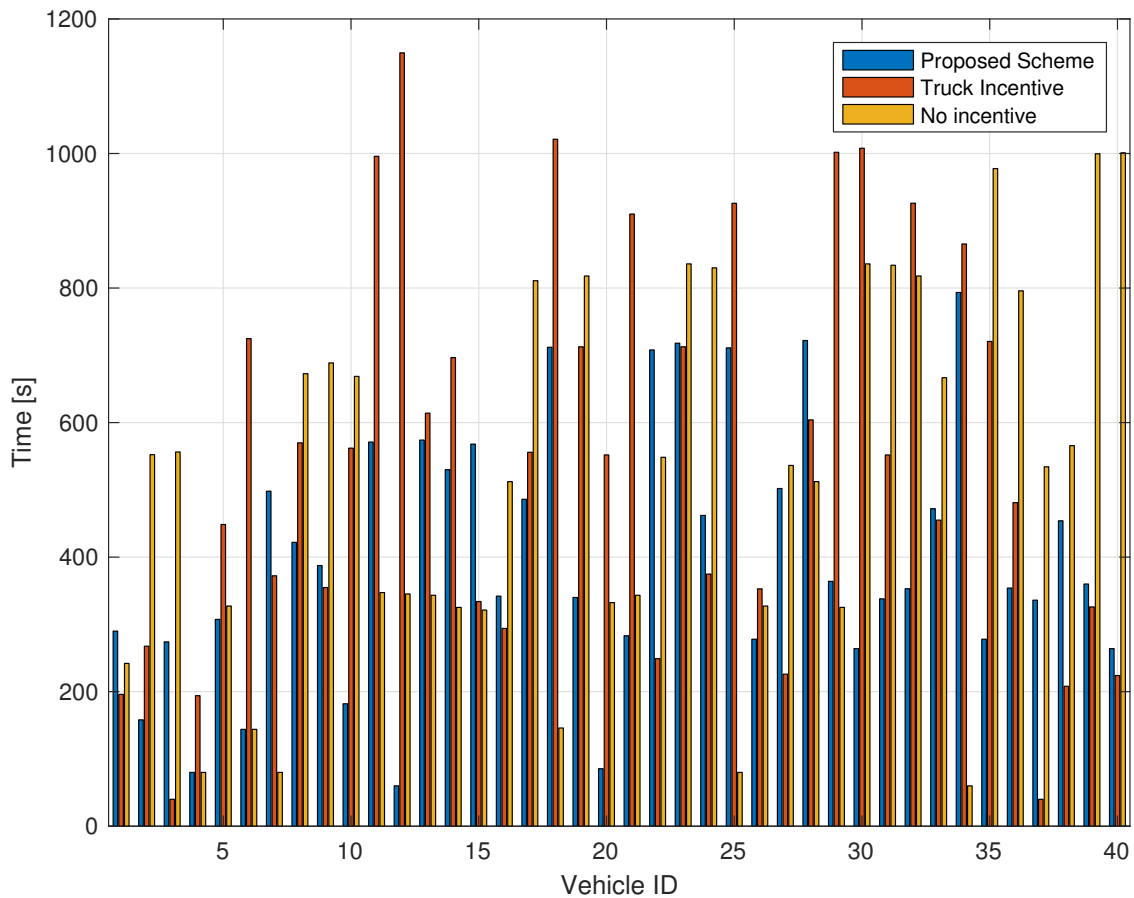


Figure 5.11: Travel time to destination for each vehicle comparing the three schemes.

Table 5.3: Statistical analysis for trip time to destination

	Mean [s]	Std. Dev. (SD) [s]
No Incentive Scheme	60.3190	32.2963
Truck Incentive Scheme [112]	54.5467	29.7141
Proposed Incentive Scheme	40.0651	19.0869

Platoon members follow the proposed control law in Section 5.2.4 and determine their maneuver decisions by starting the prediction chain from the platoon leader, i.e., the first vehicle in the platoon. However, to make platoon leader's maneuver intention predictable, the platoon leader has to adapt its maneuver only based on what has been sensed and included in its driving status message. Actually, each platoon leader, in this case, can be equivalently seen as one ACC vehicle. Assuming the ACC control law previously defined and the demanded inter-platoon time gap is found to be 1s by repeating the stability analysis as in Section 5.2.4.

Therefore, in such platooning systems, vehicles in the same platoon can keep an intra-platoon time gap as small as the adaptation period T , e.g., 100 ms when 10 Hz CAM message is used. Meanwhile, the inter-platoon time gap has to be relatively large, e.g., 1 s, to keep the traffic system stable. The reliability performance is measured by the packet reception ratio (P_{RR}) of intra-platoon V2V communication in equation (5.23).

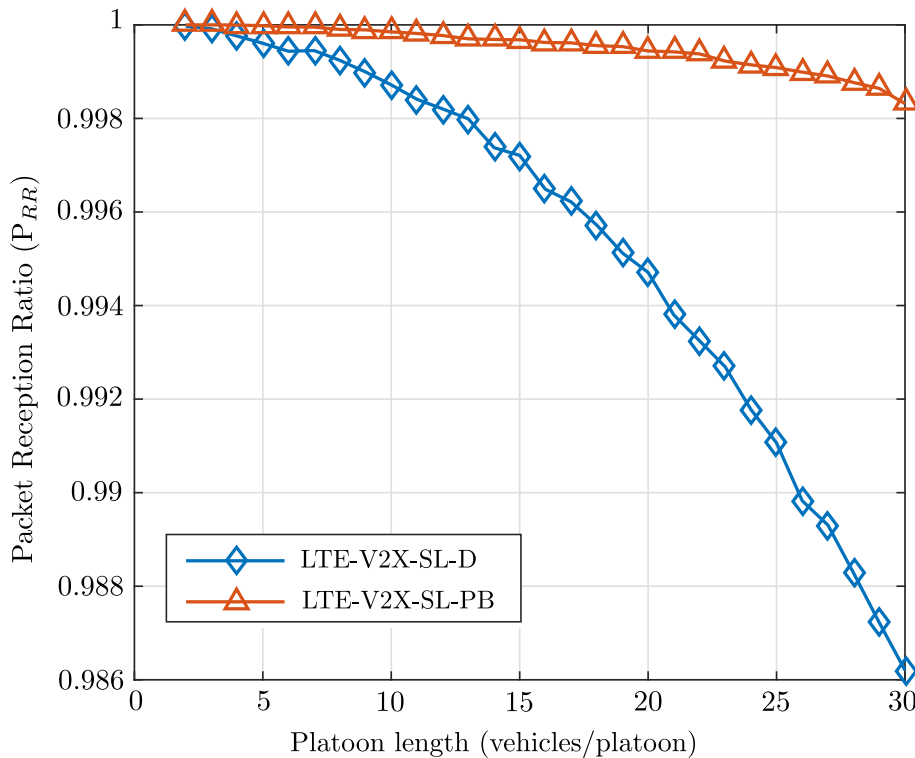
$$P_{RR} = \frac{\sum_{k=1}^K \sum_{j=1}^N R_{x_{k,j}}}{\sum_{k=1}^K \sum_{j=1}^N T_{x_{k,j}}}. \quad (5.23)$$

In which, K is the total number of scheduling period simulated, N is the total number of vehicles. $T_{x_{k,j}}$ stands for the number of effective transmissions, which can be also regarded as the number of target receivers within the same platoon, of vehicle j in a scheduling period ι . $R_{x_{k,j}}$ is the number of successful receptions among those effective transmissions of vehicle j in a scheduling period k .

The simulation result is shown in Figure 5.12. It can be seen that the intra-platoon communication using platoon based scheduling scheme has a higher P_{RR} than distributed scheduling scheme. When there are more vehicles in the platoon, the intra-platoon blocking and interference problems become more severe in distributed scheduling scheme. Therefore, the advantage of using a platoon based scheduling scheme becomes more apparent when the platoon length increases. Moreover, with the same reliability requirement, using platoon based scheduling scheme can support more vehicles in the same platoon than a distributed scheduling scheme, and the overall lane capacity may benefit from it.

5.3 Cooperative Communication Scheme

It is required to achieve a great reliability and low latency in V2V communications, and for that matter, we need to avoid collisions between the transmission in our system. In order to meet these requirements, we propose to optimize the scheduling scheme for the platoons for two different scenarios; out-of-coverage networks, and a scenario where umbrella coverage is available.

Figure 5.12: P_{RR} for platoon formation using CACC.

5.3.1 Semi-persistent scheduling optimization

The semi-persistent scheduling (SPS) combines a dynamic and persistent scheduling. SPS is particularly well-suited for vehicular communications due to the periodic nature of the exchanged messages and the required low-latency and high reliability. The principle of SPS is based on the following: the initial transmissions are persistently scheduled while the retransmissions and sporadic messages are scheduled dynamically. Each vehicle sends an uplink message to the infrastructure once it enters its coverage. Upon receiving the message, the eNB allocates part of the Transmission Time Interval-Resource Unit (TTI-RU) spectrum for the vehicle. These persistently allocated resources remain associated with the vehicle until it abandons the coverage area of the eNB or a timer expires, which are represented by the different colored pieces in Figure 5.13.

Using as the communication protocol LTE-V2X, each resource unit (RU) lasts for 10 ms and is divided in TTIs of 1 ms, which consists of a signaling access (SA) part and data. Following the standard, the resource units are periodically sent every $T = 100$ ms. Since we try to maximize the reliability of the link, the Signal-to-Interference-Noise Rate (SINR) for each link between two vehicles v_1^s and v_2^s belonging to the same platoon/coalition s , and connected to the same infrastructure n is as follows

$$\gamma_{v_{n,1}^s, v_{n,2}^s} = \frac{P_{v_{n,1}^s, v_{n,2}^s} G_{v_{n,1}^s, v_{n,2}^s}}{\sum_{j \in U} P_{n,j} G_{n,j} + \sum_{i \in V} P_{T_{n,i}} G_{n,i} I_{n,i} + \mathcal{M}}, \quad (5.24)$$

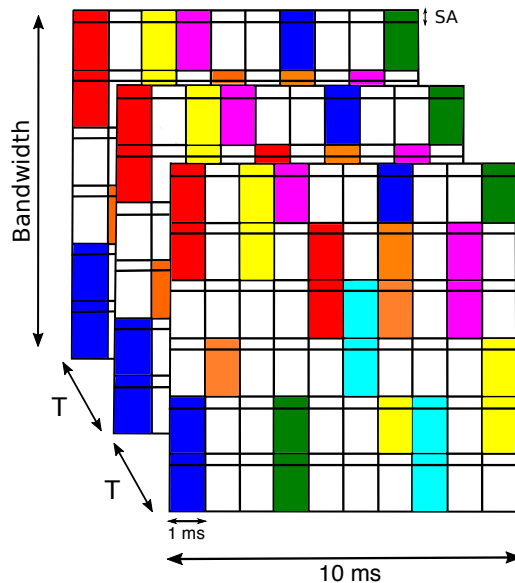


Figure 5.13: Semi-Persistent-Scheduling structure.

where $P_{v_{n,1}^s, v_{n,2}^s}$ is the transmitted power and $G_{v_{n,1}^s, v_{n,2}^s}$ is the signal gain. The first term in the denominator defines the interference created by collisions, i.e., two vehicles using the same resource block while the second term is the in-band emission interference (IBEI) produced by the leakage between sub-bands modeled as in [118, 119] and \mathcal{M} is the noise power. As shown in equation (5.24), the first term in the denominator models the interference created by the collisions of two vehicles using the same TTI-RU. However, using the SPS, this term can be neglected since each vehicle has previously allocated its resources. In addition to the persistently allocated resources, the retransmission needs to be rescheduled in a dynamic way. Therefore, the spectrum cannot be fully occupied only with the persistent resources.

The second term to optimize is the interference produced by the IBE. This interference is potentially an issue for the communication performance as studied in [120] since its value can be up to 30 dB if the variation in received power between adjacent TTI-RUs is high. Therefore, the clustering scheme shown in Section 3.3.2 where the vehicles are grouped in terms of their similarity metric, and our proposed platoon formation strategy is used to mitigate the interference. The advantage of both formation schemes is that the vehicles stay longer in the same formation, making the SPS more efficient since the persistently scheduled TTI-RU do not need to change. Adding the clustering scheme increases the complexity managing the network, however, since an infrastructure-based network is considered, the eNodeB has enough intelligence to optimally handle the resources. In addition, classifying the vehicles in platoons facilitates allocating the resources in an optimal manner, since the number of elements to consider is smaller. In the next subsections, an out-of-coverage scenario and an infrastructure-based scheme are analyzed.

5.3.2 Scheduling scheme for out-of-coverage networks

In the proposed platooning system in Section 5.2.4, V2V communication among vehicles in the same platoon is crucial to broadcast and receive control related messages. Using LTE-V SideLink (LTE-V2X-SL) with distributed scheduling achieves a higher V2V communication reliability than using IEEE 802.11p for CAM message transmission and reception. However, implementing LTE-V2X-SL with distributed scheduling directly in the proposed platooning system may experience a reliability reduction due to intra-platoon blocking and interference. Assuming each vehicle is equipped with one transceiver, it cannot transmit and receive at the same time owing to its half-duplex nature. As a result, when two vehicles broadcast their CAM messages using the same subframe, they cannot receive each other's message even if they are using different subbands. Furthermore, when two vehicles broadcast using the same resource, i.e., same subframe and same subband, not only blocking problem will be triggered, they also cause severe interference problem at other receivers.

To further improve the intra-platoon communication reliability, we propose a platoon based scheduling scheme based on the existing distributed scheduling scheme without requiring any external infrastructure. In platoon based scheduling scheme, instead of letting each vehicle perform spectrum sensing and resource selection individually, the platoon leader is in charge of scheduling for all vehicles in the same platoon. To be more specific, the platoon leader keeps sensing the channel, being aware of the idle resources and also monitoring its platoon members as well as their resource demand, i.e., a required number of 1 subframe \times 1 subband resources. When the intra-platoon V2V communication is activated, the platoon leader assigns resources in different subframes to platoon members. It makes first full use of the idle resources and randomly select from busy ones when additional ones are needed. A resource reservation timer is also generated and reduced by one after each scheduling period. Then, all vehicles within the platoon will transmit messages using assigned resources of different subframes in the next few scheduling periods until the timer expires. The platoon leader will repeat the scheduling process again at that time as depicted in Figure 5.14.

Figure 5.14 gives an example of platoon based scheduling, where one platoon consisting of four vehicles is trying to access resources for intra-platoon communication in the next scheduling period. Assuming each vehicle needs two 1 subframe \times 1 subband resources for transmission, the platoon leader selects eight idle resources of different subframes, and assign them to four vehicles. The advantage of this platoon based scheduling scheme is that by assigning resources of different subframes to vehicles in the same platoon, the intra-platoon blocking and interference problems can be solved. Note that, although there may be other methods to achieve better communication reliability in such a distributed system, letting platoon leader be a local scheduler could be the most practical way for implementation in a real scenario. This is because in platooning use cases, the platoon leader is usually in charge of the platoon management. Additionally, it keeps monitoring the status of the whole platoon and operates platoon merging or splitting. Therefore, platoon leader has the best knowledge of the platoon's overall status and resource demand.

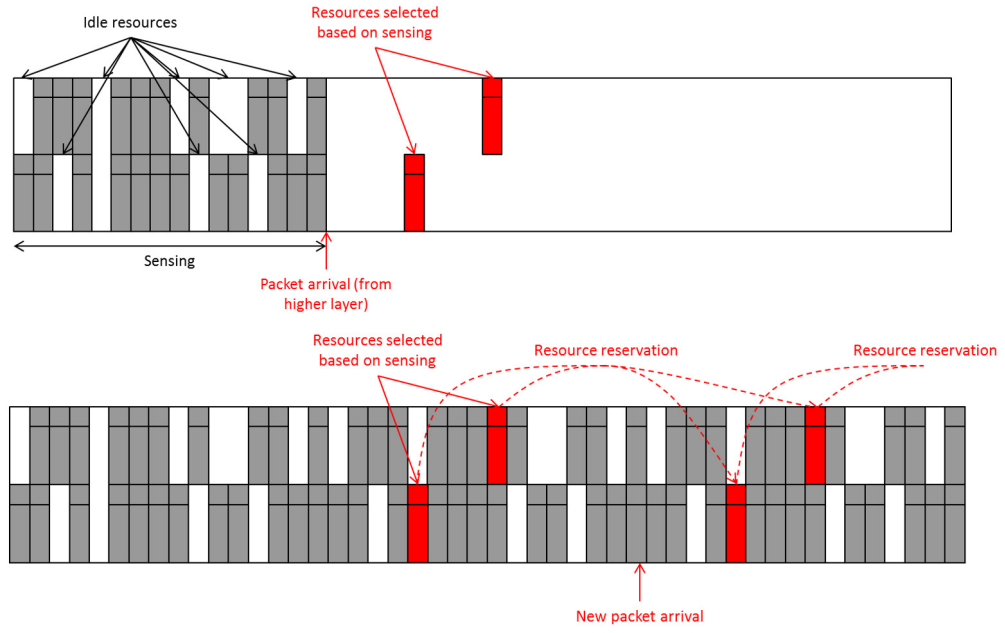


Figure 5.14: Distributed scheduling for out-of-coverage platoons.

5.3.3 Infrastructure-based prediction scheme using sub-pools

Traditionally, the SPS continues to allocate resources to a vehicle until it stays inactive for a determined period of time. However, this mechanism is not optimal, especially in a fast changing scenario, where the vehicles frequently change its position, moving to a different platoon or cell. Hence, using the information gathered by the infrastructure, it is possible to predict the vehicles next position in order to allocate the resources without waiting for inactive periods, based on a trajectory prediction using the physical limitations of the environment along with the vehicles state. This approach works not only in the case of a vehicle moving to a different cell, and hence, connecting to another eNodeB but also in the case of merging or leaving a platoon under the coverage of the same eNodeB. The environment information, i.e., the road architecture and traffic information, is used in order to predict the next position of each vehicle. A similar approach has been used in [121], where the authors focused on the density of vehicles without considering the microscopic nature of the traffic, i.e., individual state of each vehicle. An example of a complex scenario where the prediction scenario provides notorious improvement is depicted in Figure 5.15.

In this proposed scenario, a crossing is displayed with different intersections and possible directions for each vehicle. In order to create an accurate prediction, the eNodeB requires the following information:

- updated road information, i.e., connections between roads and traffic flow direction. It is also needed to periodically update this information to have the best prediction possible.
- state of each vehicle and its associated platoon: $\mathbf{y}_{n,i}^s(k) = (\mathbf{p}_{n,i}^s(k), \mathbf{h}_{n,i}^s(k), \mathbf{v}_{n,i}^s(k))^T$.

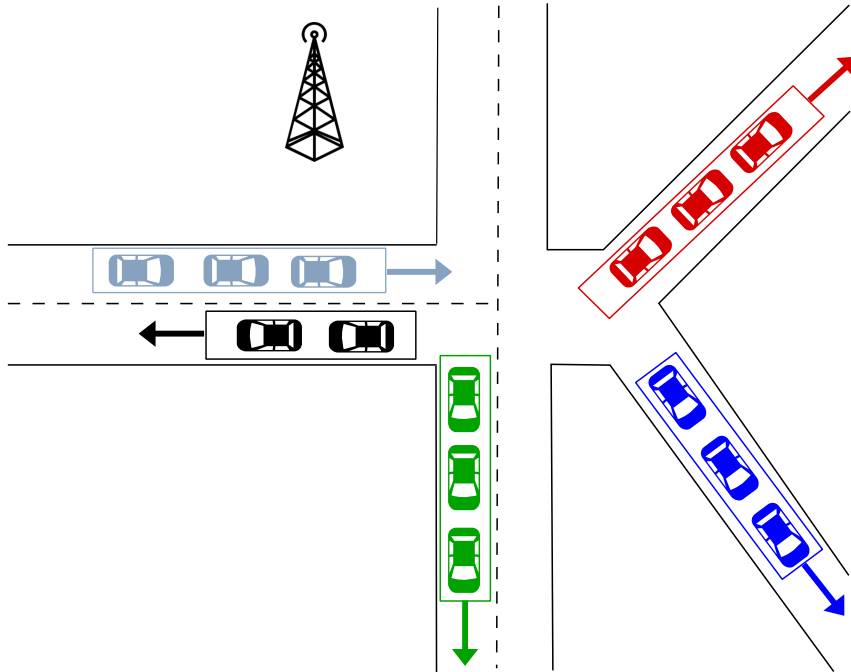


Figure 5.15: Complex prediction scenario.

- communication link between the different eNodeBs in the area. The interconnection of the eNodeBs has a double goal: first, to obtain a higher range for prediction and second, to add redundancy to the network.

Using the information of the vehicles i and $i + 1$, where $i + 1$ is the preceding car, the position prediction is done as follows

$$\mathbf{p}_{n,i}^s(k+1) = \mathbf{p}_{n,i}^s(k) + \mathbf{v}_{n,i}^s(k) \cdot k \cdot \mathbf{h}_{n,i}^s(k). \quad (5.25)$$

Moreover, in order to predict the position of the first vehicle in the platoon, i.e., the one with no preceding car, the updated road information is used to obtain the potential valid positions. Hence, with this information collected in the eNodeB, it is possible to predict the cluster members and their respective eNodeB connection.

This way of organizing the vehicles in the network solves another problem that arises when using SPS. Typically, each eNodeB has a dedicated pool of resources which is shared among all the vehicles under its coverage. However, the number of resources is sparse and it leads to disputes for these resources. Since we are organizing the vehicles into platoons, each of these platoon owns one subpool of the resources, i.e., we divide the spectrum into several subpools of resources. This scheme has a twofold goal: first there is no need for recalculating the transmission slots, and second, the interference is reduced since the IBEI is almost negligible in this scheme.

5.3.4 Numerical results

In this section, a realistic simulation using real-traffic data, from the TapasCologne project [122] is used to show the improvements obtained by means of the proposed scheme. In

order to simulate the SINR using the same formulation as in equation (5.24), the IBEI is modeled as follows:

$$I = \max\left\{-25 - 10 \log_{10} \frac{N_{RB}}{L_{CB}} - \mathcal{Z}, 20 \log_{10}(\text{EVM}) - 3 - \frac{5|\Delta_{RB} - 1|}{L_{CB}} - \mathcal{W}, \frac{-57\text{dBm}}{180\text{KHz}} - P_{RB} - \mathcal{Z}\right\}, \quad (5.26)$$

where N_{RB} is the number of RUs used for the transmission bandwidth and L_{CB} is the occupied bandwidth by the transmitted signal. In addition, P_{RB} is the transmitted power over the L_{CB} in dBm. The values of \mathcal{Z} and \mathcal{W} are provided by the LTE standard [123]. The additional parameters used for the simulation problem are presented in Table 5.1.

Table 5.4: Simulation parameters.

Parameter	Value
Bandwidth	10 MHz
Frequency	5.9 GHz
Transmission Power	23 dBm
Antenna Gain	3 dB
Channel model	Okumura-Hata
N_{RB}	50
L_{RB}	2

Optimal SPS Performance

The simulation results, displayed in Figure 5.16, compare three different implementations in terms of SINR: the one used by LTE-V2X Release 14 standard, where the vehicles are randomly allocated in the persistent slots, the orthogonal scheme proposed in [124], where the vehicles are classified into different sub-pools depending on their orthogonal direction, i.e., horizontal or vertical, and our proposed scheme. Moreover, the three schemes are implemented using the non-SPS and the SPS in order to see the improvement obtained by means of the interference mitigation.

The results displayed in Figure 5.16 show an improvement of approximately 20 dB between the schemes using the SPS and the ones without it. This improvement is due to the reduction of collisions obtained by the persistent scheduling, first term in the denominator in equation (5.24). Moreover, both the orthogonal and the proposed method in this work outperform the random scheme proposed by the standard. This enhancement is due to the platooning scheme which reduces the interference. Regarding the comparison of our method with the existing literature, it improves the already known methods achieving a higher interference mitigation obtained by the vehicle clustering. The main enhancement is based on the IBEI reduction, the second term of the denominator in equation (5.24) since the spectral clustering creates a cluster where the difference between the received power from all the vehicles is minimal.

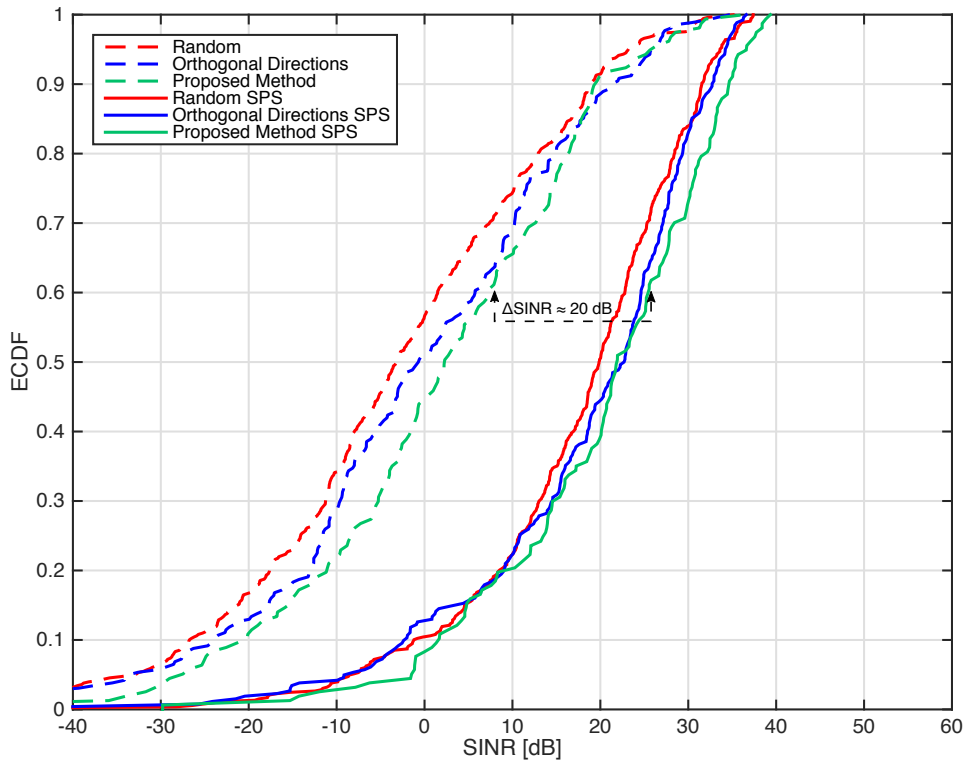


Figure 5.16: Semi-persistent scheduling scheme comparison results for the three different sub-pooling schemes.

5.4 Cooperative Connected Vehicles Security

An important topic is how to secure the wireless communications between the vehicles. In their paper, Petit and Shladover [17] classify the different potential attacks on automated systems, making a distinction between autonomous vehicles and cooperative systems. Our focus is on the latter, where the vehicles in the platoon share their status vector, i.e., position, velocity, and acceleration, encapsulated in cooperative awareness messages (CAM) with the rest of participants. The data in these messages is the main information to adjust their behavior inside the platoon, and hence, it is the main point of potential attacks. Our focus is on two different types of attack: i) non-authorized vehicle joining the platoon, and ii) fake/poisoning the vehicular communications inside the platoon. Therefore, we can classify the threads as *attacks from the outside* (the adversary has not a legitimate key and certificate) and *attacks from the inside* (the adversary somehow obtained a legitimate key and certificate). Some examples of these attacks are:

- *Unauthorized participation*: unauthorized users act as a legitimate user to participate in the system, and affect the management of the system.
- *Replay attack*: the adversary replicates messages that were sent previously. It may avoid the authentication mechanism and disturb the system. A simple solution is to

include timestamps into the messages. However, it adds more computational effort to the network and the requirement of synchronization.

- *Sibyl attacks*: the adversary may try to spread false messages or misleading information to the rest of participants. Once the user is validated in the system, it makes the receivers believe that the message comes from an authenticated source and the content of the message is true.

These attacks have different direct consequences and mitigation techniques. However, in this work, we propose a joint paradigm based on ring-based signatures to invalidate unauthorized participation, along with a combination of blockchains and smart contracts to eliminate replay and sibyl attacks.

The first concept is the ring-based signatures introduced by Rivest, Shamir, and Tauman in [125]. It takes a group of signers \mathcal{X} (in our case the platoon members) where there is no group manager (unlike group signatures [126]), and allows every group member $\mathcal{X}_i \in \mathcal{X}, i = \{1, 2, \dots, N\}$ to share messages within the group by signing them using the group public key $P_{\mathcal{X}} := \{P_1, P_2, \dots, P_N\}$ and its own private key $S_{\mathcal{X}} := \{S_1, S_2, \dots, S_N\}$. This signature scheme does not require setup procedures, group manager or external coordination between the vehicles, which makes it suitable for fast moving environments as proposed in [127]. However, in the traditional scheme defined before, the signer can send messages without any prior verification by the group/platoon. This is not suitable for our scheme where a potential attacker can overload the network by sending multiple messages (e.g., Denial of Service (DoS) attack), and congestion is particularly pernicious in time-critical applications, such as vehicular ones. Thus, we propose a consensus-based scheme in order to accept messages from a new vehicle joining the platoon, i.e., authorization scheme. This feature is explained in depth in Section. 5.4.3.

The second part of our scheme relies on the blockchain technology which was first introduced in the famous Satoshi paper [128]. The blockchain technology is defined as a digital ledger where all the transactions are recorded and publicly announced. Moreover, it uses a chained hash mechanism to make infeasible, i.e., computationally too costly, to modify previously accepted transactions. Once the vehicles form a platoon, it is required to secure the inter-vehicular communications. Hence using the blockchain distributed public ledger is possible to validate these messages as shown in [129] using a consensus-rule. However, one open question pointed in this paper is the excessive time to validate the messages in the blockchain technology since it needs to be validated by most of the users. Using as reference the Bitcoin cryptocurrency, it takes an average of approximated 10 minutes to validate each transaction which is obviously unacceptable for our time-critical application.

Therefore, we need to propose a modification to the standard blockchain transaction. The standard blockchain protocol has the great advantage of a decentralized validation architecture, i.e., there is no need for a trusted third party authority to work as a referee. However, at the same time, this is a great barrier to obtain extremely fast transactions since they need to be accepted by all the members (or at least 51%) of the network. Therefore, in this case, we propose the use of microtransactions. The idea of microtransactions relays in the creation of a relationship between two parties (by means of a smart contract), and to only publish in the blockchain whenever there is a disagreement between both parties or to publish a single transaction covering all the transactions occurred during a stipulated period of time. The smart contract concept along with blockchain has the following

advantages: i) Decentralized: there is no need to rely on an intermediary to confirm the transactions. ii) Safety: since we are using a blockchain scheme all the transaction are *carved* on a shared ledger, so there is no way to modify the values. iii) Backup: on the blockchain concept every single participant has a local copy of the last valid blockchain.

5.4.1 System model

Definitions: we call a set of possible signers a ring \mathcal{X} . Each possible signer \mathcal{X}_i is associated with a public key P_i (by means of a Public Key Infrastructure (PKI) scheme) that defines the signature scheme and specifies its verification key. The ring-signature is defined as $\sigma = (m, P_1, \dots, P_N, s, S_j)$ which produces the general ring signature σ for the message m given the public keys $\{P_1, \dots, P_N\}$ of the N ring members. The ring-verification protocol (m, σ) accepts a message m and a signature σ which includes the public keys $\{P_1, \dots, P_N\}$ of all the members.

Problem statement: create a secure and anonymous scheme for vehicles to join the platoon formation, and for the platoon members to periodically exchange messages using secure vehicle-to-vehicle communications with stringent latency requirements.

Let define the system model of a typical vehicular network based on the 3GPP Rel. 14 (LTE-V2X) implementation. The network consists on a set of vehicles \mathcal{X} forming a platoon, and an infrastructure playing the role of a Trusted Authority (TA) as shown in Figure 5.17. Using the RSA cryptosystem (it can also be applied using elliptic curve equivalents) for each vehicle \mathcal{X}_i , its public key can be defined as $P_i = (n_i, e_i)$ which specifies the trap-door one way permutation f_i of \mathbb{Z}_p as

$$f_i(x) = x^{e_i} \pmod{p}, \quad (5.27)$$

where we assume only the vehicle \mathcal{X}_i knows how to compute the inverse permutation f_i^{-1} efficiently. Each vehicle \mathcal{X}_i has an identity defined as $m_i = (I_i || R_i)$ where $||$ denotes concatenation. The identity m_i is created using a permanent vehicle ID, I_i , where one possibility is to use the license plate as suggested in [129], and a session salt R_i . This identity m_i is secured using a hash function (typically SHA-256) obtaining the value $k_i = h(m_i)$ which has the property of being pre-image resistant, i.e., it is infeasible to find a value y such that $y = k_i = h(m_i)$ providing the desired anonymity to our scheme.

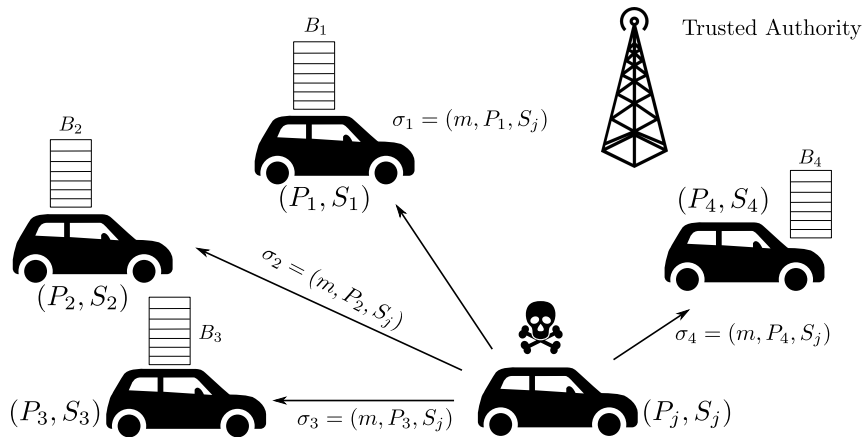


Figure 5.17: Adversary vehicle trying to join a platoon.

However, there are some open questions regarding our system model: Why do we want to organize the vehicles in platoons? What are the potential attacks to platoon formations? The concept of platooning systems has been brought up to increase the lane capacity and a representation of these systems is depicted in Figure 5.18

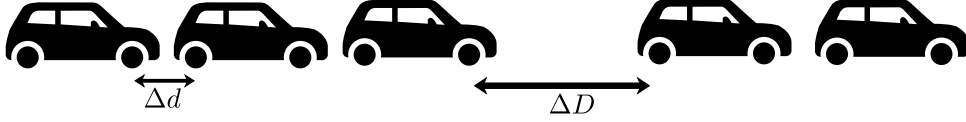


Figure 5.18: Optimal platoon formation.

where Δd and ΔD is the inter-vehicular distance and inter-platoon distance, respectively. In order to manage a platoon we need to share the vehicle status using wireless vehicle-to-vehicle communication and this is where the potential attacks may appear. Once the trusted platoon member (one already in the platoon) receives the signed message (k_j, σ_i) the protocol continues as follows: if the vehicle j is accepted in the platoon (validated by the rest of vehicles using the ring-based signature), the communication between the vehicles is periodic and requires a low delay. Therefore, we need to find a secure and almost instantaneous communication scheme (including cryptographic security). For this purpose, we propose to use a blockchain-based protocol. In the normal standard blockchain validation every single transaction is published and broadcast, and it usually takes around 10 min on average to obtain the six validations needed to trust a transaction. However, as mentioned before, we require an almost instantaneous protocol. Hence, we propose the use of the microtransactions concept using smart contracts between the vehicles. This idea is explained in Section 5.4.5.

5.4.2 Proposed security scheme

The following figure (Figure 5.19) describes the general idea about the proposed design. It is divided into three different phases: i) using a ring-based signature scheme to verify the identity of vehicle j and join the platoon. ii) establishment of a smart contract between the vehicles in the platoon to create secure channels for the microtransactions. iii) use the blockchain scheme to validate or reject the microtransactions (CAM messages) inside the secure channels.

In the case of disagreement between the reads and the received values, the receiver sends the values to the blockchain so everyone in the platoon can validate or discard the values (51 % rule). In the following, every step of the proposed scheme is described in depth.

5.4.3 Ring-based signature for platoon joining

Ring-signature generation

Let a vehicle j with a pair of keys (P_j, S_j) that wants to join an already formed platoon with N vehicles in it. Each of the vehicles has a pair of key (P_i, S_i) which correspond to the public and private key, respectively. The designated public keys are authenticated using a PKI protocol using in our case the eNodeB, binding the public keys P_i to the identity of the users $\mathcal{X}_i \in \mathcal{X}$. The binding of the vehicle identity occurs once the vehicle is registered

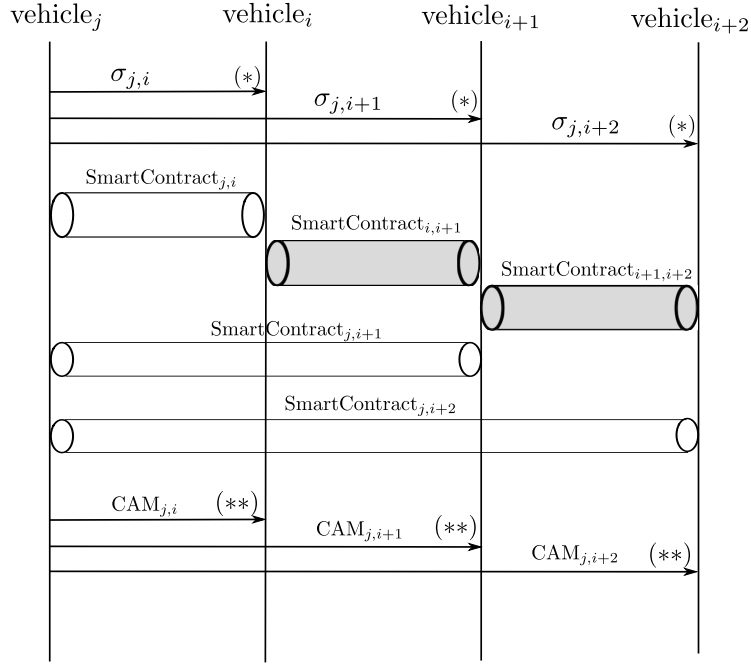


Figure 5.19: General flowchart for the proposed scheme. (*) check the identity of the vehicle j using the TA (**) verify the information sent by vehicle j comparing the values with the reads obtained from the own on-board equipment and the history of values.

in the network since the different infrastructures share their database. An emerging new approach to solve the use of certificates using the PKI is the use of blockchain technology as suggested in [130], which provides a distributed ledger for registering the identities, and what is more important provides a solution which cannot be modified from the outside. The vehicles generate an identification value (pseudonym) as

$$m_i = (I_i || R_i), \quad (5.28)$$

which is later hashed by $k_i = h(m_i)$ and it is the message used to ask for joining the platoon. The value R_i is denominated as the session salt which usually has a short life cycle. Here we propose to make the session salt expire every time a vehicle leaves a platoon reducing the number of modifications in the TA database, but providing safety against pseudonym linking attacks [131].

Ring-signature verification

Joining the platoon is a consensus-based protocol keeping the anonymity of the joining vehicle and the ones already in the platoon. For that matter we propose to use the vector $\sigma = (\sigma_{j,1}, \sigma_{j,2}, \dots, \sigma_{j,N})$ as an identification method. Each of these values is calculated as shown in Figure 5.17 using $\sigma_{j,i} = (k_j, P_i, S_j)$ which is the identifier between the adversary vehicle j and the vehicle i . The motivation behind this identification scheme is that vehicle j sends his identity to vehicle i as the designated verifier. This can be easily achieved using the individual ring signature obtained by $\sigma_{j,i}$. Using this method, the vehicle i knows that

the message is coming from the vehicle j (since no third party could have produced this ring signature due to having the value S_j encapsulated), but vehicle i cannot show to the rest of participants that the message was signed by vehicle j , since the message could have been created by vehicle i itself. Once all the values $(\sigma_{j,1}, \sigma_{j,2}, \dots, \sigma_{j,N})$ are shared between the corresponding vehicles and the vehicle j , the vector $(\sigma_{j,1}, \sigma_{j,2}, \dots, \sigma_{j,N})$ is sent to the TA. Here we can face two different outcomes: i) if k_j is stored in the TA database then the vehicle j can join the platoon. ii) if $k_j \notin \mathcal{K}$ where \mathcal{K} contains all the valid hashed identities then the vehicle is considered as an adversary. Its identity is published in the blockchain and broadcast since we know the identity (P_k, S_k) , and we can then proceed to repulse the vehicle from the network.

5.4.4 Smart contracts

Once the vehicle is accepted, it needs to establish a smart contract with the rest of platoon participants. A smart contract is defined as an operation that can be permanently executed between two different parties which have a defined agreement [132, 133]. In our scenario, a smart contract between the vehicles in the platoon is particularly suitable due to the periodic nature of the CAM messages and the stringent delay requirements. Smart contracts have the extra advantage of being completely decentralized (it only involves the two parties of the contract), and they are triggered by an event (in our case a timer or CAM messages sent periodically). Using a network of these microtransaction channels (as shown in Figure 5.19) helps to make the network more scalable, since every transaction does not need to be broadcast to every single user, but it only involves the parties in the contract. Therefore, creating tunnels using these channels, it is possible to send messages to every member of the party in a secure and decentralized manner. However, what happens if there is a disagreement between the parties in the smart contract? Here is where the blockchain technology appears as explained in next section 5.4.5.

5.4.5 Blockchain-based microtransactions

A blockchain scheme for information sharing verification is considered in order to protect our system from an inside attacker, i.e., the adversary obtained a legitimate key and it is part of the platoon. Additionally, we assume that the adversary is able to establish contracts with the rest of participants since the only requirement is to have a validated identity. The general scheme of microtransactions is shown in Figure 5.20 for a smart contract involving two vehicles.

Using the simple example from Figure 5.20 to illustrate our scheme, we have two vehicles \mathcal{X}_i and \mathcal{X}_{i+1} which are self-aware of their own state vector, i.e., position, speed, and acceleration. They have established a smart contract and they have stored a local copy of the blockchain denoted as B_i and B_{i+1} . Moreover, the vehicles can estimate the state vector of the other vehicles in the platoon by means of their on-board sensors. Using the rules established by the smart contract, the microtransactions (CAMs) are triggered every period T (defined as $T = 100$ ms by the standard [35] for vehicular safety applications). Once the vehicles receive the information from the other party, they check whether their estimates and the received values are similar. In the case of reaching an agreement, i.e.,

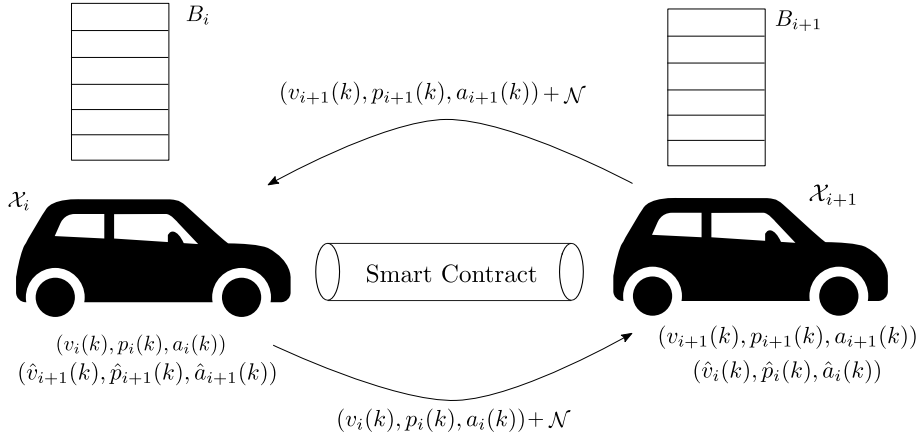


Figure 5.20: General microtransaction scheme using blockchain.

the received information and the estimated one match, the system continues working normally. In the case of having a disagreement, the receiver vehicle raises its discussion to the blockchain, i.e., broadcast the received microtransaction, and the rest of vehicles in the ring using their own estimate values, obtained by their sensors, verify whether the received microtransaction is correct.

Using the blockchain scheme, two different types of attacks are able to be blocked, i.e., replay and sibyl attacks. The first is a similar concept as the one of double-spending in the Bitcoin network. The vehicles store the received transactions along with a time-stamp, a possible solution for synchronization is using a the clock from the GPS system, in order to detect replay attacks. Moreover, since the transactions are published in the blockchain after a period of time, the vehicles can identify if a message has been previously sent. A sibyl attack can be defended as follows. The blockchain verification of a raised disagreement is based in a consensus-based model, i.e., if the majority of vehicles (51 %) find the value not acceptable, the disagreement is accepted and the vehicle is flagged as an attacker. Since the vehicles share their state vector every $T = 100$ ms, the vehicles have stored the history of values for the dynamics of each vehicle, and therefore, a prediction about the expected value can be performed as shown in equations (5.29)-(5.31). Assume that the velocity of the vehicle does not change in the platoon formation

$$\hat{v}_{i+1}(k) = v_i(k), \quad (5.29)$$

$$\hat{p}_{i+1}(k) = a_i(k) + \frac{v_i(k)}{T}, \quad (5.30)$$

$$\hat{a}_{i+1}(k) = 0.5 \frac{(v_i^2(k) - v_{i-1}^2(k))}{v_i(k) \cdot T}, \quad (5.31)$$

where the predicted acceleration $\hat{a}_{i+1}(k)$ is calculated using the field measurements obtained from [134]. The requirement of this scheme is to have synchronization between the vehicles in order to predict and estimate correctly the dynamics of the vehicles. Therefore, two different types of attacks are prevented, i.e., replay and sibyl attacks, are prevented by using the blockchain scheme. The first is a similar concept as the one of double-spending in the Bitcoin network. The vehicles store the received transactions along with a time-stamp, where a possible solution for synchronization is using the clock

from the GPS system, in order to detect replay attacks. Moreover, since the transactions are published in the blockchain after a period of time, the vehicles can identify if a message has been previously sent. Furthermore, a silyl attack can be avoided as follows. The blockchain verification of a raised disagreement is based in a consensus-based model, i.e., if the majority of vehicles (51 % of participants rule) find the value not acceptable, the disagreement is admitted and the vehicle is flagged as an attacker.

5.4.6 Scalability and time-critical applications

In order to prove the feasibility of our approach, we compare it with the traditional blockchain scheme. According to the standard blockchain scheme (peer-to-peer network), a majority of nodes in the network has to accept the transaction. Considering a network with N users at least $\frac{N+1}{2}$ users must acknowledge the transaction. Therein, the number of exchanged messages required for each transaction increases as the number of nodes grows. Therefore, we assume that the time to *mine* the hash value of the transaction is t_{hash} and the transmission time between vehicles is t_{TX} along with the time of acknowledging the transaction is t_{ACK} , the total time to accept a transaction is given by

$$t_{\text{transaction}} = t_{\text{hash}} + \frac{(t_{\text{TX}} + t_{\text{ACK}}) \cdot N}{2}. \quad (5.32)$$

Nevertheless, our approach uses microtransactions which upon having a valid smart contract between the parties does not require the validation of the remaining elements of the network (only when one of the members violates the contract terms). In consequence, the latency requirements can be met since there is no need of waiting for the network acceptance of each transaction. Additionally, our proposed scheme does not suffer from scalability issues since each smart contract is established between a pair of users, and it does not need to be constantly updated.

5.5 Summary

Throughout this chapter, a cooperative scheme for connected vehicles is implemented, assuming that the concepts developed during Chapter 3 and 4 are established. This scheme is based on two different coordination conceptions, i.e., implicit and explicit coordination. In order to prioritize safety, the vehicles are organized in platoons using a coalitional game-theory approach, where the traffic flow is optimized using several layers of utility functions. Once the vehicles are forming a coalition/platoon, a cooperative adaptive cruise control (CACC) scheme is applied to minimize the distance between the platoon members, while keeping the stability of the formation. The final section of this chapter defines a secure scheme to exchange messages (by means of a smart contract) between validated platoon members, using blockchain technology which exploits the peculiarities of the platoon formation.

6 | A Practical Vehicular Network Deployment - Two Case Studies

In this chapter, the proposed heterogeneous network is simulated using real scenarios. The objective of this simulation is to verify the positive impact of our system model including the proposed novel characteristics. Additionally, it is tested whether the network requirements are fulfilled. This chapter is divided into two different case studies with a common goal; the safety of the network participants. The first scenario is an urban environment where the complete network is deployed and a study of the required parameters using the proposed network is provided. The second case study considers a port scenario where limited equipment is available. The objective of this case study is to verify whether an analogous system model concept as the one proposed in this work is valid for these type of scenarios.

6.1 Case Study I – City of Cologne

In the first case study, the introduced network characteristics through this work are simulated in a realistic urban scenario. For this purpose, we make use of the TapasCologne dataset [135] which covers the entire region of the city of Cologne. This dataset comprises around 400 squared kilometers for a period of 24 hours, including 700.000 individual car trips. To obtain a more realistic simulation, reduce cost and motivate the implementation of the proposed scheme, the macro-cells positions are the real locations of the cellular systems provided by the public German database in 2012 obtained by the same initiative. Figure 6.1 shows the entire area of Cologne with respect to the traffic density. In order to have a feasible simulation in terms of computational time without losing generality, we select from the entire dataset a region of one square kilometer where more than 2000 different vehicles drive in a period of one day as shown in the area displayed in Figure 6.2.

The predominant vehicular density in the studied area is around 100 vehicles per minute with some specific areas where the peak of density goes up to 450 vehicles per minute. These peaks in the network represent the rush hours in the morning (8 to 9 am), and in the afternoon (5 to 6 pm), corresponding to the working hours. Therefore, our network should be able to fulfill the communication requirements at all time, even during rush hours.

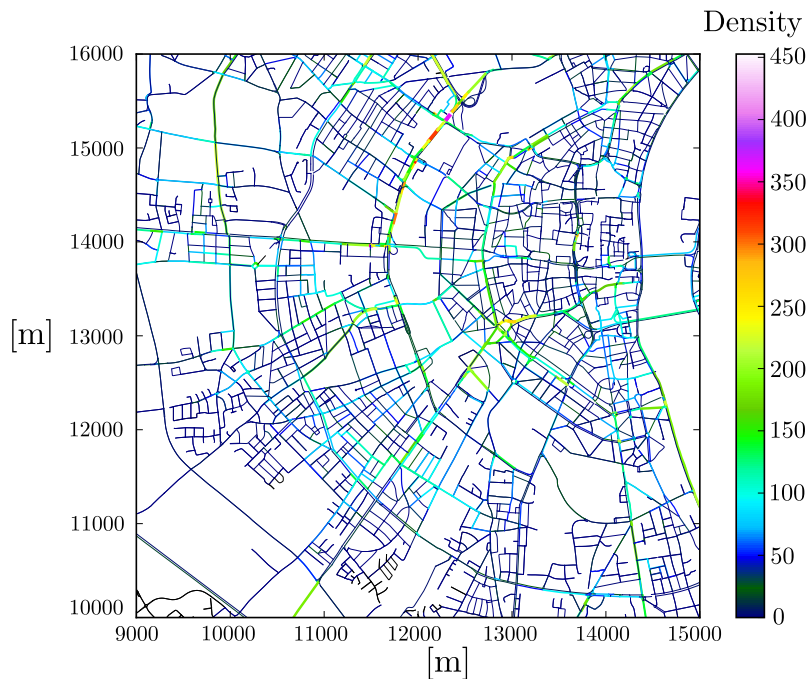


Figure 6.1: Traffic density map of Cologne.

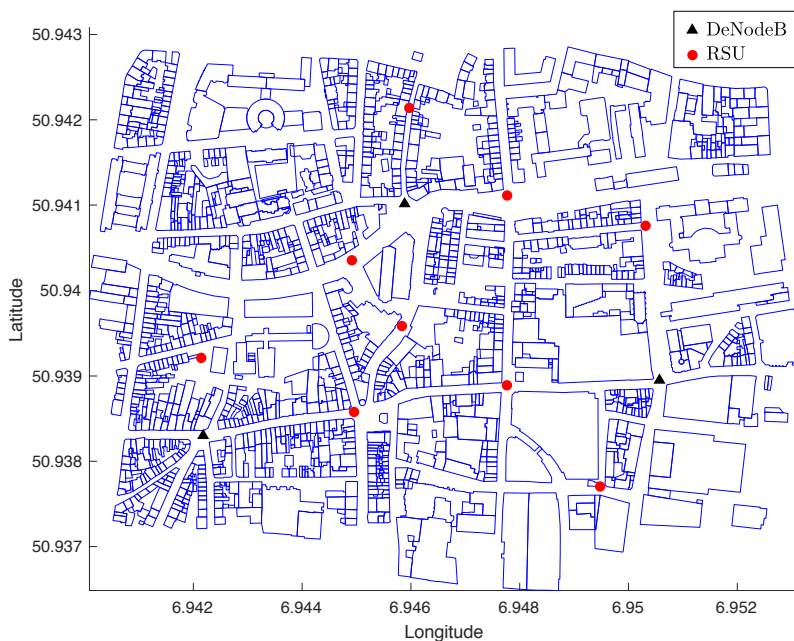


Figure 6.2: Selected area of Cologne with deployed infrastructure.

6.1.1 Performance network parameters

First, we need to define which network parameters are important for this case study, and how to evaluate them. In order to compare the performance of the proposed network

model with several state-of-the-art approaches, we define the network capacity [136] as

$$C[\text{bps}] = \sum_{m=1}^M \sum_{k=1}^K B_{m,k} \log_2(1 + \text{SINR}_{m,k}), \quad (6.1)$$

where $B_{m,k}$ is the bandwidth of each vehicle m under the coverage of the SC k , and the $\text{SINR}_{m,k}$ for each vehicle in the SC is defined as

$$\text{SINR}_{m,k} = \frac{P_{m,k} G_{m,k}}{\sum_{i=1, i \neq m}^M P_{i,k} G_{i,k} + \mathcal{N}}. \quad (6.2)$$

In our case, we assume that the communication scheme is dedicated, and therefore, there exists no interference from other types of communications. Additionally, each network member is simultaneously connected only to one macro-cell and/or infrastructure making the interference almost negligible. An important requirement to fulfill is introduced in Section. 3.1.4 as ubiquitous connectivity. Hence, we define this value as the number of road points in pixel form where the received SINR is higher than a given threshold.

6.1.2 Umbrella coverage deployment

In order to deploy the macro-cells, we use the metaheuristic algorithm defined in Algorithm 1 in Section 3.2.3. The location of the macro-cells (DeNodeB) is depicted in Figure 6.2. Using the optimal location of the macro-cells in order to obtain at least 90 % of covered points, the received power for each of these points is simulated. In order to obtain the received power, we make use of the defined radio channel model for V2N communications (see Section 4.2.3), and the resulting simulation is shown in Figure 6.3.

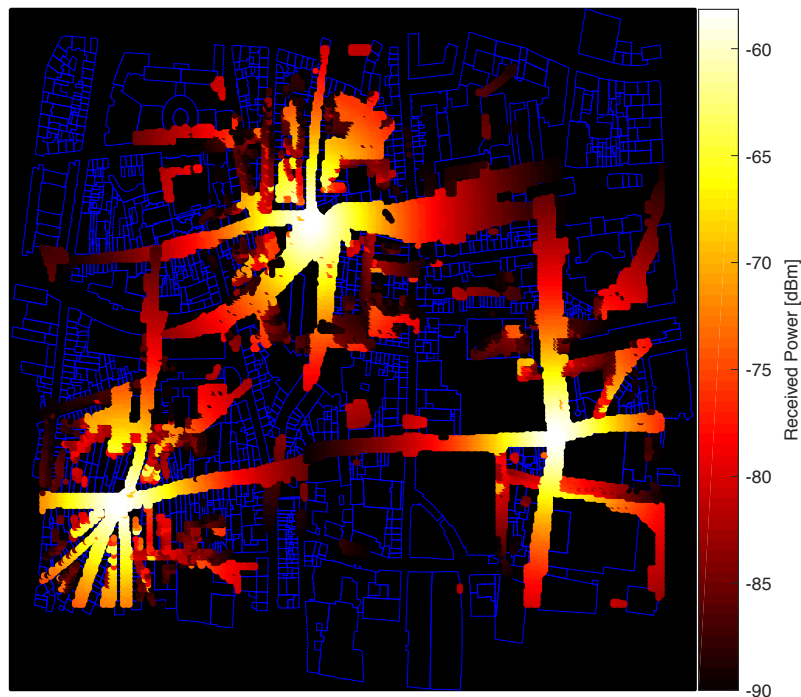


Figure 6.3: Macro-cell network deployment.

As shown in Figure 6.3, we define the threshold for the pathloss as -90 dBm. By using 3 macro-cell infrastructures to cover the entire area, we are able to fulfill the received power requirements. It is noteworthy to mention how not all the points are covered by the macrocell infrastructures ($\approx 5\%$). For these points which are not covered by the macro-cells, we use the deployment of small cells in order to cover them as defined in Section 3.3.1.

Moreover, since each macro-cell covers its own area, there is no interference between the infrastructures. This deployment is done taken into consideration the static behavior of the environment, and for the dynamic behavior, we use small cell deployment as shown in the next subsection. For the deployment of the macro-cells we disregard the data rate for each of the vehicles, since the main requirement to fulfill is the always-on concept, i.e., to guarantee that there is always a possible link between vehicle and infrastructure.

6.1.3 Small cells formation

Network deployment

Using the density-based scheme defined in Section 3.3.1, we deploy the RSUs in areas where the expected density of vehicles is higher than a given threshold following Algorithm 2. The deployed architecture is shown in Figure 6.4

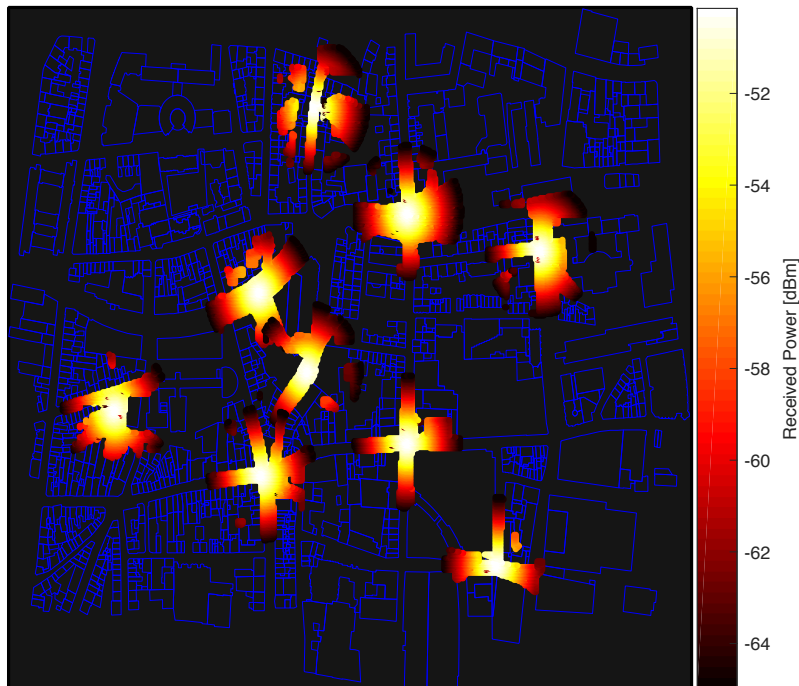


Figure 6.4: RSU deployment forming small cells.

As shown in Figure 6.4, the received signal from the small cells is higher than the one obtained from the umbrella coverage created by the cellular infrastructure (≈ 10 dB higher). The intermediate infrastructure plays a double role: It increases the received signal for all the vehicles under their coverage, and in addition, the latency is reduced

since the network is closer to the participants. The RSUs are only deployed in the areas where the expected density meets some requirements. In the rest of areas, we propose to use MRN as defined in Section 3.3.5.

6.1.4 Discussion of results for case study I

The simulation is performed using two different LTE-V modes. The first one uses a bandwidth of 2.16 MHz with 12 PRB or 144 subcarriers with 1 TTI of 1 ms, while the second mode uses a bandwidth of 1.08 MHz with 6 PRB or 72 subcarriers with 2 TTI for 1 ms each. The results for the vehicles under the coverage of the DeNodeB or a fixed SC are displayed in Figure 6.5 and Figure 6.6, respectively.

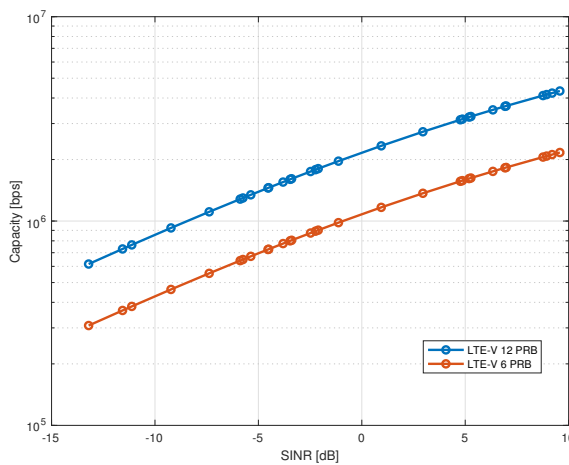


Figure 6.5: Capacity for vehicles under DeNodeB coverage.

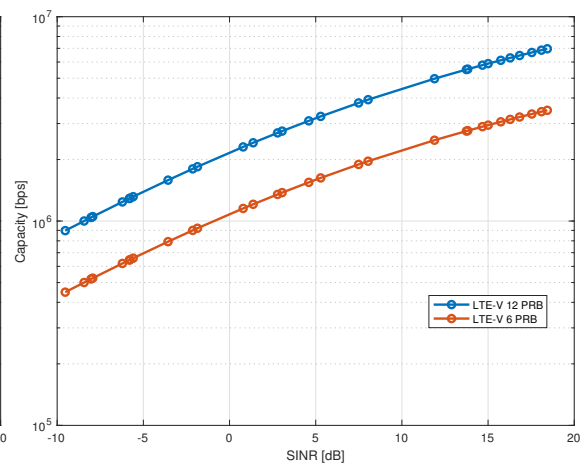


Figure 6.6: Capacity for vehicles under SC coverage.

The simulations show an increase in the obtained capacity for the vehicles under the influence of the SC in comparison with the results obtained by the DeNodeB. This corresponds to a higher received SINR for the vehicles due to the smaller distance between them and the infrastructure, along with a smaller interference due to the fewer number of vehicles under the range of the same infrastructure.

Moreover, it can be observed that the higher capacity values are within the range of Mbps which is congruent with the required value per link for cooperative perception (2.5 Mbps) and for cooperative maneuver (0.25 Mbps) according to the latest KPI requirements for LTE-V in terms of data rate [137]. Nevertheless, it can also be derived from the simulations that the potential number of vehicles simultaneously under the influence of the same infrastructure falls within the range of $\{30, 50\}$ since the capacity value has to be shared between the users.

6.2 Case Study II – Occupational Safety at Seaport

Fast development in information and communication technologies (ICT) leads to the emergence of cooperative systems, where vehicles and pedestrians equipped with on-board units can talk to each other and also with the infrastructure through road-side-units or dedicated access sites. Such cooperative sensing and controlling systems may exhibit a more advanced behavior compared to vehicles, pedestrians, and environments that do not communicate [138].

The main motivation for the deployment of vehicular communication is to have safety-related applications. For example, by collecting up-to-date information about the status of the road, the driver or pedestrian assistance systems can quickly detect potentially dangerous situations, and notify the driver and pedestrian about the approaching danger. A relatively small reduction in the driver's and pedestrian's reaction time may potentially avoid the occurrence of an accident [139]. In the seaport environment, an analogous model can be described. In this environment, a driver can be defined as a fork-lift, and a pedestrian can be an on-port worker, while the road is the internal road at the seaport transportation and operational area.

6.2.1 Innovations in maritime sector

The transportation sector scores less than the average for the economy as a whole when it comes to innovation, including the countries with a good overall climate for innovation as Finland and Sweden, for instance, [140]. Even though the transportation sector is the largest industrial research and development investor in Europe, there are considerable differences in the level of innovation activities carried out by the highly heterogeneous transport sub-sectors and their specific innovation capacities. The maritime sector in Europe is limited to mainly specialist products and military production, while the production of low-value vessels is undertaken outside Europe. In this regard, with the relatively small market of vessels production, the opportunities for the recovery of investments targeting innovations in maritime sector are rather limited [141]. Furthermore, research, innovations incubation and their diffusion impediments in waterborne transport and seaports, are much more emphasized in the so-called developing countries at South-East Europe, e.g., which have been functioning in transitional conceptions, and which permanently suffer reproduction of economic crisis [142].

An innovation is basically described as a historically irreversible change in the way of doing things [143]. A classic dictionary definition of innovation is the embodiment, combination, or synthesis of knowledge into a new idea, method, or device. Drucker [144] has defined innovation as a change that creates a new dimension of performance. Narayanan et al.[145] has used this description to define innovation as a new idea, method, process, or device that creates a high level of performance for the adopting user. Innovation includes efforts being made towards producing economic gain, either by reducing costs or through increasing income [146]. Besides commercial innovations motivated by revenue generation or cost-reduction, there are also public (or political) innovations motivated by increasing socio-economic welfare. Although there are various additional categorizations with respect to innovation, one among them is relevant from

the perspective of our study: product/service versus process; radical versus incremental; technological versus administrative; architectural versus modular; and disruptive versus sustaining innovation [147].

Although the exact classification is rather vague, we consider deployment of vehicular communication at the seaport area, with the purpose of enhancing occupational safety as service, technological, modular, and sustaining innovation. Service innovation is an intangible method of serving users with a new level of performance. It means in the context of our study that on-port workers and pedestrians will have a new vehicular communication-based service for increasing their occupational safety in a harsh working environment. Incremental innovation is commonly defined as refinement or improvement of existing innovations. In the considered case, the innovation based on vehicular communication refines the existing personal protective equipment (helmets and vests); mirrors at the corners at the open storage and warehousing areas in the seaport; horns at hard transportation and manipulative devices, by adding them a new, more sophisticated dimension. Technological innovation reflects the application of science and engineering to develop technical applications, or to accomplish a specific technical task. In the examined case it is about developing a novel technical-engineering application based on vehicular communication for increasing safety and improving environmental management at the seaport. Sustainable innovation improves performance levels of established services and provides incumbent firm an opportunity to reinforce its competences. In the examined case it means a positive change in the direction of recognizing the seaport as a safe, green and a sustainable one at the growing seaports' market. It is also important to mention within this context that the public policy, organization structure, managerial mindset, human resources, past experiences, tacit knowledge and much more, have a strong impact on the success of innovation [148].

In the following sub-section, we shall put the focus on the potential innovation success impediments vs. success conditions related to adopting vehicular communication for safety purposes in the developing seaport environment. As a base for our research, we have used [149], in which the authors have developed a methodological framework for assessing the success of the seaport-related innovations. They have analyzed three system innovation case studies related to development and implementation of the indented berth capable of serving ships from both sides, deployed at the Cares Paragon Terminal in Amsterdam; port community value-added information system (PCS) in Thessaloniki Port, and cold ironing in European ports as a process that enables a ship to turn off its engines while berthed and plugged in to an onshore power source. We have adopted a similar methodology for assessing the potential success of introducing vehicular communication for increasing on-port workers' and pedestrians' safety.

6.2.2 Case study

The initiation and adoption of vehicular communications for enhancing and upgrading the seaport safety management might be treated as a public innovation, motivated by increasing socio-economic welfare, or more precisely, on-port worker's and pedestrians' safety and wellbeing. In terms of the proposed innovation scale, it might be treated as a modular innovation, since it brings about a significant transformation in a concept within a component, i.e., the environmental seaport's safety management system. The links to the other components or systems remain unchanged and the impact is fairly low.

In our case study related to the Port of Bar (South-East Adriatic Sea) there are some additional particularities: (i) besides safety personal protective equipment (helmets and vests), mirrors at corners and horns on transportation and manipulative equipment, there is no other safety system based on advanced info-communication systems; (ii) the port functions in transitional environment since decades, which is characterized by economic uncertainty, institutional fragility, lack of human capacities and social awareness about innovation, lack of public policy instruments for business support and management training, etc. [150]. All these and much more has to be taken into consideration while proposing state of the art technology, as vehicular communications are, for uprising safety management in the harsh and dynamic seaport conditions. Namely, seaports are dangerous places for on-port workers and pedestrians in terms of operational risks connected to loading and unloading operations, port transportation and manipulative equipment, manipulative activities, warehousing, etc. Additionally, seaports usually operate 7 days a week, 24 hours a day, in all weather conditions, with multiple employees and contractors carrying out different activities [151]. It is the duty of an employer to protect the health and safety of workers and to improve occupational safe systems, but unfortunately, the accidents in seaports are not rare [152–154]. The reason for the growing number of accidents is the increase in the seaports' turnover during the past three decades. On the other side, the relatively low turnover at developing seaports, including the Port of Bar, should be in favor of workers' and pedestrians' safety, even though due to the best of our knowledge, there is no official statistical data concerning this issue in the developing and transitional countries [155]. Regardless of all above stated, permanent improvement of safety measures, it is something that simply must be done.

In the following sub-section, some infra- and supra-structural, institutional and interaction barriers vs. success conditions in the initiation, potential development and implementation phases of a novel vehicular communication system for supporting safety measures within the seaport environment are considered in more detail.

6.2.3 Barriers and success conditions

The Port of Bar is a moderately developed seaport at the South-East Adriatic Sea, without strict orientation to a specific group of cargo. Currently, it consists of four organizational units: Port of Bar, Container terminal and general cargo operator, Maritime operations, and IT operators. The port is under the direction of the Port Authority, which is located in Kotor. Also, there is a private company, which performs a range of tasks related to the protection of the environment within the port and beyond. The port has seven technological units for cargo handling: container and general cargo terminal (which is used for the simulation experiments); wood terminal; a terminal for grains; bulk cargo terminal; general cargo terminal; liquid cargo terminal, and passenger terminal. In addition to a very complex organizational structure, the port also has a specific ownership, in terms that the majority owner nowadays is a foreign company.

In such a rather complex organizational and technological environment, we tried to make a communication matrix between different actors and environmental conditions in the initial, development and implementation phases concerning vehicular communication safety system (Figure 6.7), in accordance to Arduino et al. [149] work. These communication channels are connected with certain barriers and success conditions. In

the initial phase, we presume necessity of existing positive communication between the port authorities and knowledge institutes at supra-structural, institutional, interaction, and human/administrative capacity levels. At this stage, the biggest problems are at the supra-structural and institutional levels. They can be treated as hard problems. Namely, it might be difficult to provide funds for road-side-units (RSU), tablets (for fork-lifts' drivers) and mobile hand-held devices (for on-port workers and pedestrians). Also establishing back-end info-communication support system might be a problem since it commonly requires costly infrastructure. Developing the appropriate law regulations (standards) in the domain of port environmental management system and providing funds for the aforementioned supra-structural requirements are prerequisites for establishing positive effects in this initial phase. In the development phase, it should be established positive communication with third parties in the ports (lobbyists, consultants, agents, etc.), firstly at institutional and interrelation levels. Through regulation of institutional and interaction conditions, the third parties can be prevented from making obstructions, which is among success conditions [156]. In the implementation phase, support should be provided from the external cargo operators in a manner to convict them that these safety measures are in their favor, as well. In such case, external container cargo operators might provide financial support for the project implementation. We have set this matrix (Figure 6.7), identifying the barriers and proposing general success conditions due to several in-depth interviews with the port managers, and due to our intuition and previously acquired experiences in the field.

Actions Environment	Port authorities	Container operators	Third parties	Knowledge institutes
Infrastructure: terminals, ships, roads, rail-roads, etc.	↑	↑	↑	↑
Supra-structure: transp. and manip. devices; RBS, end-nodes, etc.	1	3	2	1
Institutional issues: laws, social and economic issues	1	3	2	1
Interaction conditions	1	3	2	1
Capacities (human/ administrative)	1	3	2	1

Legend: 1 - Initial phase; 2 - Development phase; 3 - Implementation phase

Figure 6.7: Actors-environment communication matrix in providing innovation success (Source: adapted from [149], p.99)

It is to be noted that in the case of the Port of Bar there is a general orientation towards economic gain, rather than to the socio-economic welfare. The communication between the port authorities, research institutes, and universities exist, but it is rather a weak,

since the investments at the governmental level for science and education are insufficient, and the research community consequently has a weak influence on firms' innovation incubation and implementation actions. Currently, a trend of orientation towards foreign investors and relying on their development politics is prevailing. The last stated is not in favor of innovation success and should be overcome through uprising the responsible people awareness of the socio-economic well-being and environmental protection importance, and through establishing much more closer and effective communication between research institutions and maritime (seaport) industry and business sectors. So far, it has been shown that involvement of foreign investors does not support the economic gain either the socio-economic welfare of the employees and wider local/regional community. All afore stated should be kept in mind for both the inventors (research institutes and universities) and the users (seaport actors and stakeholders) regarding the provision of the fertile soil for innovation, economic growth, and social welfare.

6.2.4 An innovation success model

Vehicular communication innovative approach for enhancing on port occupational safety in the transitional environment might be treated rather as a supply-side innovation. Namely, in the considered case, the researchers' propose the innovation to the seaport's managers, while there is a risk of the managers' misreading the market and its demand for safe and green ports with zero accidents. Moreover, a good example of a supply-side approach is Sony's portable cassette player (the Sony Walkman) on the basis that "Sony does not serve markets, it creates them" [157]. In this case, the researchers have to create a market. In fact, in the initial phase of the innovation success, the researchers have to take the rule of the marketing managers and recognize uncover latent demand. They have to identify and exploit the opportunities (Figure 6.8). More precisely, they have to offer port authorities a novel safety solution based on advanced vehicular communication system as a complement to existing personal protective equipment garments, mirrors, and horns. Under the assumption of researchers' success in this first step, then, during the time, new opportunities should appear. For instance, on-port workers, pedestrians and forklifts' drivers will most probably prefer their new protective equipment, and they might ask for its refinement during the time. In such way, the researchers can blend into implementation phase supply- and demand-side approaches. After the innovation adoption, the customers will likely treat the port as a safer and green environment. This shall raise customers' confidence in the port services in terms of environmental management, and they might also like to adopt the same or similar vehicular communication system for occupational safety and production purposes within their industry or business. Afore listed should cause a vivid interplay between demand- and supply-sides within the seaport environment as a primer marketplace in this case, and beyond. We suppose that the port is proactive, so we did not take into consideration its potential reactive behavior connected with misreading opportunities and status quo (crossed fields in Figure 6.8).

In the direction of innovation success, we can also assume that the innovation initiation, implementation, routinization, and development will cause (positive) repositioning of the port at the ports' market and customers' perception map. Also, the concerned port might be used as a model to other ports in the region and wider. Afore presented a dynamic model of the innovation deployment should undoubtedly lead to innovation

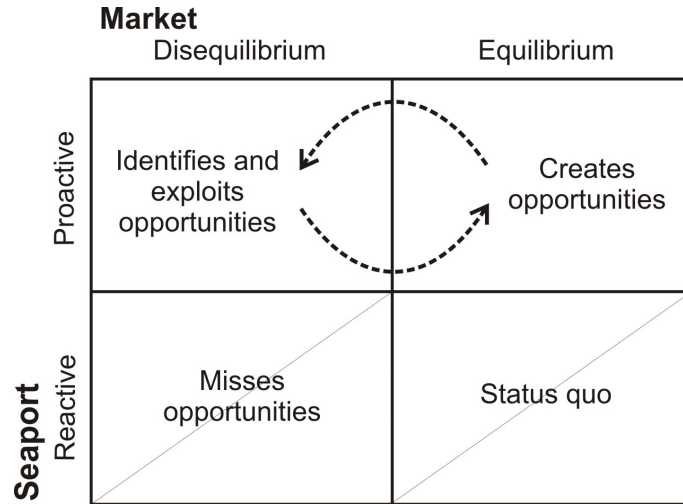


Figure 6.8: A dynamic model of market creation
(Source: adapted from [158], p.101)

success. Of course, it assumes resolving previously identified impediments. It means that the researchers have to persuade the port managers and stakeholders that they need safety and environmental management system improvements and that vehicular communication is a sound and promising path of doing so.

6.2.5 Proposed system model

Let a set of $\mathcal{N} = \{1, \dots, N\}$ port-workers and $\mathcal{M} = \{1, \dots, M\}$ fork-lifts, all of them equipped with mobile devices, enabling GPS signaling and communication. In addition, we consider a set of $\mathcal{K} = \{1, \dots, K\}$ interconnected road-side-units (RSU) covering the entire port area. It is noteworthy that for the sake of generality, we do not consider any particular communication technology in our proposed scheme. Due to the particularities of port areas, we consider concentration areas, denoted as $\mathcal{L} = \{1, \dots, L\}$, where the density of on-port workers and fork-lifts is expected to be higher. Moreover, the environmental information is known by the RSU, i.e., container positions, railway infrastructure and load and unload areas, allowing prediction and optimization of traffic and communication load.

Both the on-port workers and the fork-lifts can communicate with each other (V2V) and with a given infrastructure (V2I) due to their communication equipment as shown in Figure 6.9. Due to the restrictive requirements for safety applications in vehicular communications, i.e., high reliability and low latency, the main objective of our simulation is the study of these parameters. Ultimately, the final goal of this proposed framework is to enable the use of autonomous robots to perform the job of human workers. In order to obtain this goal, the cooperative scheme based on communication is of vital importance. Furthermore, our proposed system model includes the idea of concentration areas \mathcal{L} . These areas have a higher probability of being occupied by fork-lifts or workers since these are areas of load and unload. Hence, each worker, n , in a concentration area l can be defined as n_k^l , being k the RSU at which the worker is connected to. Analogously, the fork-lifts are denoted as m_k^l .

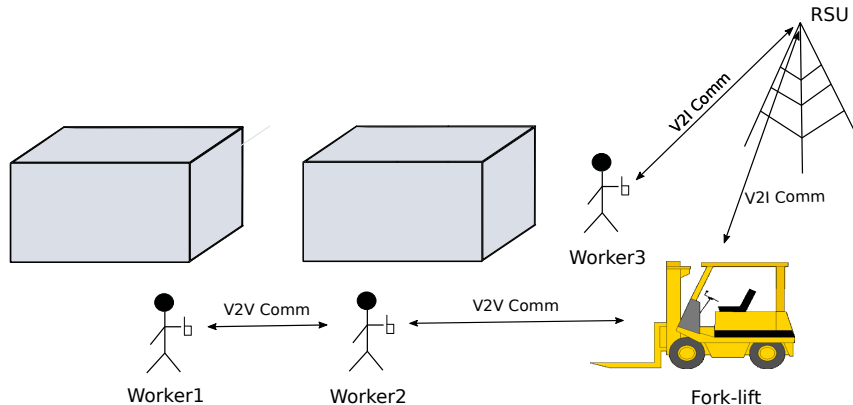


Figure 6.9: Communication network overview.

As discussed in previous section, the port under investigation has no infrastructure deployed to enable vehicular communications, hence, the first step consists on obtaining the optimal placement of the RSUs. In order to provide a suitable network for safety applications, the area covered by the RSUs has to be the totality of the port area. For this matter, we use the following radio channel model for multi-path environments [92]:

$$\mathbf{h}(t, \tau, \phi, \theta) = \sum_{n=1}^N A_n(t) e^{j\beta_n(t)} \delta(\tau - \tau_n) \delta(\phi - \phi_n) \delta(\theta - \theta_n), \quad (6.3)$$

where $A_n(t)$ is the amplitude for each received path n . Moreover, β_n denotes the phase of the received ray and θ and ϕ are the angle of arrival in azimuth and elevation plane, respectively. In order to plan the deployment of the RSUs, we define a constraint:

$$P_{rec}(t) \geq P_{th} \quad (6.4a)$$

$$\text{s.t.} \quad P_{rec}(t) = |\mathbf{h}(t, \tau, \phi, \theta)|^2. \quad (6.4b)$$

By using this constraint, it is guaranteed that the entire port area is covered within a certain received power threshold for all time instant t . Moreover, in an environment with several users sharing the same resources and infrastructure, the problem of interference arises. Hence, we define the signal-to-noise ratio (SINR) as follows, in order to model the interference and the impact in the communication:

$$\text{SINR} = \frac{P_{rec_n} G_n}{\sum_{j \in U} P_j G_j + \sum_{i \in V} P_{i,n} G_{i,n} I_{i,n} + \mathcal{W}}, \quad (6.5)$$

where P_{rec_n} is the received power and G_n is the signal gain for each user n . The first term in the denominator defines the interference created by collisions, i.e., two users using the same resource block, while the second term is the in-band emission interference (IBEI) produced by the leakage between sub-bands and \mathcal{W} is the noise power. The set U contains all the workers under the coverage of the same infrastructure sharing the same resources and V defines the set of workers located under the coverage of the infrastructure k but connected to a different infrastructure. Moreover, since the concentration areas are known

in our scenario, we want to maximize the received power in these areas, P_l , by means of an optimal beam-forming as follows:

$$\underset{\theta_i, \phi_i}{\text{maximize}} \quad |\mathbf{h}(t, \tau, \phi, \theta)^H \mathbf{w}(\theta_i, \phi_i)|^2, \quad (6.6a)$$

$$\text{s.t.} \quad \theta_i = \alpha_l \quad (6.6b)$$

$$\phi_i = \gamma_l, \quad (6.6c)$$

where the angles α_l and γ_l are defined in order to cover the desired concentration area $l \in \mathcal{L}$. $\mathbf{w}(\theta_i, \phi_i)$ is the antenna beam-forming based on the received channel state information (CSI) which depends on both angles θ_i and ϕ_i . The proposed concept of concentration areas \mathcal{L} has a double advantage. It enhances the communication signal in the areas with a higher density of users, while at the same time, decreases the interference produced by adjacent cells, since the power in these areas is smaller.

6.2.6 Simulation results

The simulation experiments related to emerging vehicular communication are done over the container and general cargo terminal at the Port of Bar. This terminal has a quadrilateral form, which can be approximated by a rectangle with dimensions 650×350 m (Figure 6.10). The container terminal is located at the pier I of the port and it covers an area of 60000 m^2 . The wharf length is 330 m and the depth of the sea is 11 m. The surface of the terminal is divided into different zones, and the connections for refrigerated containers are also provided. The terminal has an area for disposal of 2635 Twenty-Foot Equivalent Unit (TEU) in the range of the container crane. It has also 13 modular fields with a capacity of 2320 TEU per field. Additionally, the terminal has 6 modular fields for transportation and manipulation operations with 6320 TEU per field. The containers handling is realized in direct manipulation with railway wagons or other means of transportation. The general cargo terminal is located at the piers I and II of the Port of Bar, and it is equipped with necessary devices for loading, unloading and manipulating cargo (including fork-lifts). The length of the operational waterside line is 1370 m. The terminal is equipped with 15 portal cranes with a capacity of 15 Tonne per crane. The number of workers at the port depends on the workload and daily operational plans, and it varies from several workers to 20 – 25 per terminal/shift. Similar simulations have been conducted deploying three base stations and 10 mobile users, i.e., workers and fork-lifts in total [11, 12] without taking into consideration the interference between adjacent cells and users, since we assume a dedicated network.

Table 6.1: Simulation parameters

Parameter	Value
Bandwidth	10 MHz
Frequency Base Station	2.4 GHz
Frequency Workers/FL	5.9 GHz
Transmission Power	23 dBm

As described in Section 6.2.5, the communication scheme has a hybrid nature, therefore, the communication frequency is adapted accordingly to the requirements, i.e., for V2I the

used frequency is 2.4 GHz, while for V2V the used one is 5.9 GHz. Moreover, the rest of relevant parameters are defined in Table 6.1. In order to simulate the radio channel model, a combination of a deterministic ray-tracer algorithm (PIROPA) and a stochastic radio channel model (WINNER II) is used. This approach has been applied successfully in several scenarios, obtaining similar values compared with the real measurements. The simulation has been performed using a 2.6 GHz Intel Core i5 with 16 Gb of RAM, while the obtained results are presented in the next section.

The simulation scenario is depicted in Figure 6.10. The workers paths are simulated with a speed in the range of 1.4 m/s to 2.5 m/s (blue lines in Figure 6.10), while the fork-lifts move at a maximum speed of 6 m/s (red lines in Figure 6.10).

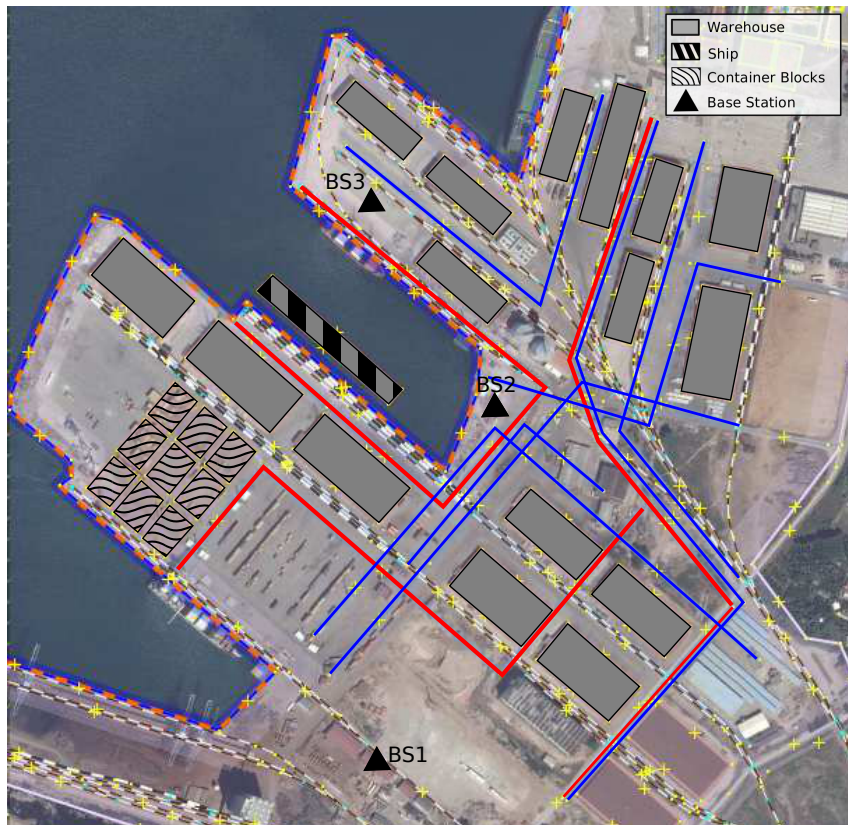


Figure 6.10: Deployed network and routes at the Port of Bar

The routes of the workers and the fork-lifts are predefined and they are known by the infrastructure and authorities, respectively. Moreover, since the proposed radio channel model has an environment-based component, it is important to know at any time the environment information, i.e., the number and location of all the containers. The situation of the containers shown in Figure 6.10 is the usual one. Therefore, the complete port area has a deterministic behavior, i.e., the ship arrivals and working areas are planned beforehand, making our approach suitable for this situation. In Figure 6.11, the received power at any port location is shown. In this situation, three base stations are deployed, at the positions shown in Figure 6.10 denoted as BS1, BS2, and BS3, covering the entire port area with the power constraint defined in equation (6.6). It is noteworthy that there are areas which are shadowed by the containers causing a lower received power. Due to this

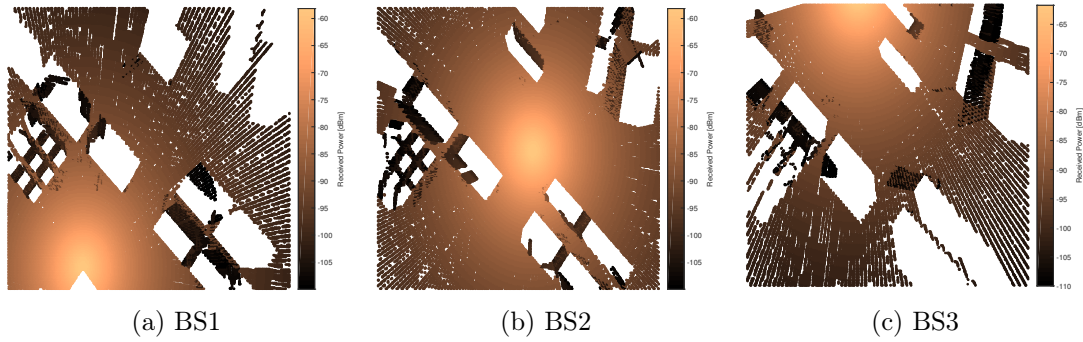


Figure 6.11: Heat map for three base stations at the Port of Bar.

obstruction, created by the different environmental elements, the already mentioned idea of concentration areas is useful. The concentration areas are defined next to the container locations as it is displayed in Figure 6.12 for BS2.

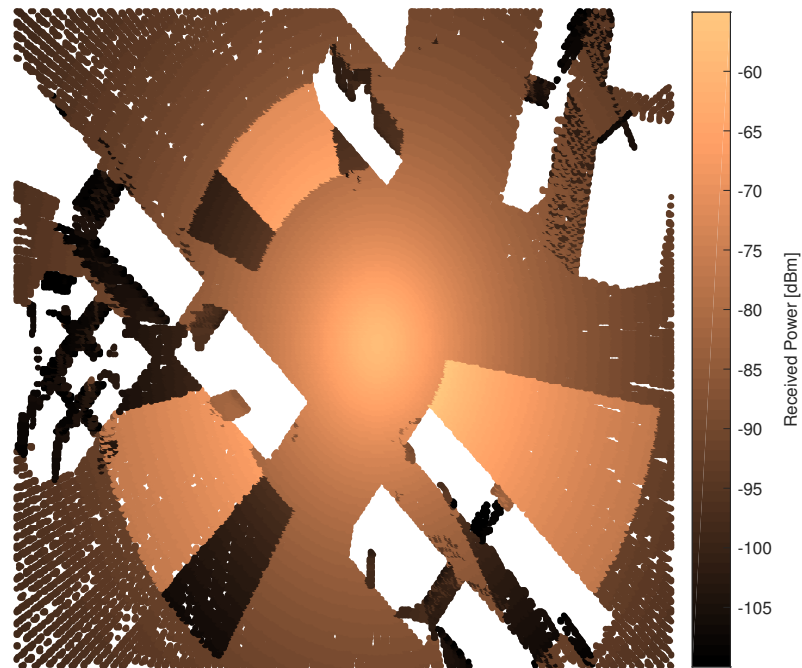


Figure 6.12: Tri-sector antenna pattern for concentration areas.

Due to this concept of concentration areas, a double goal is achieved: the areas with a lower received power are reduced and the areas next to the containers have a higher received power, increasing the reliability of communications. The final parameter to analyze is the communication between workers and fork-lifts (V2V communication). For this purpose, we simulate workers and fork-lifts in their predefined routes as shown in Figure 6.10. The results of this simulation are depicted in Figure 6.13

The study of the received power is performed using an Empirical Cumulative Distribution Function (ECDF) in order to show the coverage profile for each path. Since our study works with the obtained samples from the proposed radio channel model, using the ECDF is the most suitable way of representation. The simulation shows that the received power

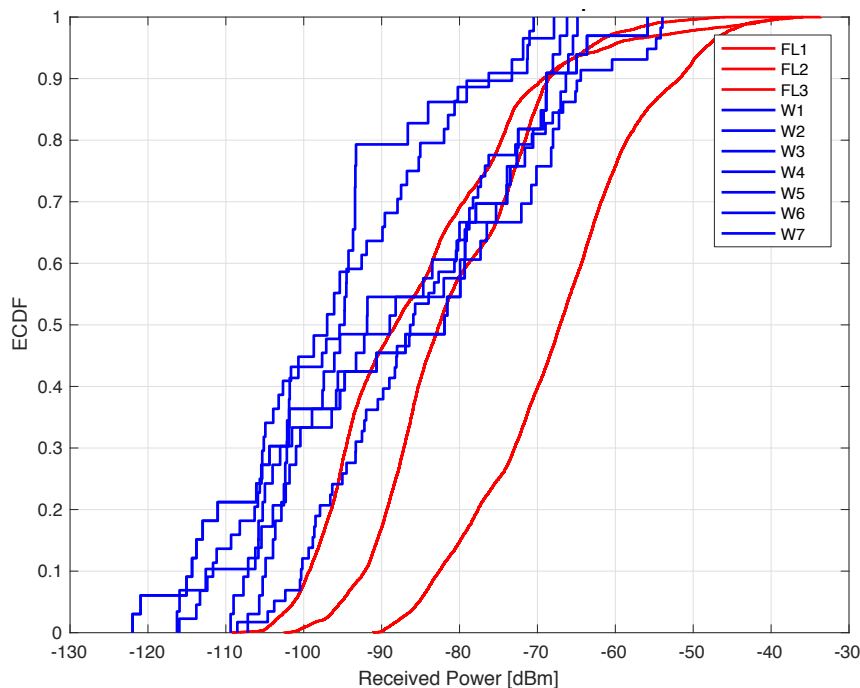


Figure 6.13: ECDF for vehicle-to-vehicle communication layer.

lies in the range of -130 dBm up to -30 dBm, which creates a feasible and reliable communication scheme. It is noteworthy to mention the higher received power by the fork-lifts due to the higher altitude of their antennas, creating regularly LoS situations. Moreover, the simulation also takes into consideration the interference defined in equation (6.5), due to the adjacent cells and the shared resources by several users at the same time.

Table 6.2: Delay, Doppler and angular parameters

	Max	Mean	Stand. Dev.
Delay Spread	$37.358 \mu\text{s}$	$11.1350 \mu\text{s}$	$5.637 \mu\text{s}$
Doppler Spread	5.345 Hz	-4.8491 Hz	1.871 Hz
Angular Spread	-	181.512°	109.245°

Moreover, due to the focus of our approach to safety, it is critical to investigate the reliability of the communications. For this purpose, the delay, Doppler and angular spread are detailed in Table 6.2. It is shown that the delay for the overall communication scheme is in the order of dozens of μs which is acceptable for safety applications. In addition, both angular and Doppler parameters are useful for the design of the receiver equipment in order to maximize the reliability of the communications.

6.2.7 Discussion of results for case study II

This paper proposes a vehicular communication network to increase the on-port safety of workers and machinery. The proposed vehicular scheme prioritizes the communication

reliability which is the main aspect of safety applications. The idea of using vehicular communications for on-port safety comes from the similar requirements of both fields, i.e., vehicle-to-vehicle and worker-to-worker communications, and also due to the great efforts are done in the research of vehicular networks in the scope of 5G technology. Our simulations show a feasible network scenario involving communication equipment for on-port workers and machinery, along with the deployment of communication infrastructures. Moreover, the concept of concentration areas, creating a heterogeneous network, is introduced enhancing the communication scheme and reducing the interferences.

Undoubtedly, the technology works, but one can not negligible the problem of innovation impenitence vs. success factors considered in the first part of the paper. Through the forthcoming work in the field, the researches should have in mind among other issues the following statements [159]: (i) The innovation cannot be restricted to the adoption of new technologies, instead it is to be conceived as a creative use of technology in order to interpret the market or integrate the knowledge; (ii) A culture of innovation can be nurtured on a continuing basis by promoting the creation of dedicated innovation networks around specific development challenges of the port that involve exchange of knowledge, technologies and resources among port operators, industrial, technology, and research and development partners.

6.3 Summary

In this chapter, two different case studies are defined and analyzed from a vehicular network perspective. The first case corresponds to an urban scenario (city of Cologne) were using real traffic data, the proposed network is deployed fulfilling the network requirements for vehicular safety applications. The network is deployed in two steps: first ubiquitous connectivity is obtained by installing macro-cells, and second, a higher reliability and lower latency are achieved by installing RSUs applying a density-based algorithm. The simulations confirm our assumptions obtaining an improved performance in the network.

The second case corresponds to a port scenario. In this case, we propose to apply the same concepts as for vehicular networks in order to provide safety to on-port workers. Since the requirements for both scenarios are similar, it makes sense to apply the same ideas for both scenarios. The simulations conclude that applying the same methods for on-port scenarios provides an increment in the on-port safety by using communication schemes.

7 | Conclusions

7.1 Summary and Contributions

This dissertation establishes a novel framework for cooperative connected vehicles using communication schemes. The content of this work is motivated by two different aspects. The first one is the vehicular communication requirements, i.e., high reliability and ultra-low latency, especially for safety-related applications. In this case, our aim is to deploy a network where these parameters can be fulfilled. The second aspect is to provide a cooperative scheme for the vehicles in order to optimize the traffic flow and increase the safety of the users by means of communication protocols.

Firstly, we define the different concepts used in vehicular networks and the stringent requirements for safety applications on the scope of a 5G technology. The main concept introduced here is the one of connected vehicles, which defines vehicles that can share information with the rest of the network by means of their communication equipment and on-board sensors. Moreover, the characteristics of vehicular scenarios and the challenges faced are defined and set as our motivation for the rest of the work.

In order to obtain a feasible framework for connected vehicles, we propose a novel heterogeneous architecture to provide ubiquitous connectivity and high reliability. Ubiquitous connectivity is established by formulating an optimization problem and by applying a heuristic algorithm to deploy macro-cells achieving umbrella coverage. In order to obtain a higher reliability, we increase the network's density, by means of installing multiple small-cells either by deploying fixed RSUs or by implementing mobile relay nodes. The infrastructures are installed using the expected density of vehicles in order to optimize the deployment and reduce the number of required infrastructures. Additionally, the remaining spots, which are not under the range of either the macro-cells or the RSUs, are covered using vehicles which play the role of mobile relay nodes. As a result of deploying the proposed network architecture, a complete coverage for the network members, in addition to high reliability for the communications are obtained, and both fulfilling the vehicular communication requirements.

In regards to characterizing the communication link between the different network layers, i.e., macro-cells, intermediate infrastructures and vehicles, we define different radio channel models. The motivation behind these several characterizations is that the different layers have diverse requirements and objectives to fulfill and therefore, require a different approach. In the case of the link between the macro-cells and vehicles or RSUs, we apply a semi-stochastic radio channel model. This particular radio channel model exploits the environment information by means of a ray-tracer algorithm and includes on

top of it, the fading behavior by means of a stochastic approach. The communication link between vehicles (V2V) requires a different approach. In this case, we do not focus on the overall behavior or peak data rate, but rather on the singular cases where the communication link is not good enough. For this matter, we use a three-wave channel model in order to characterize the communication reliability up to 10^{-5} error probability. Furthermore, we apply the concept of predictor antennas to obtain an accurate estimation of the radio channel impulse response for the preceding vehicles exploiting the platoon formation.

The main contribution of this dissertation is the formulation of a novel cooperative scheme for connected vehicles. This scheme comprises the formation of platoons and their management once they are created. We prove that under some communication constraints the platoon is stable, and moreover, it is the optimal formation in terms of safety and traffic flow. In order to motivate the creation of platoons, we design a theoretical framework based on a game-theory approach which provides a better performance when compared with previous work found in the literature. The core of our cooperative scheme is based on a repulsion/attraction approach, where a penalty is given whenever a user behaves selfishly, i.e., not making an optimal decision for the overall network; and a reward is granted when joining a platoon or forming a new one. Additionally, taking advantage of the achieved platoon formation for the vehicles, we propose an optimal scheduling scheme in order to enhance the communication network avoiding collisions in the transmissions, improving the reliability. The last part of this chapter deals with the aspect of safety in V2V communications. In order to provide a secure communication scheme, we make use of a ring-based signature and blockchain concepts to share the messages in a safe and anonymous manner.

The final part of this dissertation defines two different case studies to investigate the beneficial impact of the concepts developed in this work. The first case study describes a real-world urban scenario and evaluates whether the proposed network fulfills the required parameters. The second case study investigates whether analogous concepts as the ones for vehicular communications can be used in on-port scenarios in order to increase occupational safety. Our simulation results show that for the given port scenario, this approach is able to provide a higher safety for the on-port workers than the existing solutions.

7.2 Future Research

Connected vehicles is a relatively new topic and therefore, there is plenty of room for improvement and testing new ideas. A key technology further enabling the idea of ITS and autonomous driving is machine learning. Using our proposed framework as a starting point, it would be possible to apply machine learning concepts in two different cases:

- Network optimization predicting the traffic flow and resource allocation of the network: Using the available datasets, including the density of vehicles and the location of pedestrians, it is possible to train the network in order to achieve a better performance.

- Supervised learning for the adaptive behavior of the vehicles, achieving a faster consensus state. Additionally, the reward and penalty functions can be optimized using previous experiences.

It is also interesting to consider schemes which increase the communication reliability, especially in V2V communications. Some research has already been conducted in this field by the author of this dissertation, but further extensive considerations need to be investigated. Moreover, the general system implemented here does not consider the dynamic on-vehicle data processing time. It is necessary to include this variable and observe its impact on the overall system performance, especially on the platoon stability.

Moreover, since the currently proposed framework is mainly theoretical even though supported by simulations, the straightforward next step is to perform a real test for both network and cooperative scheme. This would be possible in the near future since it is expected to have new chips (Qualcomm late 2018) enabling LTE-V2X mode 3 and 4. The last aspect of the future research involving connected vehicles is to measure the acceptance of society regarding this new technology, and to which extent do the different industries involved are willing to modify their business models.

List of Acronyms

3GPP	Third Generation Partnership Project
5G	Fifth Generation of Mobile Communications
5GAA	5G Automotive Association
eNodeB	Evolved Node B
ACC	Adaptive Cruise Control
AIFS	Arbitration Inter-frame Space
ARMA	Autoregressive Moving Average
C-ITS	Cooperative Intelligent Transportation Systems
CACC	Cooperative Adaptive Cruise Control
CAM	Cooperative Awareness Message
CSMA/CA	Carrier Sense Multiple Access with Collision Avoidance
D2D	Device to Device
DeNodeB	Donor Evolved Node B
DoS	Denial of Service
DCF	Distributed Coordination Function
DCU	Data Center Unit
DENM	Decentralized Environmental Notification Message
ECDF	Empirical Cumulative Distribution Function
FD-MIMO	Full Dimension Multiple Input Multiple Output
FUA	Fast Uplink Access
GBSM	Geometry-Based Stochastic Model
GHO	Group Handover
I2I	Infrastructure to Infrastructure Communication
IoT	Internet of Things
ITS	Intelligent Transportation Systems

List of Acronyms

LIDAR	Light Detection and Ranging
LTE	Long Term Evolution
LTE-V2X	Long Term Evolution-Vehicle to Everything
LTE-V2X-SL	LTE-V SideLink
M2M	Machine-to-Machine
MAC	Media Access Control
MRN	Moving Relay Node
MSC	Mobile Small Cell
NMSE	Normalized Mean Square Error
NTU	Non-Transferable Utility
OBU	On-board Unit
PCF	Punctual Coordination Function
PDCP	Packet Data Convergence Protocol
PIROPA	Parallel Implemented Ray Optical Prediction Algorithm
PKI	Public Key Infrastructure
QoS	Quality of Service
RLC	Radio Link Control
RRC	Radio Resource Control
RSSI	Received Signal Strength Indicator
RSU	Road Side Unit
SC	Small Cell
SC-FDMA	Single Carrier Frequency Division Multiple Access
SINR	Signal-to-Interference-Noise Rate
SPS	Semi-Persistent Scheduling
TA	Trusted Authority
TEU	Twenty-Foot Equivalent Unit
TTI	Transmission Time Interval
TTI-RU	Transmission Time Interval-Resource Unit
UE	User Equipment
URLLC	Ultra-Reliable and Low-Latency Communications
V2I	Vehicle to Infrastructure Communication
V2N	Vehicle to Network Communication

V2P	Vehicle to Pedestrian Communication
V2V	Vehicle to Vehicle Communication
V2X	Vehicle to Everything Communication
VANET	Vehicular Ad-hoc Network

List of Figures

2.1	In-vehicle ITS technologies [15].	6
2.2	Vehicle-to-X application roadmap [16].	6
2.3	Automation levels according to SAE International Standard.	8
2.4	In-vehicle sensors and active safety systems.	10
2.5	Standard platoon formation.	11
2.6	V2X communication network overview.	12
2.7	Flowchart for the CSMA/CA according to the standard.	14
2.8	LTE-V2X Release 14 architecture.	15
2.9	LTE resource block architecture.	16
2.10	Modes of operation for V2X communications.	17
2.11	Packet structure consisting of metadata (preamble + header) and payload (a) Traditional long packet for current cellular systems. (b) Short packet for vehicular communications.	19
3.1	Cloud-assisted heterogeneous network overview.	22
3.2	Comparison of the results from metaheuristic algorithm and linear integer optimization with three different transmitted powers.	29
3.3	Geometry for RSU deployment.	32
3.4	Gap statistic for dataset 1.	35
3.5	Gap statistic for dataset 2.	35
3.6	K-means clustering algorithm.	36
3.7	Spectral clustering of one cluster obtained using K-means.	37
3.8	Number of beacons in a cluster.	38
3.9	Head-cluster dynamics prediction.	40
3.10	Estimated prediction accuracy for each update period Δt	41
3.11	Cluster lifetime comparison.	42
3.12	Flowchart for the MRN selection.	44
3.13	Flowchart for the group handover selection.	45
4.1	WINNER II channel model overview.	51
4.2	Full-Dimension MIMO for backhaul links.	54
4.3	General scheme for predictor antennas using a platoon formation.	57
4.4	General scheme for predictor antennas using a platoon formation.	58
4.5	RSSI comparison for the two different models.	59
4.6	NMSE comparison.	59
4.7	Outage probability in the three-waves channel model.	62
4.8	Outage probability in the three-waves channel model for URC relevant values.	62
4.9	Overtaking scenario for V2V communication.	64

List of Figures

4.10	Outage probability for V2V communication link in an overtaking scenario.	65
4.11	Doppler Shift value for V2V communication link in an overtaking scenario.	65
4.12	Crossing scenario for V2V communication.	66
4.13	Outage probability for V2V communication in a crossing scenario.	66
4.14	Doppler Shift value for V2V communication in a crossing scenario.	66
5.1	Block diagram using an implicit coordination scheme for obstacle detection.	68
5.2	General platoon formation.	71
5.3	Dynamic coalition formation game overview.	74
5.4	Time synchronized discrete control.	77
5.5	Traffic system response with 0.1s time gap.	78
5.6	Traffic system response with 0s time gap.	79
5.7	Stability analysis for the proposed platoon scheme.	81
5.8	Roadmap network for the simulation example.	82
5.9	Graph form of the network including the weights for each edge.	82
5.10	Load for each path comparing the three schemes.	83
5.11	Travel time to destination for each vehicle comparing the three schemes.	84
5.12	P_{RR} for platoon formation using CACC.	86
5.13	Semi-Persistent-Scheduling structure.	87
5.14	Distributed scheduling for out-of-coverage platoons.	89
5.15	Complex prediction scenario.	90
5.16	Semi-persistent scheduling scheme comparison results for the three different sub-pooling schemes.	92
5.17	Adversary vehicle trying to join a platoon.	94
5.18	Optimal platoon formation.	95
5.19	General flowchart for the proposed scheme. (*) check the identity of the vehicle j using the TA (**) verify the information sent by vehicle j comparing the values with the reads obtained from the own on-board equipment and the history of values.	96
5.20	General microtransaction scheme using blockchain.	98
6.1	Traffic density map of Cologne.	102
6.2	Selected area of Cologne with deployed infrastructure.	102
6.3	Macro-cell network deployment.	103
6.4	RSU deployment forming small cells.	104
6.5	Capacity for vehicles under DeNodeB coverage.	105
6.6	Capacity for vehicles under SC coverage.	105
6.7	Actors-environment communication matrix in providing innovation success (Source: adapted from [149], p.99)	109
6.8	A dynamic model of market creation (Source: adapted from [158], p.101)	111
6.9	Communication network overview.	112
6.10	Deployed network and routes at the Port of Bar	114
6.11	Heat map for three base stations at the Port of Bar.	115
6.12	Tri-sector antenna pattern for concentration areas.	115
6.13	ECDF for vehicle-to-vehicle communication layer.	116

List of Tables

3.1	Cloud-assisted heterogeneous network notation.	23
3.2	Symbol notation.	26
3.3	Static optimization constraint values.	27
3.4	Estimated mean values for each update period.	42
4.1	Environment-based channel model parameters	53
4.2	Statistical analysis for both models.	59
5.1	Simulation parameters.	82
5.2	Statistical analysis for the load per path.	83
5.3	Statistical analysis for trip time to destination	84
5.4	Simulation parameters.	91
6.1	Simulation parameters	113
6.2	Delay, Doppler and angular parameters	116

Bibliography

- [1] J. A. L. Calvo, X. Xu, and F. Schröder, “Investigation on mobile radio propagation channel models based on measurement data,” in *18th International Student Conference on Electrical Engineering*, Prague, Czech Republic, May 2014, pp. 1–5.
- [2] J. A. L. Calvo, F. Schröder, and R. Mathar, “Hybrid environment-based channel model for vehicular communications,” in *2015 14th International Conference on ITS Telecommunications (ITST)*, Copenhagen, Denmark, Dec. 2015, pp. 6–11.
- [3] J. A. L. Calvo, F. Schröder, X. Xu, and R. Mathar, “A validation using measurement data of a radio channel model with geographical information,” in *9th European Conference on Antennas and Propagation (EUCAP 2015)*, Lisbon, Portugal, Apr. 2015, pp. 1–4.
- [4] J. A. L. Calvo, H. A. Tokel, and R. Mathar, “Environment-based roadside unit deployment for urban scenarios,” in *27th Annual International Symposium on Personal, Indoor, and Mobile Radio Communication (PIMRC)*, Valencia, Spain, Sep. 2016, pp. 2037–2042.
- [5] J. A. L. Calvo and R. Mathar, “A two-level cooperative clustering scheme for vehicular communications,” in *The 6th International Conference on Information Communication and Management*, Hertfordshire, United Kingdom, Oct. 2016, pp. 205–210.
- [6] —, “A multi-level cooperative perception scheme for autonomous vehicles,” in *2017 15th International Conference on ITS Telecommunications (ITST)*, Warsaw, Poland, May 2017, pp. 1–5.
- [7] —, “An optimal LTE-V2I-based cooperative communication scheme for vehicular networks,” in *IEEE International Symposium on Personal, Indoor and Mobile Radio Communications (PIMRC)*, Montreal, QC, Canada, Oct. 2017.
- [8] C. Zhang, Y. Zang, J. A. L. Calvo, and R. Mathar, “A novel V2V assisted platooning system: Control scheme and MAC layer designs,” in *IEEE International Symposium on Personal, Indoor and Mobile Radio Communications (PIMRC)*, Montreal, QC, Canada, Oct. 2017.
- [9] J. A. L. Calvo and R. Mathar, “Secure blockchain-based communication scheme for connected vehicles,” in *2018 European Conference on Networks and Communications (EuCNC)*, Ljubljana, Slovenia, Jun. 2018.

Bibliography

- [10] —, “Connected vehicles coordination: A coalitional game-theory approach,” in *2018 European Conference on Networks and Communications (EuCNC)*, Ljubljana, Slovenia, Jun. 2018.
- [11] S. Bauk, J. A. L. Calvo, R. Mathar, and A. Schmeink, “V2P/I communication for increasing occupational safety at a seaport,” in *59th IEEE International Symposium Electronics in Marine (ELMAR)*, Zadar, Croatia, 2017, pp. 79–82.
- [12] S. Bauk, J. A. L. Calvo, A. Schmeink, and R. Mathar, “Enhancing on port safety by vehicular communication approach,” in *6th IEEE Mediterranean Conference on Embedded Computing (MECO)*, Bar, Montenegro, Jun. 2017, pp. 338–341.
- [13] L. Figueiredo, I. Jesus, J. A. T. Machado, J. R. Ferreira, and J. L. M. de Carvalho, “Towards the development of intelligent transportation systems,” in *ITSC 2001. 2001 IEEE Intelligent Transportation Systems. Proceedings (Cat. No.01TH8585)*, 2001, pp. 1206–1211.
- [14] 5G Automotive Association, *The Case for Cellular V2X for Safety and Cooperative Driving (White Paper)*, 2016.
- [15] M. Aoyama, “Computing for the next-generation automobile,” *Computer*, vol. 45, pp. 32–37, 2012.
- [16] R. Baldessari, B. Bödekker, M. Deegener, A. Festag, W. Franz, C. C. Kellum, T. Kosch, A. Kovacs, M. Lenardi, C. Menig, T. Peichl, M. Röckl, D. Seeberger, M. Straßberger, H. Stratil, H.-J. Vögel, B. Weyl, and W. Zhang, “Car-2-car communication consortium - manifesto,” Tech. Rep., 2007.
- [17] J. Petit and S. E. Shladover, “Potential cyberattacks on automated vehicles,” *IEEE Transactions on Intelligent Transportation Systems*, vol. 16, no. 2, pp. 546–556, April 2015.
- [18] S. Hassler, “Self-driving cars and trucks are on the move [spectral lines],” *IEEE Spectrum*, vol. 54, no. 1, pp. 6–6, January 2017.
- [19] Mobileye. (2015) Collision avoidance system. protecting your fleet and improving your bottom line. [Online]. Available: <http://www.mobileye.com>
- [20] R. Hult, G. R. Campos, E. Steinmetz, L. Hammarstrand, P. Falcone, and H. Wymeersch, “Coordination of cooperative autonomous vehicles: Toward safer and more efficient road transportation,” *IEEE Signal Processing Magazine*, vol. 33, no. 6, pp. 74–84, Nov 2016.
- [21] M. Treiber and A. Kesting, “Traffic flow dynamics,” *Traffic Flow Dynamics: Data, Models and Simulation*, Springer-Verlag Berlin Heidelberg, 2013.
- [22] S. Singh, “Critical reasons for crashes investigated in the national motor vehicle crash causation survey,” 2015.
- [23] SAE International, “Taxonomy and definitions for terms related to on-road motor vehicle automated driving systems, SAE J3016,” 2014.
- [24] World Health Organization, “Global health workforce statistics database,” 2016. [Online]. Available: (<http://www.who.int/hrh/statistics/hwfstats/>)
- [25] Eurostat, “Transport accident statistics,” 2015.

- [26] Y. Horita and R. S. Schwartz, “Extended electronic horizon for automated driving,” in *ITS Telecommunications (ITST), 2015 14th International Conference on*, Dec 2015, pp. 32–36.
- [27] Google Inc., “Google self-driving car project,” 2016.
- [28] R. Coppola and M. Morisio, “Connected car: Technologies, issues, future trends,” *ACM Comput. Surv.*, vol. 49, no. 3, pp. 46:1–46:36, Oct. 2016.
- [29] B. Schwarz, “Lidar: Mapping the world in 3d,” *Nature Photonics*, vol. 4, no. 7, pp. 429–430, 2010.
- [30] M. Wörner, F. Schuster, F. Dölitzscher, C. G. Keller, M. Haueis, and K. Dietmayer, “Integrity for autonomous driving: A survey,” in *2016 IEEE/ION Position, Location and Navigation Symposium (PLANS)*, April 2016, pp. 666–671.
- [31] F. Garcia, D. Martin, A. de la Escalera, and J. M. Armingol, “Sensor fusion methodology for vehicle detection,” *IEEE Intelligent Transportation Systems Magazine*, vol. 9, no. 1, pp. 123–133, Spring 2017.
- [32] N. Lyamin, Q. Deng, and A. Vinel, “Study of the platooning fuel efficiency under ETSI ITS-G5 communications,” in *2016 IEEE 19th International Conference on Intelligent Transportation Systems (ITSC)*, Nov 2016, pp. 551–556.
- [33] Y. Zheng, S. E. Li, K. Li, F. Borrelli, and J. K. Hedrick, “Distributed model predictive control for heterogeneous vehicle platoons under unidirectional topologies,” *IEEE Transactions on Control Systems Technology*, vol. 25, no. 3, pp. 899–910, May 2017.
- [34] L. Wu, N. Zhang, B. Sheng, and Q. Zhou, “Event-based control and scheduling for platoon system with communication constraints,” in *2017 36th Chinese Control Conference (CCC)*, July 2017, pp. 7926–7931.
- [35] 3GPP, “3rd generation partnership project: technical specification group radio access network: study on LTE-based V2X services (release 14),” 2016.
- [36] Rohde & Schwarz, *Device to Device Communication in LTE (White Paper)*, 2015.
- [37] D. Jiang and L. Delgrossi, “IEEE 802.11p: Towards an international standard for wireless access in vehicular environments,” in *Vehicular Technology Conference, 2008. VTC Spring 2008. IEEE*, May 2008, pp. 2036–2040.
- [38] R. Blasco, H. Do, S. Shalmashi, S. Sorrentino, Y. Zang, “3GPP LTE enhancements for V2V and comparison to IEEE 802.11p,” in *11th ITS European Congress, no. EU-SP0264*, 2016, pp. 6–9.
- [39] P. Popovski, “Ultra-reliable communication in 5G wireless systems,” in *1st International Conference on 5G for Ubiquitous Connectivity*, Nov 2014, pp. 146–151.
- [40] K. Lee, J. Kim, Y. Park, H. Wang, and D. Hong, “Latency of cellular-based V2X: Perspectives on TTI-proportional latency and TTI-independent latency,” *IEEE Access*, vol. 5, pp. 15 800–15 809, 2017.

Bibliography

- [41] Y. Polyanskiy, H. V. Poor, and S. Verdu, "Channel coding rate in the finite blocklength regime," *IEEE Transactions on Information Theory*, vol. 56, no. 5, pp. 2307–2359, May 2010.
- [42] P. Schulz, M. Matthe, H. Klessig, M. Simsek, G. Fettweis, J. Ansari, S. A. Ashraf, B. Almeroth, J. Voigt, I. Riedel, A. Puschmann, A. Mitschele-Thiel, M. Muller, T. Elste, and M. Windisch, "Latency critical iot applications in 5G: Perspective on the design of radio interface and network architecture," *IEEE Communications Magazine*, vol. 55, no. 2, pp. 70–78, February 2017.
- [43] J. G. Andrews, "Seven ways that HetNets are a cellular paradigm shift," *IEEE Communications Magazine*, vol. 51, no. 3, pp. 136–144, March 2013.
- [44] L. Chen, Y. Huang, F. Xie, Y. Gao, L. Chu, H. He, Y. Li, F. Liang, and Y. Yuan, "Mobile relay in LTE-advanced systems," *IEEE Communications Magazine*, vol. 51, no. 11, pp. 144–151, November 2013.
- [45] F. h. Tseng, L. d. Chou, H. c. Chao, and J. Wang, "Ultra-dense small cell planning using cognitive radio network toward 5G," *IEEE Wireless Communications*, vol. 22, no. 6, pp. 76–83, December 2015.
- [46] A. Goldsmith, S. A. Jafar, N. Jindal, and S. Vishwanath, "Capacity limits of MIMO channels," *IEEE Journal on selected areas in Communications*, vol. 21, no. 5, pp. 684–702, 2003.
- [47] H. Ji, Y. Kim, J. Lee, E. Onggosanusi, Y. Nam, J. Zhang, B. Lee, and B. Shim, "Overview of full-dimension MIMO in LTE-advanced pro," *arXiv preprint arXiv:1601.00019*, 2015.
- [48] Y.-H. Nam, M. S. Rahman, Y. Li, G. Xu, E. Onggosanusi, J. Zhang, and J.-Y. Seol, "Full dimension MIMO for LTE-advanced and 5G," in *Information Theory and Applications Workshop (ITA), 2015*. IEEE, 2015, pp. 143–148.
- [49] H. Halbauer, S. Saur, J. Koppenborg, and C. Hoek, "3D beamforming: Performance improvement for cellular networks," *Bell Labs Technical Journal*, vol. 18, no. 2, pp. 37–56, 2013.
- [50] E. G. Larsson, O. Edfors, F. Tufvesson, and T. L. Marzetta, "Massive MIMO for next generation wireless systems," *IEEE Communications Magazine*, vol. 52, no. 2, pp. 186–195, February 2014.
- [51] A. Zakrzewska, D. López-Pérez, S. Kucera, and H. Claussen, "Dual connectivity in LTE HetNets with split control- and user-plane," in *2013 IEEE Globecom Workshops (GC Wkshps)*, Dec 2013, pp. 391–396.
- [52] H. Ishii, Y. Kishiyama, and H. Takahashi, "A novel architecture for LTE-B :C-plane/U-plane split and phantom cell concept," in *2012 IEEE Globecom Workshops*, Dec 2012, pp. 624–630.
- [53] S. Yutao, *On the Benefits of Moving Relay Nodes in Wireless Networks*. Department of Signals and Systems, Communication Systems, Chalmers University of Technology,, 2012.

- [54] J. Barrachina, P. Garrido, M. Fogue, F. Martinez, J.-C. Cano, C. Calafate, and P. Manzoni, "Road side unit deployment: A density-based approach," *Intelligent Transportation Systems Magazine, IEEE*, vol. 5, no. 3, pp. 30–39, Fall 2013.
- [55] S. I. Sou, "A power-saving model for roadside unit deployment in vehicular networks," *IEEE Communications Letters*, vol. 14, no. 7, pp. 623–625, July 2010.
- [56] Savari, "Streetwave roadside unit: Support V2X safety and mobility applications." [Online]. Available: <http://www.savarinetworks.com/products/streetwave/>
- [57] I. Gurobi Optimization, "Gurobi optimizer reference manual," 2016. [Online]. Available: <http://www.gurobi.com>
- [58] Q. Ming-yao, M. Li-xin, Z. Le, and X. Hua-yu, "A new tabu search heuristic algorithm for the vehicle routing problem with time windows," in *Management Science and Engineering, 2008. ICMSE 2008. 15th Annual Conference Proceedings., International Conference on*, Sept 2008, pp. 1648–1653.
- [59] R. Daher and A. Vinel, "Roadside networks for vehicular communications: Architectures, applications, and test fields," 2012.
- [60] W. W. Yongping Xiong, Jian Ma and D. Tu, "Roadgate: Mobility-centric roadside units deployment for vehicular networks," in *International Journal of Distributed Sensor Networks*, vol. 2013, 2013, p. 10.
- [61] J. Lee and C. Kim, "A roadside unit placement scheme for vehicular telematics networks," in *Advances in Computer Science and Information Technology*, ser. Lecture Notes in Computer Science, T.-h. Kim and H. Adeli, Eds. Springer Berlin Heidelberg, 2010, vol. 6059, pp. 196–202.
- [62] K. Ayvaz, E. Kurtarangil, and B. Canberk, "A relay-based coverage area model for optimal connectivity in vehicular networks," in *2014 IEEE International Black Sea Conference on Communications and Networking (BlackSeaCom)*, May 2014, pp. 129–133.
- [63] A. B. Reis, S. Sargento, F. Neves, and O. Tonguz, "Deploying roadside units in sparse vehicular networks: What really works and what does not," *IEEE Transactions on Vehicular Technology*, vol. 63, no. 6, pp. 2794–2806, July 2014.
- [64] N. Wisitpongphan, F. Bai, P. Mudalige, V. Sadekar, and O. Tonguz, "Routing in sparse vehicular ad hoc wireless networks," *IEEE Journal on Selected Areas in Communications*, vol. 25, no. 8, pp. 1538–1556, Oct 2007.
- [65] R. Graham, B. Lubachevsky, K. Nurmela, and P. Östergård, "Dense packings of congruent circles in a circle," *Discrete Mathematics*, vol. 181, no. 1, pp. 139 – 154, 1998.
- [66] J. A. L. Calvo, G. Alirezaei, and R. Mathar, "Wireless powering of drone-based manets for disaster zones," in *The 2017 IEEE International Conference on Wireless for Space and Extreme Environments (WiSEE'17)*, Montreal, Canada, Oct. 2017.
- [67] S. Kuklinski and G. Wolny, "Density based clustering algorithm for VANETs," in *Testbeds and Research Infrastructures for the Development of Networks Communities and Workshops, 2009. TridentCom 2009. 5th International Conference on*, April 2009, pp. 1–6.

Bibliography

- [68] S. A. Mohammad and C. W. Michele, "Using traffic flow for cluster formation in vehicular ad-hoc networks," in *Local Computer Networks (LCN), 2010 IEEE 35th Conference on*, Oct 2010, pp. 631–636.
- [69] E. Souza, I. Nikolaidis, and P. Gburzynski, "A new aggregate local mobility clustering algorithm for VANETs," in *Communications (ICC), 2010 IEEE International Conference on*, May 2010, pp. 1–5.
- [70] A. Vinel, "3GPP LTE versus IEEE 802.11p/WAVE: Which technology is able to support cooperative vehicular safety applications?" *IEEE Wireless Communications Letters*, vol. 1, no. 2, pp. 125–128, April 2012.
- [71] R. Sivaraj, A. K. Gopalakrishna, M. G. Chandra, and P. Balamuralidhar, "QoS-enabled group communication in integrated VANET-LTE heterogeneous wireless networks," in *2011 IEEE 7th International Conference on Wireless and Mobile Computing, Networking and Communications (WiMob)*, Oct 2011, pp. 17–24.
- [72] R. Atat, E. Yaacoub, M. S. Alouini, and F. Filali, "Delay efficient cooperation in public safety vehicular networks using LTE and IEEE 802.11p," in *2012 IEEE Consumer Communications and Networking Conference (CCNC)*, Jan 2012, pp. 316–320.
- [73] S. Ucar, S. C. Ergen, and O. Ozkasap, "Multihop-cluster-based IEEE 802.11p and LTE hybrid architecture for VANET safety message dissemination," *IEEE Transactions on Vehicular Technology*, vol. 65, no. 4, pp. 2621–2636, April 2016.
- [74] A. Y. Ng, M. I. Jordan, and Y. Weiss, "On spectral clustering: Analysis and an algorithm," in *Advances in Neural Information Processing Systems*. MIT Press, 2001, pp. 849–856.
- [75] G. L. Scott and H. C. Longuet-Higgins, "Feature grouping by relocalisation of eigenvectors of the proximity matrix." in *BMVC*. Citeseer, 1990, pp. 1–6.
- [76] R. Tibshirani, G. Walther, and T. Hastie, "Estimating the number of clusters in a data set via the gap statistic," *Journal of the Royal Statistical Society: Series B (Statistical Methodology)*, vol. 63, no. 2, pp. 411–423, 2001.
- [77] Z. Huang, "Extensions to the k-means algorithm for clustering large data sets with categorical values," *Data Min. Knowl. Discov.*, vol. 2, no. 3, pp. 283–304, Sep. 1998.
- [78] J. L. M. Jiang and Y. Tay. (1999) Cluster based routing protocol. [Online]. Available: <https://tools.ietf.org/html/draft-ietf-manet-cbrp-spec-01>
- [79] S. Sivavakeesar and G. Pavlou, "Associativity-based stable cluster formation in mobile ad hoc networks," in *Second IEEE Consumer Communications and Networking Conference, 2005. CCNC. 2005*, Jan 2005, pp. 196–201.
- [80] P. Fan, J. G. Haran, J. Dillenburg, and P. C. Nelson, *Cluster-Based Framework in Vehicular Ad-Hoc Networks*. Berlin, Heidelberg: Springer Berlin Heidelberg, 2005, pp. 32–42.

- [81] A. Vinel, Y. Koucheryavy, S. Andreev, and D. Staehle, "Estimation of a successful beacon reception probability in vehicular ad-hoc networks," in *Proceedings of the 2009 International Conference on Wireless Communications and Mobile Computing: Connecting the World Wirelessly*, ser. IWCMC '09. New York, NY, USA: ACM, 2009, pp. 416–420.
- [82] M. J. Lighthill and G. B. Whitham, "On kinematic waves. ii. a theory of traffic flow on long crowded roads," *Proceedings of the Royal Society of London A: Mathematical, Physical and Engineering Sciences*, vol. 229, no. 1178, pp. 317–345, 1955.
- [83] R. Haberman and R. W. Kolkka, "Mathematical models," 1977.
- [84] A. B. Reis, S. Sargento, and O. K. Tonguz, "Parked cars are excellent roadside units," *IEEE Transactions on Intelligent Transportation Systems*, vol. 18, no. 9, pp. 2490–2502, Sept 2017.
- [85] Y. Sui, J. Vihriala, A. Papadogiannis, M. Sternad, W. Yang, and T. Svensson, "Moving cells: a promising solution to boost performance for vehicular users," *IEEE Communications Magazine*, vol. 51, no. 6, pp. 62–68, June 2013.
- [86] M. Patra, R. Thakur, and C. S. R. Murthy, "Improving delay and energy efficiency of vehicular networks using mobile femto access points," *IEEE Transactions on Vehicular Technology*, vol. 66, no. 2, pp. 1496–1505, Feb 2017.
- [87] W. Viriyasitavat, M. Boban, H. M. Tsai, and A. Vasilakos, "Vehicular communications: Survey and challenges of channel and propagation models," *IEEE Vehicular Technology Magazine*, vol. 10, no. 2, pp. 55–66, June 2015.
- [88] X. Xu, M. Reyer, F. Schröder, A. Engels, and R. Mathar, "A semi-stochastic radio propagation model for wireless MIMO channels," in *International Symposium on Wireless Communication 2011*, Aachen, Deutschland, Nov. 2011, pp. 619–623.
- [89] F. Schöder, M. Reyer, and R. Mathar, "Field strength prediction for environment aware mimo channel models," in *6th European Conference on Antennas and Propagation (EUCAP)*, March 2012.
- [90] P. Kyösti, J. Meinilä, L. Hentilä, X. Zhao, T. Jämsä, C. Schneider, M. Narandzić, M. Milojević, A. Hong, J. Ylitalo, V.-M. Holappa, M. Alatossava, R. Bultitude, Y. de Jong, and T. Rautiainen, "WINNER II channel models," EC FP6, Tech. Rep., Sep. 2007. [Online]. Available: <http://www.ist-winner.org/deliverables.html>
- [91] J. P. Kermoal, L. Schumacher, K. I. Pedersen, P. E. Mogensen, and F. Frederiksen, "A stochastic mimo radio channel model with experimental validation," *IEEE Journal on Selected Areas in Communications*, vol. 20, no. 6, pp. 1211–1226, Aug 2002.
- [92] M. Steinbauer, A. F. Molisch, and E. Bonek, "The double-directional radio channel," *IEEE Antennas and Propagation Magazine*, vol. 43, pp. 51–63, Aug 2001.
- [93] 3GPP, "Evolved universal terrestrial radio access (E-UTRA); physical channels and modulation. specification 36.211." Tech. Rep., 2016.

Bibliography

- [94] G. Xu, Y. Li, J. Yuan, R. Monroe, S. Rajagopal, S. Ramakrishna, Y. H. Nam, J. Y. Seol, J. Kim, M. M. U. Gul, A. Aziz, and J. Zhang, “Full dimension MIMO (FD-MIMO): Demonstrating commercial feasibility,” *IEEE Journal on Selected Areas in Communications*, vol. 35, no. 8, pp. 1876–1886, Aug 2017.
- [95] T. R. Ramya and S. Bhashyam, “On using channel prediction in adaptive beamforming systems,” in *2007 2nd International Conference on Communication Systems Software and Middleware*, Jan 2007, pp. 1–6.
- [96] M. Sternad, M. Grieger, R. Abildgaard-Olesen, T. Svensson, D. Aronsson, and A. Belen Martinez, “Using “predictor antennas” for long-range prediction of fast fading for moving relays,” in *2012 IEEE Wireless Communications and Networking Conference*, 2012, pp. 253–257.
- [97] D. Aronsson, *Channel estimation and prediction for MIMO OFDM systems: Key design and performance aspects of Kalman-based algorithms*. Institutionen för teknikvetenskap, 2011.
- [98] R. Parasuraman, S. Caccamo, F. Baberg, and P. Ogren, “CRAWDAD dataset kth/rss (v. 2016-01-05),” Downloaded from <https://crawdad.org/kth/rss/20160105>, Jan. 2016.
- [99] J. Maurer, T. Fugen, T. Schafer, and W. Wiesbeck, “A new inter-vehicle communications (IVC) channel model,” in *Vehicular Technology Conference, 2004. VTC2004-Fall. 2004 IEEE 60th*, vol. 1, Sept 2004, pp. 9–13.
- [100] J. Karedal, F. Tufvesson, N. Czink, A. Paier, C. Dumard, T. Zemen, C. Mecklenbrauker, and A. Molisch, “A geometry-based stochastic mimo model for vehicle-to-vehicle communications,” *Wireless Communications, IEEE Transactions on*, vol. 8, no. 7, pp. 3646–3657, July 2009.
- [101] T. Mangel, O. Klemp, and H. Hartenstein, “A validated 5.9 GHz non-line-of-sight path-loss and fading model for inter-vehicle communication,” in *ITS Telecommunications (ITST), 2011 11th International Conference on*, Aug 2011, pp. 75–80.
- [102] P. C. F. Eggers, M. Angelichinoski, and P. Popovski, “Wireless channel modeling perspectives for ultra-reliable low latency communications,” *ArXiv e-prints*, May 2017.
- [103] J. Nuckelt, T. Abbas, F. Tufvesson, C. Mecklenbrauker, L. Bernado, and T. Kurner, “Comparison of ray tracing and channel-sounder measurements for vehicular communications,” in *2013 IEEE 77th Vehicular Technology Conference (VTC Spring)*, June 2013, pp. 1–5.
- [104] J. Björsell, M. Sternad, and M. Grieger, “Using predictor antennas for the prediction of small-scale fading provides an order-of-magnitude improvement of prediction horizons,” in *2017 IEEE International Conference on Communications Workshops (ICC Workshops)*, May 2017, pp. 54–60.
- [105] Z. Chen, T. Chu, and J. Zhang, “Swarm splitting and multiple targets seeking in multi-agent dynamic systems,” in *49th IEEE Conference on Decision and Control (CDC)*, Dec 2010, pp. 4577–4582.

- [106] C. W. Reynolds, “Flocks, herds and schools: A distributed behavioral model,” in *ACM SIGGRAPH computer graphics*, vol. 21, no. 4. ACM, 1987, pp. 25–34.
- [107] A. Espinosa, J. Lerch, R. Kraut, E. Salas, S. M. Fiore, and J. A. C. bowers (editors), “Explicit vs. implicit coordination mechanisms and task dependencies: One size does not fit all,” 2002.
- [108] T. H. Chan and L. Ning, “Fast convergence for consensus in dynamic networks,” in *International Colloquium on Automata, Languages, and Programming*. Springer, 2011, pp. 514–525.
- [109] D. Cheng, J. Wang, and X. Hu, “An extension of lasalle invariance principle and its application to multi-agent consensus,” *IEEE Transactions on Automatic Control*, vol. 53, no. 7, pp. 1765–1770, Aug 2008.
- [110] J. P. LaSalle, “Stability theory and invariance principles,” in *Dynamical Systems, Volume 1*. Elsevier, 1976, pp. 211–222.
- [111] F. Farokhi and K. H. Johansson, “A game-theoretic framework for studying truck platooning incentives,” in *16th International IEEE Conference on Intelligent Transportation Systems (ITSC 2013)*, Oct 2013, pp. 1253–1260.
- [112] A. Gattami, A. A. Alam, K. H. Johansson, and C. J. Tomlin, “Establishing safety for heavy duty vehicle platooning: A game theoretical approach,” *IFAC Proceedings Volumes*, vol. 44, no. 1, pp. 3818 – 3823, 2011, 18th IFAC World Congress.
- [113] M. Hözl, N. Koch, M. Puviani, M. Wirsing, and F. Zambonelli, “The ensemble development life cycle and best practices for collective autonomic systems,” in *Software Engineering for Collective Autonomic Systems*. Springer, 2015, pp. 325–354.
- [114] K. Y. Liang, J. Mårtensson, and K. H. Johansson, “Heavy-duty vehicle platoon formation for fuel efficiency,” *IEEE Transactions on Intelligent Transportation Systems*, vol. 17, no. 4, pp. 1051–1061, April 2016.
- [115] R. J. Aumann and B. Peleg, “Von Neumann-Morgenstern solutions to cooperative games without side payments,” *Bull. Amer. Math. Soc.*, vol. 66, no. 3, pp. 173–179, 05 1960.
- [116] R. J. Aumann and J. H. Dreze, “Cooperative games with coalition structures,” *International Journal of Game Theory*, vol. 3, no. 4, pp. 217–237, Dec 1974.
- [117] J. Ploeg, N. van de Wouw, and H. Nijmeijer, “Lp string stability of cascaded systems: Application to vehicle platooning,” *IEEE Transactions on Control Systems Technology*, vol. 22, no. 2, pp. 786–793, March 2014.
- [118] D. Li and Y. Liu, “In-band emission in LTE-A D2D: Impact and addressing schemes,” in *2015 IEEE 81st Vehicular Technology Conference (VTC Spring)*, May 2015, pp. 1–5.
- [119] 3GPP TR 36.843 V12.0.1, “Study on LTE device to device proximity services, radio aspects.”

Bibliography

- [120] W. B. Yang, M. Souryal, and D. Griffith, "LTE uplink performance with interference from in-band device-to-device (D2D) communications," in *2015 IEEE Wireless Communications and Networking Conference (WCNC)*, March 2015, pp. 669–674.
- [121] Z. Liang and Y. Wakahara, "City traffic prediction based on real-time traffic information for intelligent transport systems," in *2013 13th International Conference on ITS Telecommunications (ITST)*, Nov 2013, pp. 378–383.
- [122] TAPASCologne. Institute of Transportation Systems at the German Aerospace Center, "Tapascologne project."
- [123] 3GPP TS 36.101 V12.4.0: "Evolved Universal Terrestrial Radio Access (E-UTRA); User Equipment (UE) radio transmission and reception."
- [124] J. Yang, B. Pelletier, and B. Champagne, "Enhanced autonomous resource selection for LTE-based V2V communication," in *2016 IEEE Vehicular Networking Conference (VNC)*, Dec 2016, pp. 1–6.
- [125] R. L. Rivest, A. Shamir, and Y. Tauman, "How to leak a secret," in *Advances in Cryptology — ASIACRYPT 2001*, C. Boyd, Ed. Berlin, Heidelberg: Springer Berlin Heidelberg, 2001, pp. 552–565.
- [126] D. Chaum and E. Van Heyst, "Group signatures," in *Advances in Cryptology—EUROCRYPT'91*. Springer, 1991, pp. 257–265.
- [127] Y. Jiang, Y. Ji, and T. Liu, "An anonymous communication scheme based on ring signature in VANETs," *ArXiv e-prints*, Oct. 2014.
- [128] S. Nakamoto, "Bitcoin: A peer-to-peer electronic cash system," <http://bitcoin.org/bitcoin.pdf>.
- [129] S. Rowan, M. Clear, M. Gerla, M. Huggard, and C. M. Goldrick, "Securing vehicle to vehicle communications using blockchain through visible light and acoustic side-channels," *CoRR*, vol. abs/1704.02553, 2017. [Online]. Available: <http://arxiv.org/abs/1704.02553>
- [130] C. Fromknecht, D. Velicanu, and S. Yakoubov, "A decentralized public key infrastructure with identity retention," *IACR Cryptology ePrint Archive*, vol. 2014, p. 803, 2014.
- [131] J. Petit, F. Schaub, M. Feiri, and F. Kargl, "Pseudonym schemes in vehicular networks: A survey," *IEEE Communications Surveys Tutorials*, vol. 17, no. 1, pp. 228–255, Firstquarter 2015.
- [132] P. Cuccuru, "Beyond bitcoin: an early overview on smart contracts," *International Journal of Law and Information Technology*, vol. 25, no. 3, pp. 179–195, 2017.
- [133] M. Bartoletti and L. Pompianu, "An empirical analysis of smart contracts: platforms, applications, and design patterns," *ArXiv e-prints*, Mar. 2017.
- [134] J. Xu, W. Lin, X. Wang, and Y.-M. Shao, "Acceleration and deceleration calibration of operating speed prediction models for two-lane mountain highways," *Journal of Transportation Engineering, Part A: Systems*, vol. 143, no. 7, p. 04017024, 2017.

- [135] S. Uppoor, O. Trullols-Cruces, M. Fiore, and J. M. Barcelo-Ordinas, “Generation and analysis of a large-scale urban vehicular mobility dataset,” *IEEE Transactions on Mobile Computing*, vol. 13, no. 5, pp. 1061–1075, May 2014.
- [136] C. E. Shannon, “A mathematical theory of communication,” *Bell system technical journal*, vol. 27, 1948.
- [137] 3GPP TR 22.886 Release 15, “Study on enhancement of 3GPP support for 5G V2X services,” 2018.
- [138] M. Wang, W. Daamen, S. P. Hoogendoorn, and B. van Arem, “Rolling horizon control framework for driver assistance systems. part ii: Cooperative sensing and cooperative control,” *Transportation Research Part C: Emerging Technologies*, vol. 40, pp. 290 – 311, 2014.
- [139] H. Zhou, S. Xu, D. Ren, C. Huang, and H. Zhang, “Analysis of event-driven warning message propagation in vehicular ad hoc networks,” *Ad Hoc Networks*, vol. 55, pp. 87 – 96, 2017.
- [140] Dialogic and NEA, “International innovation benchmark,” (2002).
- [141] T. Wiesenthal, A. Condeço-Melhorado, and G. Leduc, “Innovation in the European transport sector: A review,” *Transport Policy*, vol. 42, pp. 86 – 93, 2015.
- [142] M. Draškovic, S. Bauk, D. Streimikiene, and V. Draskovic, “Testing the level of alternative institutions as a slowdown factor of economic development: the case of montenegro,” in *Amfiteatru Economic*, vol. 19, no. 45, 2017.
- [143] J. Schumpeter and U. Backhaus, “The theory of economic development,” *Joseph Alois Schumpeter*, pp. 61–116, 2003.
- [144] P. Drucker, *Innovation and entrepreneurship*. Routledge, 2014.
- [145] V. K. Narayanan and G. C. O’Connor, *Encyclopedia of technology and innovation management*. John Wiley & Sons, 2010.
- [146] J. Sundbo, *The theory of innovation: entrepreneurs, technology and strategy*. Edward Elgar Publishing, 1998.
- [147] R. Garcia and R. Calantone, “A critical look at technological innovation typology and innovativeness terminology: a literature review,” *Journal of Product Innovation Management*, vol. 19, pp. 110 – 132, 2002.
- [148] J. A. Gambatese and M. Hallowell, “Enabling and measuring innovation in the construction industry,” *Construction Management and Economics*, vol. 29, pp. 553–567, 2011.
- [149] G. Arduino, R. Aronietis, Y. Crozet, K. Frouws, C. Ferrari, L. Guihéry, S. Kapros, I. Kourounioti, F. Laroche, M. Lambrou, M. Lloyd, A. Polydoropoulou, A. Roumboutsos, E. V. de Voorde, and T. Vanelslander, “How to turn an innovative concept into a success? An application to seaport-related innovation,” *Research in Transportation Economics*, vol. 42, pp. 97 – 107, 2013.
- [150] OECD/Eurostat, “Oslo Manual. Guidelines for collecting and interpreting innovation data, 3rd Ed. 2005,” 2005.

Bibliography

- [151] B. Roberts and M. Gray, “Improving pedestrian safety in container ports and terminals,” Port Technology International, Tech. Rep., 2013.
- [152] UKDT-UK Department for Transport, “Transport Statistics Bulletin – Port Employment and Accident Rates,” 2009/10.
- [153] —, “Port Employment and Accident Rates Survey:,” 2009/10.
- [154] R.-M. Darbra and J. Casal, “Historical analysis of accidents in seaports,” *Safety Science*, vol. 42, pp. 85 – 98, 2004.
- [155] S. Bauk, A. Schmeink, and J. Colomer, “An RFID model for improving workers’ safety at the seaport in transitional environment,” *Transport*, vol. 31, pp. 1–11, Oct. 2016.
- [156] F. Parola and S. Maugeri, “Origin and taxonomy of conflicts in seaports: Towards a research agenda,” *Research in Transportation Business & Management*, vol. 8, pp. 114 – 122, 2013.
- [157] P. Kotler, S. Burton., and K. L. Keller, *Marketing management*, 1st ed. Pearson Prentice Hall Frenchs Forest, N.S.W, 2009.
- [158] J. Darroch and M. P. Miles, “Sources of innovation,” in *Wiley Encyclopedia of Management*. Wiley Online Library, 2010.
- [159] M. De Martino, L. Errichiello, A. Marasco, and A. Morvillo, “Logistics innovation in seaports: An inter-organizational perspective,” in *Research in Transportation Business & Management*, 2013.

Curriculum Vitae

Jose Angel Leon Calvo

Feb. 28, 1988	Born in Madrid, Spain
Sep. 1994 - Jun. 2000	Elementary school "Amor de Dios" Alcorcon, Madrid
Sep. 2000 - Jun. 2006	High school "Amor de Dios" Alcorcon, Madrid
Jul. 2006	General qualification for University entrance
Sept. 2006 - Jun. 2008	Telecommunication Engineering Department of Electrical Engineering Universidad Politecnica de Madrid, Madrid, Spain
Sept. 2008 - Jun. 2014	Telecommunication Engineering Department of Electrical Engineering Universidad Carlos III de Madrid, Madrid, Spain
Sept. 2013 - May. 2014	Student Researcher Institute for Communication Technologies (ICE) RWTH Aachen University, Aachen, Germany
Sept. 2013 - Sept. 2014	Erasmus Student Master of Science Electrical Engineering RWTH Aachen University, Aachen, Germany
Sep. 2014	Master of Science Telecommunication Engineering Department of Electrical Engineering Universidad Carlos III de Madrid, Madrid, Spain
Since Oct. 2014	Research Assistant Institute for Theoretical Information Technology RWTH Aachen University, Aachen, Germany